

Universität Leipzig
Fakultät für Physik und Geowissenschaften
Institut für Geographie

Carbonate chemistry and CaCO_3 precipitation as ikaite in Antarctic sea ice

Analysis in the Southern Ocean and off Adélie Land, Antarctica

Wissenschaftliche Arbeit
zur Erlangung des akademischen Grades
Diplom-Geograph

vorgelegt von: Michael Fischer
Matrikel: 9106936
Studiengang Geographie

Betreuer: Prof. Dr. Hans Neumeister
Universität Leipzig
Institut für Geographie

Dr. Gerhard Dieckmann
Alfred Wegener Institut für Polar- und Meeresforschung
In der Helmholtz-Gemeinschaft Deutscher Forschungszentren

Die Welt ist ein Buch, und wer zu
Hause bleibt, liest nur die erste Seite

unbekannt

Fischer, Michael (2009):

Carbonate chemistry and CaCO₃ precipitation as ikaite in Antarctic sea ice: Analysis in the Southern Ocean and off Adélie Land, Antarctica. 108 pages, 47 figures, 16 tables, Leipzig, University of Leipzig, Diploma thesis

Erklärung

Hiermit erkläre ich ehrenwörtlich, dass ich die vorliegende Diplomarbeit ohne unzulässige Hilfe Dritter und Benutzung anderer als der angegebenen Hilfsmittel angefertigt habe. Die aus fremden Quellen direkt oder indirekt übernommenen Gedanken sind als solche kenntlich gemacht.

An der geistigen Erstellung der vorliegenden Diplomarbeit war außer mir niemand beteiligt. Dritte haben von mir weder unmittelbar noch mittelbar geldwerte Leistungen für Arbeiten erhalten, die im Zusammenhang mit dem Inhalt der vorliegenden Arbeit stehen.

Diese Diplomarbeit wurde bisher weder im Inland noch im Ausland in gleicher oder ähnlicher Form oder auszugsweise einer Prüfungsbehörde vorgelegt.

Ich erkläre mich damit einverstanden, dass meine Diplomarbeit nach positiver Begutachtung in der Zweigstelle Geographie der Universitätsbibliothek Leipzig zur allgemeinen Benutzung zur Verfügung steht. Die Urheberrechte müssen jedoch gewahrt bleiben.

Leipzig, den 20.05.2009

Michael Fischer

Danksagung

Die vorliegende Diplomarbeit entstand im Rahmen des Internationalen Polarjahres 2007/2008 in dem sich Wissenschaftler aus über 60 Nationen zusammen geschlossen haben, um gemeinsam die Polargebiete genauer zu erforschen.

An dieser Stelle möchte ich all jenen danken, die durch fachliche und persönliche Unterstützung zum Gelingen meiner Diplomarbeit beigetragen haben.

Herrn Prof. Dr. Hans Neumeister danke ich für die Betreuung und für die wichtigen Anregungen bei der Bearbeitung des Themas.

Bei Herrn Dr. Gerhard Dieckmann bedanke ich mich für die Motivation für das Thema, die Bereitstellung wichtiger Daten sowie der Unterstützung, Anregungen und der konstruktiven Kritik im Feld und während der Ausgestaltung Arbeit.

Bei Herrn Prof. Dr. Dieter Wolf-Gladrow und Herrn Dr. Gernot Nehrke vom Alfred Wegener Institut für Polar- und Meeresforschung bedanke ich mich für die fachliche Unterstützung und Diskussion im Bereich der Carbonatchemie und Mineralogie.

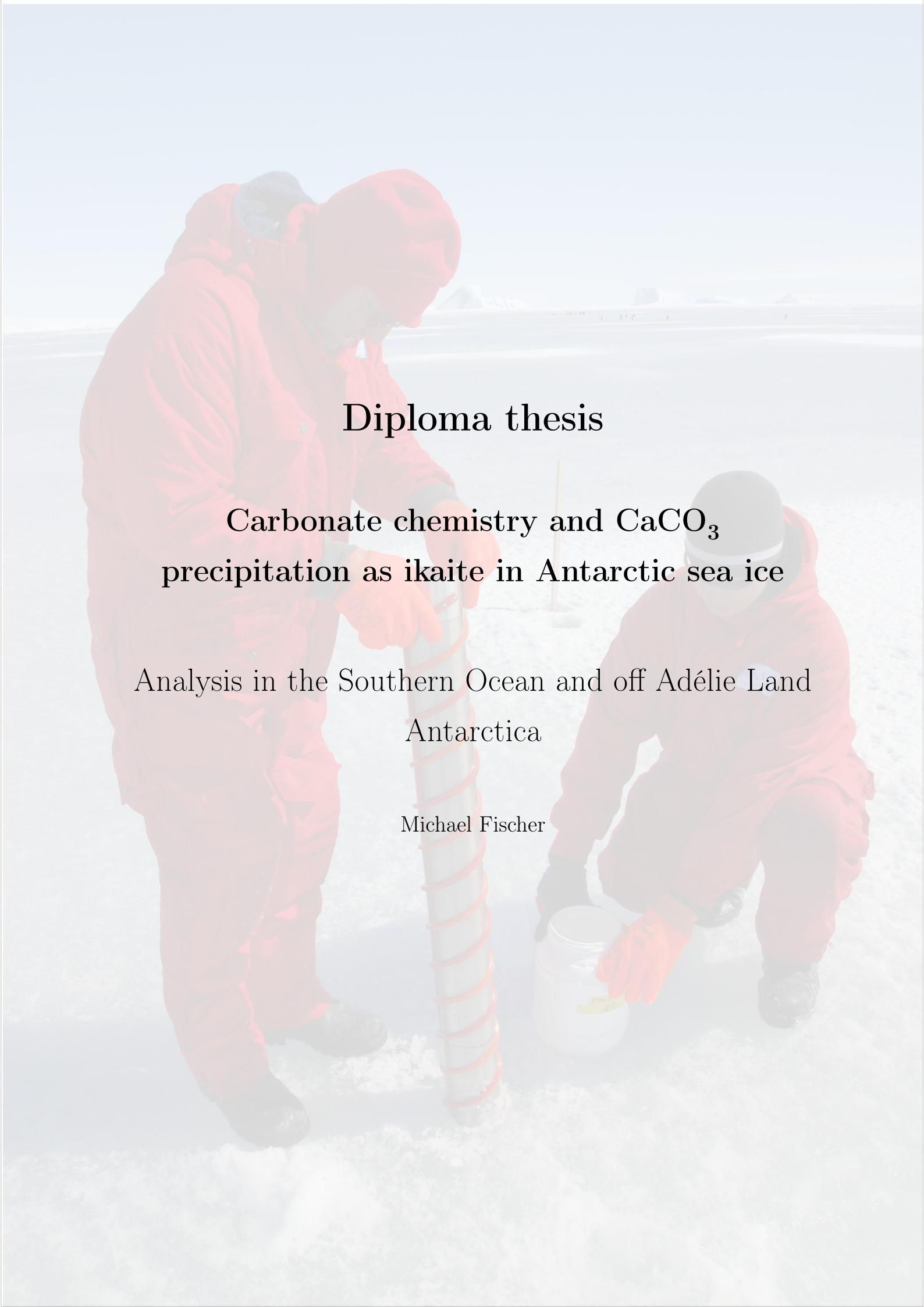
Herrn Dr. Andreas Krell danke ich für die Bereitstellung der Proben und Daten aus dem Südozean vom "Sea Ice Physics and Ecosystem eXperiment" (SIPEX).

Ich danke Ilsetraut Stölting vom Alfred Wegener Insitut für Polar- und Meeresforschung für die Unterstützung bei der Calcium-Messung.

Erika Allhusen danke ich für die logistische Unterstützung und die nützlichen Ratschläge vor und während der Expedition.

Gedankt sei hier auch der Schiffscrew der "L'Astrolabe", den Piloten der Australian Antarctic Division und allen Mitarbeitern der Forschungsstation Dumont d'Urville, die logistisch dazu beigetragen haben diese Forschungsarbeit zu ermöglichen.

Vor allem aber möchte ich mich bedanken bei meiner Familie und meinen Freunden, die hier nicht namentlich erwähnt werden, ohne deren Unterstützung diese Arbeit nie hätte entstehen können.



Diploma thesis

Carbonate chemistry and CaCO_3
precipitation as ikaite in Antarctic sea ice

Analysis in the Southern Ocean and off Adélie Land
Antarctica

Michael Fischer

Summary

This study analyses the carbonate chemistry and the precipitation of CaCO_3 as ikaite in Antarctic sea ice. Based upon these findings this study provides data on the geochemical composition of sea ice brine, while at the same time supplying modelers with the first data on the temporal and spatial occurrence of ikaite in Antarctic sea ice. The main study area is located off Adélie Land Antarctica at $\text{S}66^\circ 39' 13''$, $\text{E}140^\circ 00' 05''$. Additional samples are from the Southern Ocean between the latitude $\text{S}64^\circ 13'$ and $\text{S}65^\circ 36'$ and the longitude $\text{E}116^\circ 49'$ and $\text{E}128^\circ 04'$.

The determination of the geochemical composition of sea ice brine is based on measurements of pH , total alkalinity, and calculations using different sets of dissociation constants for carbonic acid. The results highlight difficulties of the used dissociation constants in hypersaline solutions at subzero temperatures. Differences of more than $18 \mu\text{mol/l}$ CO_2 in sea ice brine are likely to occur. Therefore it is not possible to use the findings in this study for CO_2 budget calculations in polar regions before a valid set of dissociation constants for carbonic acid in hypersaline solutions is provided.

The amount of ikaite was determined on different spatial scales in young (≈ 3 month), single year land-fast sea ice, and pack ice. Values up to 125 mg per liter melted sea ice were measured. The highest concentrations were found in single-year land-fast sea ice. A stratigraphical investigation displays an enrichment of the mineral within the top layer of the ice. However, in lower levels the concentration of ikaite drops to less than 1 mg/liter melted sea ice. The analysis of the temporal distribution of $\text{CaCO}_3 \cdot 6\text{H}_2\text{O}$ during austral spring demonstrate that the precipitation of CaCO_3 is a dynamic process affecting the carbon cycle. Unexpected findings of ikaite in Antarctic firn ice show that the mineral seems to be transported by aeolian processes from the sea ice to Antarctic inland.

Finally this study encourages a new determination of the dissociation constants of carbonic acid in hypersaline solution at subzero temperatures. Furthermore the requirement of a development of an appropriate method in the study of the biogeochemistry of sea ice brine is shown revealing the importance of small-scale processes. Resulting from the findings a further investigation of this boundary layer including the atmosphere and the underlying water column is proposed.

Keywords: ikaite, carbonate chemistry, sea ice, brine, carbon cycle, Adélie Land, Antarctica

Contents

Summary	I
Contents	II
List of figures	V
List of tables	VIII
1 Introduction	1
1.1 Issue	3
1.1.1 Placement of this study within the fields of research of the Alfred Wegener Institute for Polar and Marine Research	3
1.1.2 Goal of this study	4
1.1.3 Structure of this study	5
1.2 Conventions	5
2 Theory	6
2.1 Sea ice	6
2.2 Brine	7
2.3 Carbonate chemistry	9
2.3.1 The carbonate system	9
2.3.2 Equilibrium constants of the carbonate system in seawater	10
2.3.3 pH scales	16
2.3.4 Conversion between pH_{NBS} and pH_{SWS}	18
2.3.5 Total alkalinity and DIC	19
2.3.6 From TA and pH to CO_2 , HCO_3^- , CO_3^{2-} , and DIC	20
2.4 The polymorphs of $CaCO_3$	21
2.5 The mineral ikaite and its natural abundance	22
3 Methodology and study area	25
3.1 Study area	25
3.1.1 Climate	25
3.1.2 Sea ice cover	29

3.2	Methodology during the expedition in Terre Adélie	30
3.2.1	Sampling	30
3.2.2	Sackhole method	31
3.2.3	Brine salinity	31
3.2.4	Extraction of the CaCO_3 crystals from the ice core	34
3.2.5	pH in brine solution	34
3.2.6	Total alkalinity	36
3.2.7	Examining spatial distribution of ikaite with the help of Kriging	37
3.3	Methodology during the SIPEX expedition in the southern ocean . . .	37
3.4	ICP OES	38
3.5	Calculation of the concentrations in the carbonate system	39
4	Results	40
4.1	Meteorological data during the sampling period at Dumont d'Urville . .	40
4.2	Geochemistry of sea ice brine	42
4.2.1	Salinity and temperature of sea ice brine	42
4.2.2	pH values in the brine solution	43
4.2.3	Total Alkalinity	46
4.2.4	Concentration of the species in the carbonate system in sea ice brine	46
4.3	Distribution of ikaite	52
4.3.1	Total amount of ikaite in sea ice	52
4.3.2	Stratigraphic distribution of ikaite in land-fast ice off Adélie Land on the scale 0.1 – 1 <i>m</i>	53
4.3.3	Stratigraphic distribution of ikaite in sea ice on the SIPEX cruise on the scale 0.1 – 1 <i>m</i>	55
4.3.4	Stratigraphic distribution of ikaite in land-fast ice off Adélie Land on the scale ≤ 10 <i>cm</i>	61
4.3.5	Temporal distribution of ikaite in land-fast ice off Adélie Land .	61
4.3.6	Spatial distribution of ikaite	63
4.3.7	Additional measurements of ikaite	64
4.3.8	Ikaite in continental firn ice	65
5	Discussion and conclusion	66
5.1	Discussion of methodology	66
5.1.1	Sampling techniques	66
5.1.2	Measured chemical values	67
5.2	Discussion of results	68

<i>CONTENTS</i>	IV
5.2.1 Species in the carbonate system	68
5.2.2 Distribution of ikaite	72
5.2.3 Ikaite in firn ice	74
5.2.4 Spatial distribution	74
5.2.5 Significance for the CO ₂ cycle in polar regions	74
5.3 Conclusion	76
Bibliography	78
A Meteorological data	86
B Data from the sampling site off Adélie Land	89
B.1 Air temperature, salinity and temperature of sea ice brine	89
B.2 Calculated concentration of H ⁺ _{sws}	90
B.3 Total alkalinity	91
C Dissociation constants	93
D Amount of the mineral ikaite in sea ice	96
E SIPEX data	103

List of Figures

2.1	Phase diagram of sea ice. From Assur (1958)	8
2.2	pK_1 as function of salinity ($T = 271, 15K$)	13
2.3	pK_2 as function of salinity ($T = 271, 15K$)	14
2.4	Ion pair ($\text{Ca}_2^+\text{CO}_3^{2-}$) and hydration cage. Part of the crystal structure of ikaite. Ca (blue) is in dodecahedral coordination with O atoms (red) of the carbonate (black planar) and water molecules, while hydrogen bonds (dotted) exists between H-atoms (yellow) of the water molecules and the O-atoms of the carbonate ion.	22
2.5	Ikaite crystals from tufa columns collected in Ikka Fjord. A) Micrograph of frozen ikaite ($\sim 140^\circ\text{C}$) in the cryo-SEM. The photo illustrates non-recrystallized ikaite crystals with mucilaginous biofilm (b) embedding the crystals. These membranes are suggested to seal the ikaite crystals from the aggressive seawater environment, where ikaite is strongly undersaturated. Photo by O.B. Lyshede. B) Micrograph of a freeze-dried crystal. Freeze drying results in recrystallization of ikaite to calcite but retains the morphology of the original crystals. Photo by B. Buchardt. (Buchardt et al., 2001)	23
2.6	Ikaite from Antarctic sea ice (Dieckmann, unpublished data)	24
3.1	Map Antarctic Ocean - Terre Adélie, Archipel de pointe géologie	26
3.2	Average maximum temperatures at Dumont d'Urville (1956 - 2002) Source: IPEV, Base Dumont d'Urville	27
3.3	Average duration of precipitation in hours at Dumont d'Urville (1956-2002) Source: IPEV, Base Dumont d'Urville	28
3.4	9 cm diameter corer (Photo: Camille Fresser)	30
3.5	Drilling a sackhole with an ice corer (Photo: Camille Fresser)	32
3.6	Schematic body of sea ice with typically winter temperatures and salinity profiles of first-year sea ice according to Eicken (2003).	32

3.7	A drilled ice core (a), leaving a sack hole (b) which is covered by a plastic lid while brine percolates from the surroundings into the sackhole (c). The ice core (d) contains CaCO_3 crystals and is stored in a clean plastic container for further processing. - Schematic figure. The texture does not necessarily represent the structure of the sea ice during this study. .	33
3.8	Photograph of ikaite crystals taken from a single bulk sea ice sample showing various crystal shapes and sizes: a) idiomorphic; and b) shape of brine pockets or channels (Dieckmann et al., 2008).	35
4.1	Meteorological data at Dumont d'Urville, Ile des Petrels, Terre Adélie - Antarctica ($\text{S}66^{\circ}39.5'$ / $\text{E}140^{\circ}00.3'$, 41m a.s.l.) during the sampling period focusing on temperature, global radiation, wind speed, and cloudiness	41
4.2	Relation of salinity and temperature in sea ice brine	42
4.3	Salinity and temperature of the brine during the sampling period . . .	43
4.4	Concentration of H^+_{SWS}	45
4.5	Total alkalinity in $\mu\text{mol}/\text{kg}$	45
4.6	Concentration of the species of the carbonate system calculated with the dissociation constants of Dickson and Millero (1987)	47
4.7	Concentration of the species of the carbonate system calculated with the dissociation constants of Millero et al. (2006)	51
4.8	Ice core ROV3, $T_{\text{air}} = -4.8^{\circ}\text{C}$, land-fast ice	53
4.9	Ice core ROV4, $T_{\text{air}} = -3.2^{\circ}\text{C}$, land-fast ice	54
4.10	Ice core ROV6, $T_{\text{air}} = -3.1^{\circ}\text{C}$, land-fast ice	54
4.11	Ice core ROV7, $T_{\text{air}} = -1.9^{\circ}\text{C}$, land fast ice	54
4.12	Ice core ROV9, $T_{\text{air}} = 0.1^{\circ}\text{C}$, land-fast ice	55
4.13	Ice core ROV13, $T_{\text{air}} = -2.3^{\circ}\text{C}$, land-fast ice	55
4.14	SIPEX ice core 1 at $\text{S}64^{\circ}13.773$ $\text{E}127^{\circ}57.132$, $T_{\text{air}} = -15.6^{\circ}\text{C}$, total ice thickness: 51 cm	56
4.15	SIPEX ice core 2 at $\text{S}64^{\circ}29.42$ $\text{E}128^{\circ}03.29$, $T_{\text{air}} = -18.6^{\circ}\text{C}$, total ice thickness: 98 cm	56
4.16	SIPEX ice core 3 at $\text{S}64^{\circ}23.390$ $\text{E}127^{\circ}11.293$, $T_{\text{air}} = -20.1^{\circ}\text{C}$, total ice thickness: 49 cm	57
4.17	SIPEX ice core 4, position = N/A, $T_{\text{air}} = \text{N/A}$	57
4.18	SIPEX ice core 5 at $\text{S}65^{\circ}31.465$ $\text{E}124^{\circ}45.121$, $T_{\text{air}} = -18^{\circ}\text{C}$, total ice thickness: 85 cm, more or less fast ice station between grounded icebergs	57
4.19	SIPEX ice core 6 at $\text{S}65^{\circ}35.304$ $\text{E}122^{\circ}35.043$, $T_{\text{air}} = -11.7^{\circ}\text{C}$, total ice thickness: 81 cm, heavily rafted floes, very fragile skeletal layer at bottom	58

4.20	SIPEX ice core 7 at S65°33.492 E121°31.640, $T_{air} = -12.3^{\circ}\text{C}$, total ice thickness: 53 cm	58
4.21	SIPEX ice core 8 at S65°33.281 E118°52.480, $T_{air} = -7^{\circ}\text{C}$, total ice thickness: 37 cm	58
4.22	SIPEX ice core 9 at S65°20.612 E118°33.809, $T_{air} = -11.1^{\circ}\text{C}$, total ice thickness: 98 cm, region of heavily rafted and deformed ice	59
4.23	SIPEX ice core 10 at S64°56.549 E119°07.976, $T_{air} = -14.8^{\circ}\text{C}$, total ice thickness: 133 cm, coring site on an adjacent rafted area, negative freeboard	59
4.24	SIPEX ice core 11 at S65°01.496 E117°42.015, $T_{air} = -7.3^{\circ}\text{C}$, total ice thickness: 101 cm, rafted floe, ice surface very rough	59
4.25	SIPEX ice core 12, $T_{air} = -6.9^{\circ}\text{C}$, total ice thickness: 187 cm, close to station 11 (1.5 nm)	60
4.26	SIPEX ice core 13 at S64°44.436 E116°49.274, $T_{air} = -7.8^{\circ}\text{C}$, total ice thickness: 78 cm, rafted floes	60
4.27	SIPEX ice core 14 at S64°18.483 E116°49.594, $T_{air} = -10^{\circ}\text{C}$, total ice thickness: 64 cm	60
4.28	Ikaite on the pico scale a) ROV7 with snow on top, b) ROV7 without snow on top	62
4.29	Ikaite on the pico scale a) ROV6 sample from young ice (≤ 3 month), and b) ROV15 sample from single year ice but older than the sea ice from the stations ROV3 to ROV13	62
4.30	Temporal distribution of ikaite during Austral spring - sum parameter from sack hole ice cores	63
4.31	Contour map of the distribution of ikaite in the first 10 cm of land-fast ice in an area of 20m ² , amount of ikaite in mg/liter melted sea ice . . .	64
4.32	Contour map of sea ice thickness of a 20m ² , sea ice thickness in cm . .	65
5.1	Comparison of the calculated concentrations of the species in the carbonate system using the dissociation constants of Dickson and Millero (1987) and Millero et al. (2006)	69

List of Tables

2.1	Summary of pH scale and media used by various workers in order to determine the dissociation constants of carbonic acid in seawater	12
2.2	The pH scales and the differences between them (Zeebe and Wolf-Gladrow, 2001)	17
2.3	The six variables of the CO ₃ -system (Zeebe and Wolf-Gladrow, 2001) .	20
3.1	Ice thickness of land fast ice at the beginning of austral spring near Dumont d'Urville on 11/07/2007	29
4.1	Calculated total hydrogen ion activity coefficient as function of temperature and salinity	43
4.2	Calculated concentrations of the species in the carbonate system in sea ice brine, using pK_1 and pK_2 according to Dickson (1987)	48
4.3	Calculated concentrations of the species in the carbonate system in sea ice brine, using pK_1 and pK_2 according to Millero (2006)	49
5.1	Amount of ikaite in selected types of sea ice	75
A.1	Meteorological data during the sampling period	86
B.1	Salinity and temperature of sea ice brine and air temperature	89
B.2	Calculated concentration of H ⁺ _{SWs} using f_H from section 4.2.2	90
B.3	Total alkalinity in $\mu\text{mol/l}$	91
C.1	pK_1 calculated at different salinities using the equations of different authors (see section 2.3.2)	93
C.2	pK_2 calculated at different salinities using the equations of different authors (see section 2.3.2)	94
D.1	Quantity of ikaite in sea ice in the Southern Ocean	96
E.1	SIPEX data	103

Chapter 1

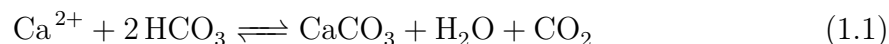
Introduction

When astronauts observed our planet from outer space, they called it the 'blue planet'. About 70% of the earth's surface is covered by water. Hence, our planet should be called 'water' instead of earth. While there is a huge knowledge about terrestrial geoprocesses, little is known about our oceans. A common saying among scientists states that we know more about the moon than about our oceans.

Large parts of the oceans belong to the polar regions underlying the annual growth and decay of sea ice. During the last decades, enormous efforts have been undertaken to study this special biome. Sea ice research spans many modern scientific disciplines including, among others, geophysics, glaciology, geology, chemistry, biogeochemistry and numerous branches of biology (Dieckmann and Hellmer, 2003). Sea ice is a complex substratum and environment which covers over 10% of the world's oceans at its maximum extent. This has a major impact on the gas exchange between atmosphere and ocean while at the same time biogeochemical processes, which occur within the sea ice, affect diffusion and flux to both atmosphere and ocean. However, little is known as yet about these processes and their effect on e.g. the carbon cycle.

During sea ice formation, the dissolved salts in the parent seawater mass are quantitatively expelled from the ice crystal matrix and become concentrated in the residual brine. The dissolved salts are trapped amongst the ice crystals, raising the ionic strength (salinity) of the brine. Due to gravity drainage, a large part of the hyper-saline brine escapes from the growing ice column into the underlying oceanic water column, with the remaining brine residing in pockets and channels within the sea ice (Eicken, 2003). This hyper-saline solution undergoes substantial changes with respect to mineral-liquid thermodynamic equilibria which are influenced by salinity and temperature of the sea ice system (Dieckmann et al., 2008). On the basis of these thermodynamic equilibria, the precipitation of CaCO_3 is expected under conditions of natural sea ice formation (Gitterman, 1937; Anderson and Jones, 1985; Marion, 2001,

cited in Papadimitriou et al. (2004)) and is proposed for more than 50 years (Assur, 1958). The precipitation of CaCO_3 is described by the chemical equation:



Though the precipitation of calcium carbonate was predicted for a long time, no one has presented a physico-chemical support for this idea (Marion, 2001). Evidence has only been indirect (Killawee et al., 1998; Papadimitriou et al., 2004; Tison et al., 2002, cited in Dieckmann et al. (2008)). Dieckmann et al. (2008) were the first to find calcium carbonate within Antarctic sea ice. They report the discovery of hydrous calcium carbonate as ikaite crystals from the Weddell Sea and off Adélie Land. "The discovery of $\text{CaCO}_3 \cdot 6\text{H}_2\text{O}$ crystals in natural sea ice provides the necessary evidence for the evaluation of previous assumptions and lays the foundation for further studies to help elucidate the role of ikaite in the carbon cycle of the seasonally sea ice covered regions" (Dieckmann et al., 2008).

The mineral is rendered a major and hitherto overlooked component of the carbon cycle in the seasonal ice zone of the polar oceans and that it is a faithful recorder of key components of the internal sea ice physical-chemical composition and processes with far reaching implications (Kennedy and Thomas, personal commun.).

Rysgaard et al. (2007) show that brine rejection from sea ice increases the density in the underlying water column and thereby contributes to the formation of deep and intermediate water masses. Together with brine DIC is rejected from growing sea ice to the underlying water column. They ascribe the high $p\text{CO}_2$ levels found below sea ice to possible calcium carbonate precipitation. This sea ice-driven carbon pump affects the partial pressure of CO_2 in surface water significantly in polar seas and potentially sequesters large amounts of CO_2 to the deep ocean. However, they encourage an improved understanding of the process described above. Furthermore they bewail a missing of biogeochemical studies on sea ice in terms of scaling and the range of parameters that can be reliably measured. "In particular, an increased effort into understanding physical chemistry at low temperatures is required as are seasonal studies of comprehensive suites of biogeochemical parameters in both seasonal and multi-year sea ice" (Rysgaard et al., 2007, p. 6). Also Delille et al. (2007, p. 1368) assert that "precipitation of carbonate minerals within sea ice could drive significant CO_2 uptake, but such a phenomenon remains to be investigated and has not been systematically observed."

Besides its function as component in the carbon cycle, the mineral is rendered a key role in tropospheric ozone depletion events (ODEs) at high latitudes (Sander et al., 2006). They simulated the chemistry occurring in polar regions over recently formed

sea ice and relate the ODE to the transformation of inert sea-salt bromide to reactive bromine monoxide (BrO) when precipitation of calcium carbonate from freezing sea water is taken into account. Additionally, the recent discovery of ikaite in firn ice of the Antarctic continent, which appears to be derived from sea ice 300 km away, may have implications as a sea ice proxy (Sala et al., 2008).

Resulting from these findings, the goal of this study is a systematical analysis of geochemical parameters in sea ice focusing on carbonate chemistry on a temporal scale. As Dieckmann et al. (2008) provide only sparse data on the quantity of precipitated CaCO_3 the amount of precipitated mineral will additionally be investigated on a temporal and spatial scale.

1.1 Issue

1.1.1 Placement of this study within the fields of research of the Alfred Wegener Institute for Polar and Marine Research

This study is integrated in the research field "Earth and Environment" at the Helmholtz Association, which focuses on the understanding of the fundamental functions of System Earth. The aim is to describe the complex changes to the earth and the environment as precisely as possible. The "grand challenges" facing the "Earth and Environment" research field are tackled within four programmes. One of these programmes is the new research programme PACES which stands for "Programme Marine, Coastal and Polar Systems: Polar Regions and Coasts in a changing Earth System", which is coordinated by the Alfred Wegener Institute for Polar and Marine Research Bremerhaven (AWI).

This programme aims at identifying the role of processes at high latitudes on past, current and future changes of the earth system. The Polar Regions play a special role within the earth system. The systems therein are linked by a large number of processes and interdependencies. Each, however, poses its own very special challenge, emanating from its unique environment and role within the Earth System, which needs to be met individually. Therefore, this study is integrated in the sub-project WP 1.3 (A Bi-Polar Perspective of Sea Ice - Atmosphere - Ocean - Ecosystem Interactions) within topic 1 ("The changing Arctic and Antarctic").

This sub-project focuses on the investigation of the interaction processes between sea ice, atmosphere, and ocean in order to help to understand the changes in Antarctic and Arctic sea ice conditions as well as their impact on ecosystems and food webs. Consequently, the effects of changing sea ice conditions on the sea ice ecosystem with

emphasis on biogeochemistry, growth and production of sea ice biota, and associated food web will be investigated as well as species diversity. The functioning of the sea ice ecosystem is inextricably linked to the freeze and melt cycle, and to physical and geochemical features such as ice texture, snow cover, temperature, and brine composition. These factors affect the species diversity, growth and life cycles of sea ice biota, as well as those of associated organisms such as krill, copepods, and amphipods.

In the scope of this research, the present study investigates the geochemical feature of brine composition. It focuses on carbonate chemistry since this is directly linked to the CO_2 cycle (Rysgaard et al., 2007). The production of carbonate minerals in sea ice represents a component of the polar carbon cycle which so far is still not quantified. Key aspects of the dynamics of this mineral need to be studied before a true appreciation of its role can be assessed. Therefore, this study will be the first which provides data on a temporal scale both for carbonate chemistry in sea ice brine and precipitation of calcium carbonate. Consequently, this study will lead to a better understanding of the chemical constraints within sea ice affecting the growth and the production of sea ice biota. Furthermore, the study provides data which are necessary for further research on ocean acidification, carbon cycling, climate modeling, and an enhanced Earth System Model (ESM). This new ESM will be achieved within topic 4 (Synthesis) of the research programme PACES, since present ESMs are unable to model the polar regions with the precision required for qualified predictions.

1.1.2 Goal of this study

As described above the present study investigates the carbonate chemistry and the occurrence of calcium carbonate within Antarctic sea ice during austral spring. These aspects will be investigated in view of the following objectives:

- To investigate the carbonate chemistry within brine solution on a temporal scale and to analyze uncertainties in CO_2 calculations in highly saline solutions.
- To determine the quantity of $\text{CaCO}_3 \cdot 6\text{H}_2\text{O}$ in Antarctic sea ice
- To investigate possible temporal fluctuations of the quantity of precipitated calcium carbonate during austral spring
- To investigate the small and mesoscale distribution of the mineral within the sea ice

The resulting data will provide the required information on the geochemical composition of sea ice brine, and at the same time provide modelers with the first values

on the temporal and spatial occurrence of ikaite in Antarctic sea ice. Based upon these findings, this study will give an overview on the carbonate chemistry in brine solution and the distribution of CaCO_3 at the same temporal scale, and also identifies gaps in the research on geochemical features of sea ice. This will enable future researchers to plan their experimental set ups, and in this way it will help to improve the understanding of the carbonate chemistry of sea ice in the polar and global carbon cycle.

1.1.3 Structure of this study

After an introduction to the topic, the placement of this study within the research of the Alfred Wegener Institute, and the illustration of the objectives in chapter 1, a theoretical overview on sea ice and brine geochemistry will be given in chapter 2. This is followed by the description of the methodology used in this study and the presentation of the study area (Chapter 3). In chapter 4 the results will be visualized. The complete data sets and tables can be found in the appendix on page 86. The results will be divided into the geochemistry of sea ice and the distribution of ikaite within sea ice. Stratigraphic distribution of ikaite in pack ice from the Southern Ocean, as well as in land-fast ice off Adélie Land will be shown. The distribution of ikaite in land-fast ice is presented on different spatial scales. The chapter will be completed with an overview on the temporal and spatial distribution of ikaite in sea ice off Adélie Land and additional measurements on sea and continental firn ice. A discussion of the methodology and the results follows in chapter 5. While the conclusion completes the study.

1.2 Conventions

In this study, the abbreviation DIC (dissolved inorganic carbon) is used as synonym for the total dissolved inorganic carbon ascribed in some studies as C_T or TCO_2 . For total alkalinity, the abbreviation TA is used. In the literature, also A_T is found. However, according to Wolf-Gladrow et al. (2007) the present study determines the practical alkalinity (PA). The abbreviation TA will be used as a synonym for PA in this study. So far there is no standard spatial scale obtainable from the literature. The terms pico-scale and nano-scale are used according to Neumeister (2007). Pico refers to the scale smaller than $0.1m$, and nano to the scale between 0.1 and $1m$.

Chapter 2

Theory

2.1 Sea ice

At its maximum extent, sea ice covers about 7 per cent of the earth's surface (Comiso, 2003), and is therefore one of the largest biomes on earth (Dieckmann and Hellmer, 2003). Sea ice is a thin boundary layer between ocean and atmosphere, which influences and is influenced by the fluxes of heat, moisture and momentum across the ocean-atmosphere interface. This layer has become one of the most important components in the research on the past, present, and future climate, since it has been so far a widely overlooked component in the carbon cycle in polar regions.

Sea ice is different to lake ice. While fresh water usually has a freezing point of 0°C , sea water has its freezing point at -1.86°C , with a salinity of 34. Lake ice is very transparent, while sea ice is opaque due to a network of brine inclusions. Both the freezing point and the grade of transparency originate from the salinity of the natural water from which the different types of ice arise. During sea ice formation, the dissolved salts in the parent seawater mass are quantitatively expelled from the ice crystal matrix and become concentrated in the residual brine which is trapped amongst the ice crystals in small pockets and channels. This results in a milky appearance of the sea ice and a reflection of the incoming rays which are scattered back to a large extent.

Whenever the ocean is supercooled, sea ice begins to form. There are two different ways of sea ice formation. The grease ice pathway occurs under calm conditions and mostly in the Arctic. In the Antarctic there is a predominance of the pancake cycle which occurs under rough conditions. Both cycles start with frazil ice which forms due to thermohaline mixing and wind stress. Frazil ice consists of ice crystals in the form of needles, spicules, or platelets which are in suspension until a surface layer of ice slush builds up. In quiescent growth, this ice is consolidated to so called "grease ice". Layer upon layer is added forming nilas ice which is about 5 - 10 cm thick. The nilas ice

might be rafted and develop so called finger ice. With increasing thickness the ice is called congelation ice and finally forms a blank sheet of ice. As already mentioned, in the Antarctic pancake ice is the predominant type of ice due to the rougher conditions. Pancake ice forms when frazil ice consolidates and then accretes into larger patches of ice. By rubbing against each other pancakes begin to evolve. Decimeter-sized floes with raised edges develop. These floes congeal to larger units, developing large ice floes or continuous sheets of ice, respectively (Eicken, 2003).

The typical stratigraphy of sea ice consists of granular ice at the top ("a few tens of centimeters at most in the Arctic, but substantially more in other, more dynamic environments such as the Antarctic" (Eicken, 2003)) followed by a transition zone of granular and columnar ice, and finally pure columnar ice. Under rough conditions floes might slide over each other, resulting in a recurrence stratigraphy. This phenomenon can be seen regularly in pack ice where the rapid thickening of sea ice due to deformation of the sea ice cover through rafting and ridging can be observed. On a larger scale there is another form of sea ice besides pack ice. During cold periods such as winter, late autumn, or early spring, land-fast-ice can be found in the polar regions, but occurs more often in the Antarctic due to the Antarctic continent (Thomas and Dieckmann, 2003).

There are huge differences between Arctic and Antarctic sea ice. While the maximum extent in the Antarctic is 20 per cent higher than in the Arctic, the minimum extent is the other way around. Arctic sea ice extends the sea ice cover in the Antarctic at the minimum extent by a factor of roughly 2.6 (Comiso, 2003). The average thickness of sea ice amounts to about 0.5 to 0.6m in the Antarctic and several meters in the Arctic (Wadhams, 2000, cited in Dieckmann and Hellmer (2003)), although multiyear ice with more than 2m can be found along the southern continent. Land-fast ice accounts for 5 per cent of the sea ice cover in the Antarctic (Fedotov et al., 1998, cited in Dieckmann and Hellmer (2003)). Another important factor is the residence time of sea ice according to a specific time scale. In the Antarctic this time is significantly shorter (1-2 years) than in the Arctic (5-7 years) (Dieckmann and Hellmer, 2003).

2.2 Brine

Brine is the highly concentrated sea water retained within the sea ice body. The salt is expelled from the ice matrix during sea ice formation and is not incorporated into the ice matrix. Therefore, a decreasing temperature steadily raises the ionic strength of the remaining brine. Salinity and temperature are correlated. The salinity rises and can reach more than 100 psu at subzero temperatures. For example, in a closed

system which originates from sea water with a salinity of 34 psu, the brine salinity attains 87 psu at a temperature of -5°C (Thomas and Papadimitriou, 2003). Brine consists of different ions such as Na^+ , Cl^- , SO_4^{2-} , H^+ , OH^- , K^+ , Ca_2^+ , Mg_2^+ , HCO_3^- , and CO_3^{2-} . The increasing concentration of the ions in brine solution leads to supersaturation with respect to different ions, and this leads to the precipitation of different salts. Anderson and Jones (1985) state that calcium carbonate is the first salt which precipitates just below freezing point. Sodium sulphate precipitates at -8.2°C , calcium sulphate at -10°C , and sodium chloride at -22°C . In addition they assume, but have not proven, that solid salts that form in sea ice are hydrates, i.e. $\text{CaCO}_3 \cdot 6\text{H}_2\text{O}$, $\text{Na}_2\text{SO}_4 \cdot 10\text{H}_2\text{O}$, and $\text{NaCl} \cdot 2\text{H}_2\text{O}$. Assur (1958) proposed a phase diagram for standard sea ice (Figure 2.1), which includes the already mentioned salts but also $\text{MgCl}_2 \cdot 8\text{H}_2\text{O}$, KCl , $\text{MgCl}_2 \cdot 12\text{H}_2\text{O}$, and $\text{CaCl}_2 \cdot 6\text{H}_2\text{O}$. Weeks and Ackley (1986) predict that the latter would precipitate below -18°C . More important is the precipitation of CaCO_3 since this is directly related to the CO_2 cycle. Little is known about its distribution, the exact processes leading to its precipitation, and the fate of the crystals (Thomas and Papadimitriou, 2003; Papadimitriou et al., 2004; Dieckmann et al., 2008).

Assur (1958) was the first to predict CaCO_3 in the form of ikaite ($\text{CaCO}_3 \cdot 6\text{H}_2\text{O}$) but

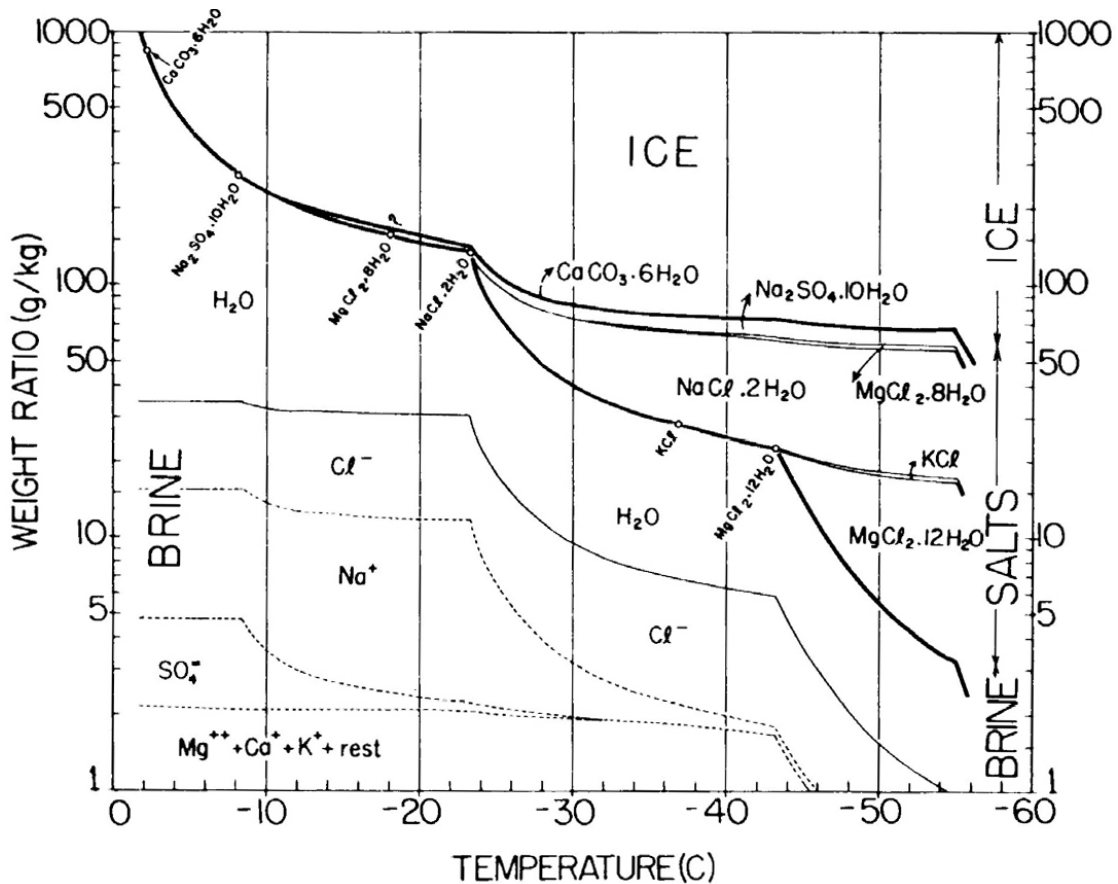


Figure 2.1: Phase diagram of sea ice. From Assur (1958)

evidence of its formation in sea ice has only been indirectly obtained (Killawee et al., 1998; Tison et al., 2002; Papadimitriou et al., 2004, cited in Dieckmann et al. (2008)). Although Marion (2001) proposed that the CaCO_3 mineral that precipitates during seawater freezing is probably calcite and not ikaite, Dieckmann et al. (2008) were the first to confirm ikaite in sea ice. Since calcium carbonate is assumed to play a major role within the CO_2 cycle in polar regions and has further implications (Jones and Coote, 1981; Sander et al., 2006; Rysgaard et al., 2007; Morin et al., 2008; Sala et al., 2008), this study focuses on the precipitation of CaCO_3 and the carbonate chemistry within sea ice. In the next section, the carbonate chemistry in highly saline solution will be described in more detail.

2.3 Carbonate chemistry

After nitrogen and oxygen, carbon dioxide is one of the most abundant gases in the earth's atmosphere. Therefore, it is the second most important greenhouse gas besides water vapour. Unlike oxygen and nitrogen, most of the carbon dioxide on earth is dissolved in sea water (Zeebe and Wolf-Gladrow, 2001). The oceans contain sixty times more carbon than the atmosphere and the carbonate chemistry therein determines the partial pressure of CO_2 ($p\text{CO}_2$) of the atmosphere on long time scales (Nehrke, 2007).

2.3.1 The carbonate system

In order to understand and to calculate the carbonate chemistry within saline solutions, it is necessary to identify the equilibria and in this was the dissociation constants that control the carbonate system. This system contains only a few essential components, CO_2 , HCO_3^- , CO_3^{2-} , H^+ , and OH^- . If one wants to be more precise H_2CO_3 (true carbonic acid) has also to be taken into account. However, the concentration of H_2CO_3 is much smaller than the one of $\text{CO}_2(\text{aq})$ ($\lesssim 0.3\%$) and thus, in the literature, the two electrically neutral forms of H_2CO_3 and CO_2 are denoted mostly as CO_2 (Zeebe and Wolf-Gladrow, 2001). Sometimes also H_2CO_3^* or $\text{CO}_{2\text{T}}$ is used. In this thesis the notation CO_2 will be used:

$$[\text{CO}_2] = [\text{CO}_2(\text{aq})] + [\text{H}_2\text{CO}_3] \quad (2.1)$$

¹It is safe to say that free protons do not exist in any significant amount in aqueous solutions. Rather the proton is bonded to a water molecule thus forming an H_3O^+ ion; this in turn is hydrogen bonded to three other water molecules to form an H_9O_4^+ ." (Dickson, 1984, p. 2299) "Thus, the symbol ' H^+ ' represents hydrate complexes rather than the concentration of free hydrogen ions [...] it is however convenient to refer to $[\text{H}^+]$ as the hydrogen ion concentration." (Zeebe and Wolf-Gladrow, 2001, p. 54)

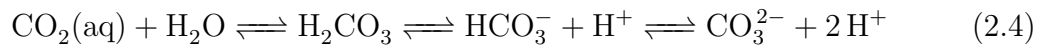
With the solubility coefficient of CO_2 in seawater, K_0 , the concentration of CO_2 is given by Henry's law, when carbon dioxide gas dissolves in water (Nehrke, 2007; Zeebe and Wolf-Gladrow, 2001).



By focusing on the equilibrium and not on reaction pathways, the hydroxylation



can be neglected and the relation of the carbonate species in water can be shown as the following equilibrium (Zeebe and Wolf-Gladrow, 2001):



The hydration of CO_2 is described by the first dissociation constant (K_1) and the following dissociation of bicarbonate is given by the second dissociation constant (K_2) of carbonic acid. Related to concentrations (see equations 2.8 and 2.11 on page 15), the stoichiometric equilibrium constants K_1 and K_2 are used to describe the carbonate system in water.



Since this system is an aqueous one, the dissociation of water has also to be taken into account (Nehrke, 2007).



2.3.2 Equilibrium constants of the carbonate system in seawater

Like other authors (Millero, 1979; Dickson and Millero, 1987; Goyet and Poisson, 1989; Dickson, 1990; Millero et al., 1993; Roy et al., 1993; DOE, 1994; Lee et al., 2000; Lueker et al., 2000; Zeebe and Wolf-Gladrow, 2001; Mojica-Prieto and Millero, 2002; Millero et al., 2002, 2006) Wanninkhof et al. (1999, p.291) identify various independent determinations of the dissociation constants of carbonic acid and assert that "these results have been corrected, refit, and combined by others creating a virtual cottage industry of laboratory and field verification, and cross checks." Therefore, it is difficult to assess the proper constants that should be used for this special issue of determination of the carbonate system within hypersaline solutions. Dissociation constants for carbonic acid in sea water have been determined over the last seventy-six years. The first has been Buch et al. (1932), followed by Lyman (1956). Both were reviewed by

Mehrbach et al. (1973) and Hansson (1973a). Furthermore the latter have determined K_1 and K_2 again. While Hansson (1973a) used artificial seawater to determine the equilibrium constants for carbonic acid, Mehrbach et al. (1973) used natural seawater for their measurements. Another discrepancy are the pH scales used by different authors. Table 2.1 on the next page shows the used type of seawater and pH scales. Hansson (1973b) has been the first introducing a new pH scale in marine carbonate chemistry. Since Hansson (1973a) and Mehrbach et al. (1973) used different pH scales, Dickson and Millero (1987) refitted both determinations of the dissociation constants to pH_{SW_S} (seawater scale) to allow a comparison between those sets of constants. In addition they proposed new equations for the corrected pK_1 and pK_2 . However, they do not clearly prefer a set of constants. The U.S. Department of Energy (DOE) recommended the dissociation constants based on Roy et al. (1993). Whereas Lee et al. (2000) and Lueker et al. (2000) come to the conclusion that the constants of Mehrbach et al. (1973) as refitted by Dickson and Millero (1987) do the best job. Also Zeebe and Wolf-Gladrow (2001) noted that Mehrbach constants do a good job in field studies as they have been determined in natural seawater. The latest work has been published by Millero et al. (2006) claiming their equations to be valid from $S = 0$ to 50 and $T = 0$ to 50°C for most estuarine and marine waters. It has to be pointed out, that their equations for determining pK_1 and pK_2 are based on 466 (for pK_1) and 458 (for pK_2) values, respectively. Earlier works from other authors base on much less samples and a smaller salinity range (see table 2.1 on the following page). Furthermore Millero et al. (2006) assume that seawater is diluted with pure water. All determinations of the first and the second dissociation constant mentioned above, have been done in natural or artificial seawater, respectively. However, there is no work at all where those constants have been determined in hyper saline solutions ($35 \leq S \leq 120$) at subzero temperatures. Only a validation of pK_1 and pK_2 at subzero temperatures has been done (Marion, 2001; Millero et al., 2002, cited in Delille et al. (2007)). Thus, no validation exists for high salinities. If one calculates pK_1 and pK_2 at a given temperature as a function of salinity the values of the constants vary strongly among different authors. The values have been plotted in figure 2.2 and 2.3 where the differences, especially for the constants of Millero et al. (2006), are clearly shown (corresponding equations are given in table 2.1). The values of pK_1 according to the equations of Hansson (1973a), Dickson and Millero (1987), Goyet and Poisson (1989), and Roy et al. (1993) are very similar. Whereas the values of Mehrbach et al. (1973) and Millero et al. (2006) differ considerable with increasing salinity.

Table 2.1: Summary of pH scale and media used by various workers in order to determine the dissociation constants of carbonic acid in seawater

Author	T(°C)	Salinity	pH scale	Media	pK_1	No.	pK_2	No.
Hansson (1973a) ^a	5 - 30	20 - 40	pH(T)*	ASW	5.8502	70	8.9419	70
Mehrbach et al. (1973) ^b	2 - 35	19 - 43	pH(NBS)	SW	6.00004	30	9.1141	33
Dickson and Millero (1987) ^c	2 - 35	0 - 40	pH(SWS)	SW	5.83723	30	8.9554	33
Goyet and Poisson (1989) ^d	-1 - 40	10 - 50	pH(SWS)	ASW	5.8487	93	8.9189	93
Roy et al. (1993) ^e	0 - 45	5 - 45	pH(SWS)	ASW	5.8473	56	8.9159	56
Mojica-Prieto and Millero (2002) ^f	5 - 45	12 - 45	pH(SWS)	SW	5.83584	59	8.9498	140
Millero et al. (2006) ^g	0 - 50	1 - 50	pH(SWS)	SW	5.84014	466	8.9636	458

where pH(NBS) = standard pH scale, pH(T) = total scale, pH(SWS) = the seawater scale, ASW = artificial seawater, SW = natural seawater

* Hansson (1973a) defined his pH scale as seawater scale. In this work his pH scale is described after Zeebe and Wolf-Gladrow (2001) as total scale as his medium did not contain fluoride ions and therefore the protonation of F^- is not taken into account.

$$^a pK_1 = 851.4/T + 3.237 - 0.0106S + 0.000105S^2; pK_2 = -3885.4/T + 125.844 - 18.141 \ln T - 0.0192S + 0.000132S^2$$

$$^b pK_1 = -13.7201 + 0.031334T + 3235.76/T + 1.300 \cdot 10^{-5} S \cdot T - 0.1032S^{0.5}; pK_2 = 5371.9645 + 1.671221T + 0.22913S + 18.3802 \log S - 128375.28/T - 2194.3055 \log T - 8.0944 \cdot 10^{-4} S \cdot T - 5617.11 \log S/T + 2.136S/T$$

$$^c pK_1 = 3670.7/T - 62.008 + 9.7944 \ln T - 0.0118S + 0.000116S^2; pK_2 = 1394.7/T + 4.777 - 0.0184S + 0.000118S^2$$

$$^d pK_1 = 807.18/T + 3.374 - 0.00175S \ln T + 0.000095S^2; pK_2 = 1486.6/T + 4.491 - 0.00412S \ln T + 0.000215S^2$$

$$^e pK_1 = 845/T + 3.248 - 0.0098S + 0.000087S^2; pK_2 = 1377.3/T + 4.824 - 0.0185S + 0.000122S^2$$

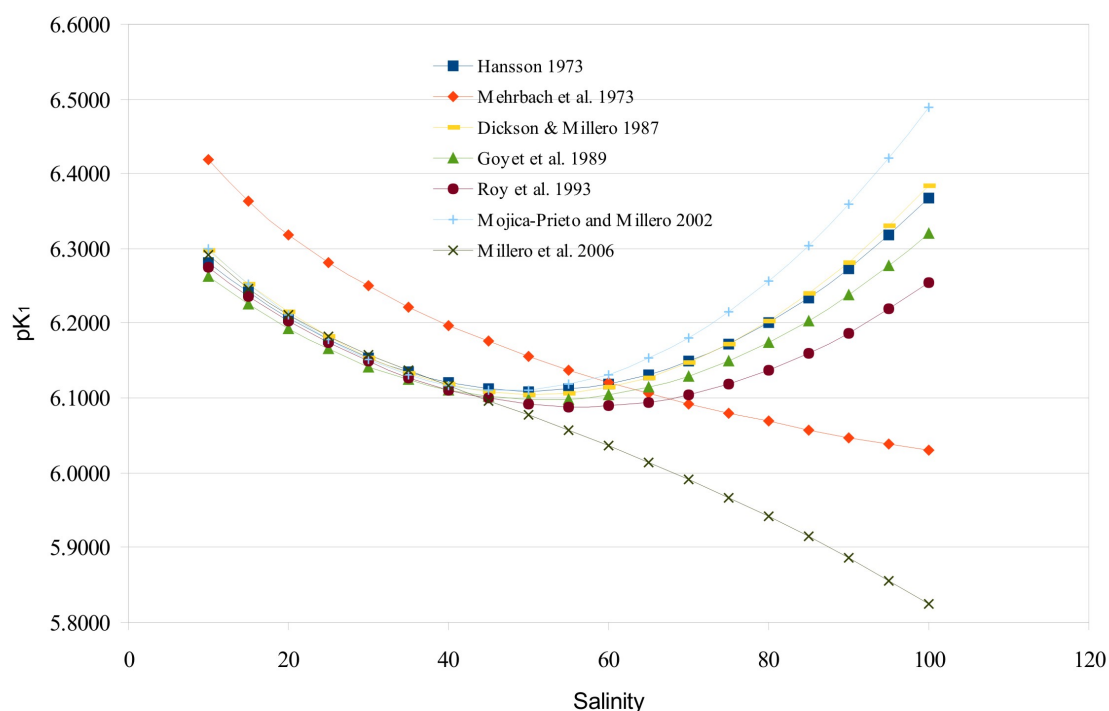
$$^f pK_1 = -43.6977 - 0.0129037S + 1.364 \cdot 10^{-4} S^2 + 2885.378/T + 7.045159 \ln T; pK_2 = -452.0940 + 13.142162S - 8.101 \cdot 10^{-4} S^2 + 21263.61/T + 68.483143 \ln T + (-581.4428S + 0.259601S^2)/T - 1.967035S \ln T$$

$$^g pK_1 = 13.4191S^{0.5} + 0.0331S - 5.33 \cdot 10^{-5} S^2 + (-530.123S^{0.5} - 6.103S)/T - 2.06950S(0.5) \ln T + (-126.34048 + 6320.813/T + 19.568224 \ln T); pK_2 = 21.0894S^{0.5} + 0.1248S - 3.687 \cdot 10^{-4} S^2 + (-772.483S^{0.5} - 20.051S)/T - 3.336S^{0.5} \ln T$$

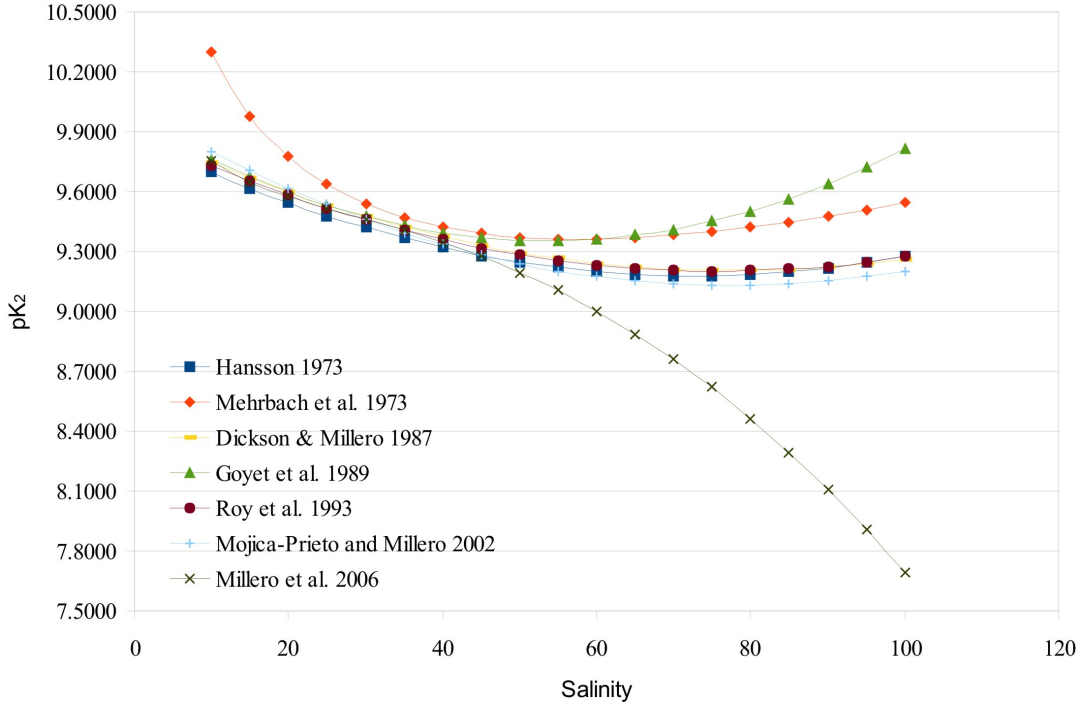
The same is noted for pK_2 , except for the values of Mehrbach et al. (1973) as they now draw near the majority. One might tend to ignore the set of constants of Millero et al. (2006) since they show a huge variation compared to the constants of all other authors. On the other hand the effect of salinity on the dissociation constants of carbonic acid are described in the literature as increase of the pK values if there is a decrease of salinity (Zeebe and Wolf-Gladrow, 2001). Regarding this statement, all other constants have to be used carefully in hyper saline solutions since their pK values reincrease at a salinity of about 50.

In the recent literature very few studies have been carried out on the geochemistry

Figure 2.2: pK_1 as function of salinity ($T = 271, 15K$)



of brine in sea ice. Anderson and Jones (1985) and Rysgaard et al. (2007) have done different measurements on bulk sea ice. Whereas Gleitz et al. (1995) followed by Delille et al. (2007) and Papadimitriou et al. (2007) have done direct measurements on brine in sea ice. To calculate the concentration of the different species in the carbonate system they used different sets of dissociation constants for carbonic acid. Gleitz et al. (1995) used a modified computer program developed by Campbell et al. (1993), where they applied pK_1 and pK_2 based on Roy et al. (1993). The constants based on Dickson and Millero (1987) were used by Delille et al. (2007), whereas Papadimitriou et al. (2007) used the most recent determination of pK_1 and pK_2 at this time from Mojica-Prieto and Millero (2002). Thus, there is no clear choice of the dissociation constants for carbonic acid in seawater for the investigation of geochemistry of sea ice. Based on

Figure 2.3: pK_2 as function of salinity ($T = 271, 15K$)

the recommendation of Lee et al. (2000), Lueker et al. (2000), and Zeebe and Wolf-Gladrow (2001), it has been decided to use the dissociation constants for carbonic acid in seawater from Dickson and Millero (1987) in this study. Since Delille et al. (2007) have carried out their study at the same location as this study, while using the dissociation constants of Dickson and Millero (1987), it is possible to compare the data obtained in those studies. Due to uncertainties in the literature in the choice of the proper equilibrium constants for carbonic acid when determining the carbonate chemistry in sea ice brine an additional set of constants should be used. Since Millero et al. (2006) based their determination of pK_1 and pK_2 on much more measurements than others and only their pK 's drop with an increase of salinity as described by Zeebe and Wolf-Gladrow (2001), this set of constants will be used as well. Therefore pK_1 and pK_2 are given by the following equations:

The equilibrium constant for equation 2.5

$$K_1 = [\text{H}^+][\text{HCO}_3^-]/[\text{CO}_2^*] \quad (2.8)$$

is given by Mehrbach et al. (1973) as refitted by Dickson and Millero (1987); $pH_{SW,S}$, $\text{mol}\cdot\text{kg}\cdot\text{soln}^{-1}$

$$pK_1 = 3670.7/T - 62.008 + 9.7944 \ln T - 0.0118S + 0.000116S^2 \quad (2.9)$$

Check value: $pK_1 = 5.83723$ at $S = 35$, $T = 298.15K$

and by Millero et al. (2006)

$$pK_1 = 13.4191S^{0.5} + 0.0331S - 5,33 \cdot 10^{-5}S^2 + (-530.123S^{0.5} - 6.103S)/T - 2.06950S^{0.5} \ln T + (-126.34048 + 6320.813/T + 19.568224 \ln T) \quad (2.10)$$

Check value: $pK_1 = 5.84014$ at $S = 35$, $T = 298.15\text{K}$

For equation 2.6 the equilibrium constant

$$K_2 = [\text{H}^+][\text{CO}_3^{2-}]/[\text{HCO}_3^-] \quad (2.11)$$

is given by Mehrbach et al. (1973) as refitted by Dickson and Millero (1987); $pH_{SW,S}$, $\text{mol}\cdot\text{kg}\cdot\text{soln}^{-1}$

$$pK_2 = 1394.7/T + 4.777 - 0.0184S + 0.000118S^2 \quad (2.12)$$

Check value: $pK_2 = 8.9554$ at $S = 35$, $T = 298.15\text{K}$

and by Millero et al. (2006)

$$pK_2 = 21.0894S^{0.5} + 0.1248S - 3.687 \cdot 10^{-4}S^2 + (-772.483S^{0.5} - 20.051S)/T - 3.336S^{0.5} \ln T \quad (2.13)$$

Check value: $pK_2 = 8.9636$ at $S = 35$, $T = 298.15\text{K}$

To calculate the concentration of CO_2 from TA and pH in the carbonate system in seawater according to the equations in section 2.3.6 there are another three essential equilibrium constants. These constant are K_0 (solubility coefficient of CO_2), K_B (dissociation constant of boric acid), and K_W (ion product of water). Additionally the total boron concentration (B_t) is needed.

The solubility coefficient of CO_2

$$K_0 = [\text{CO}_2^*]/f(\text{CO}_2) \quad (2.14)$$

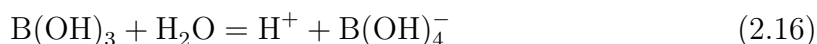
is given by the expression (DOE, 1994, and references therein)

$$\ln K_0 = 93.4517 \left(\frac{100}{T/K} \right) - 60.2409 + 23.3585 \ln \left(\frac{T/K}{100} \right) + S \left(0.023517 - 0.023656 \left(\frac{T/K}{100} \right) + 0.0047036 \left(\frac{T/K}{100} \right)^2 \right) \quad (2.15)$$

$k^\circ = 1 \text{ mol} \cdot \text{kg}\cdot\text{soln}^{-1}$

Check values: $\ln K_0 = -3.5617$ at $S = 35$ and $t = 25^\circ \text{C}$ (298.15K)

The dissociation of boric acid is described by



with the dissociation constant

$$K_B = [\text{H}^+][\text{B(OH)}_4^-]/[\text{B(OH)}_3] \quad (2.17)$$

Based on Dickson (1990) and recommend by DOE (1994) and Zeebe and Wolf-Gladrow (2001) the constant is given by the expression:

$$\begin{aligned} \ln K_B = & (-8966.90 - 2890.53S^{1/2} - 77.942S + 1.728S^{3/2} - 0.0996S^2) / T \\ & + 148.0248 + 137.1942S^{1/2} + 1.62142S \\ & - (24.4344 + 25.085S^{1/2} + 0.2474S) \ln T + 0.053105S^{1/2}T \end{aligned} \quad (2.18)$$

B_T is the total boron concentration and is related to salinity in seawater by:

$$B_T(\text{mol}(\text{kg} - \text{soln})^{-1}) = [\text{B(OH)}_3] + [\text{B(OH)}_4^-] \quad (2.19)$$

$$= 4.16 \cdot 10^{-4} \frac{S}{35} \quad (2.20)$$

(DOE, 1994)

Millero (1995) define the ion product of water K_W by

$$\begin{aligned} \ln K_W = & 148.9802 - 13847.26/T - 23.6521 \ln T \\ & + (118.67/T - 5977 + 1.0495 \ln T) S^{1/2} - 0.01615S \end{aligned} \quad (2.21)$$

2.3.3 pH scales

"The field of pH scales and the study of proton transfer reactions in sea water is one of the more confused areas of marine chemistry." (Dickson, 1984, p. 2299) Therefore this section gives a short overview over the pH scales used in oceanography. In the literature and as seen in section 2.3.2 different pH -scales are in use in marine chemistry: The NBS Scale, the $pH(\text{SWS})$ scale, the total scale and the free scale (Dickson, 1984; Wedborg et al., 1999; Zeebe and Wolf-Gladrow, 2001).

The common definition of pH (lat.: potentia hydrogenii) is the negative common logarithm of the concentration of hydrogen ions (Sørensen, 1909, cited in Zeebe and Wolf-Gladrow (2001)). This is a simple definition, but does not reflect the reality. As already mentioned in section 2.3.1 there are no free protons in any significant amount in aqueous solutions. Bonded to a water molecule the proton forms an H_3O^+ ion, which itself is

Table 2.2: The pH scales and the differences between them (Zeebe and Wolf-Gladrow, 2001)

pH scale	applicable in	reference state	difference to free scale*
pH_{NBS}	freshwater	pure water	
pH_F	seawater	artificial seawater	
pH_T	seawater	artificial seawater	≈ 0.11
pH_{SWS}	seawater	artificial seawater	≈ 0.12

* At $S = 35$, $T = 25^\circ\text{C}$

bonded to three other water molecules forming an H_9O_4^+ ion. However it is convenient and thermodynamically correct to refer to $[\text{H}^+]$ as the hydrogen ion concentration. In the traditional choice in solution chemistry the pH is defined from the activity of the hydrogen ion as

$$pH = -\log a_{\text{H}^+} \quad (2.22)$$

It has to be mentioned, that measuring pH as defined in equation 2.22 is not possible, as individual ion activities cannot be measured experimentally. Therefore and recommended by NBS ² (National Bureau of Standards) and IUPAC (International Union of Pure and Applied Chemistry) an operational definition of the pH scale has been introduced. This scale is referred in the literature as pH_{NBS} or NBS pH scale and is defined by a series of standard buffers whose values are close to the best estimates of $-\log a_{\text{H}^+}$ (Grasshoff et al., 2002).

When pH is measured in seawater the different ionic strengths have to be considered. Due to the differences in ionic strength (≈ 0.1 for NBS standard buffer solutions and ≈ 0.7 for seawater) when using NBS buffers in pH measurements in seawater an error larger than the desired accuracy of 0.01 - 0.001 pH units may occur (Wedborg et al., 1999, cited in Zeebe and Wolf-Gladrow (2001)). To improve pH measurements in a saline medium Hansson (1973b) introduced a new pH scale, called the 'total scale' ³ and therefore a new set of standard buffers were adopted. This new definition of the pH_T contains sulphate ions (see equation 2.25). Hansson (1973b) "proposed a fluoride-free synthetic seawater as the standard state, since fluoride is only a minor

²now NIST (National Institute of Standards and Technology)

³Hansson (1973a) defined his pH scale as seawater scale. In this work his pH scale is described after Zeebe and Wolf-Gladrow (2001) as total scale as his medium did not contain fluoride ions and therefore the protonation of F^- is not taken into account.

component of seawater.” (Wedborg et al., 1999, p. 112) However, in recent literature another pH scale is widely used, the seawater scale (pH_{SWs}). Suggested by Dickson and Riley (1979), Dickson (1984) and Dickson and Millero (1987) the protonation of F^- ions is also taken into account (see equation 2.26). As it can be seen in table 2.2 the difference between pH_T and pH_{SWs} is small, because the concentration of HF in seawater is small. For completeness the free scale (pH_F) has also to be mentioned. Conceptually this scale is the clearest using the concentration of free hydrogen ions. However, $[H^+]_F$ has to be calculated according to equation 2.23:

$$[H^+]_F = [H^+]_T - [HSO_4^-] \quad (2.23)$$

because only $[H^+]_T$ can be determined analytically. Therefore the concentration of HSO_4^- has to be determined which is not a simple task (Zeebe and Wolf-Gladrow, 2001).

$$pH_F = -\log [H^+]_F \quad (2.24)$$

$$pH_T = -\log ([H^+]_F + [HSO_4^-]) = -\log [H^+]_T \quad (2.25)$$

$$pH_{SWs} = -\log ([H^+]_F + [HSO_4^-] + [HF]) = -\log [H^+]_{SWs} \quad (2.26)$$

Readers with interest in more detail in pH in seawater see Hansson (1973b), Culberson and Pytkowicz (1973), Dickson and Riley (1979), Dickson (1984), Dickson and Millero (1987), Del Valls and Dickson (1998), Zeebe and Wolf-Gladrow (2001), and Grasshoff et al. (2002).

2.3.4 Conversion between pH_{NBS} and pH_{SWs}

During the expedition pH was measured using standard NIST buffers (see section 3.2.5). Since most of the equilibrium constants of the carbonate system are determined using the seawater scale (see section 2.3.2) the obtained pH values have to be converted from pH_{NBS} to pH_{SWs} to get accurate results when using the equations in section 2.3.6. The two pH scales are related by the expression:

$$10^{-pH(NBS)} = f_H[H]_{sws} \quad (2.27)$$

where f_H is the total hydrogen ion activity coefficient (Culberson and Pytkowicz, 1973, cited in Dickson and Millero (1987)). Dickson and Millero (1987) obtained f_H by interpolating the experimental data of Mehrbach et al. (1973) using a quadratic function of salinity. Due to measurements of subzero temperatures, this study determines f_H as a

function of salinity and temperatures according to the experimental data of Mehrbach et al. (1973) using the following equation:

$$f_H = 1.8460 - 0.0042 (T + 273.15) + 0.0031S \quad (2.28)$$

(Wolf-Gladrow, 2008, personal comm.)

2.3.5 Total alkalinity and DIC

Total alkalinity (TA) and dissolved inorganic carbon ($\text{DIC} = [\text{CO}_2] + [\text{HCO}_3^-] + [\text{CO}_3^{2-}]$) are closely linked. The alkaline characteristics and the large amount of DIC in seawater are already known since the 19th century. Due to a higher alkalinity of seawater with respect to freshwater the DIC content is also higher in seawater (Wolf-Gladrow et al., 2007). If TA and DIC are given, one can calculate, together with salinity and temperature, all other quantities of the carbonate system. Alkalinity itself is "one of the most central but perhaps not the best understood concept in aquatic chemistry" (Morel and Hering, 1993, cited in Zeebe and Wolf-Gladrow (2001)). A good overview is given by Dickson (1981); Zeebe and Wolf-Gladrow (2001) and Wolf-Gladrow et al. (2007). Dickson defines the total alkalinity of a natural water "as the number of moles of hydrogen ion equivalent to the excess of proton acceptors (bases formed from weak acids with a dissociation constant $K \leq 10^{-4.5}$ at 25°C and zero ionic strength) over proton donors (acids with $K > 10^{-4.5}$) in one kilogram of sample" (DOE, 1994). The expression for this definition is:

$$\begin{aligned} TA = & [\text{HCO}_3^-] + 2[\text{CO}_3^{2-}] + [\text{B}(\text{OH})_4^-] + [\text{OH}^-] \\ & + [\text{HPO}_4^{2-}] + 2[\text{PO}_4^{3-}] + [\text{H}_3\text{SiO}_4^-] \\ & + [\text{NH}_3] + [\text{HS}^-] - [\text{H}^+]_F - [\text{HSO}_4^-] - [\text{HF}] - [\text{H}_3\text{PO}_4] \end{aligned} \quad (2.29)$$

However, seawater is more complicated, since it contains many more ions and a number of weak acids. From a geochemical point of view Zeebe and Wolf-Gladrow (2001) show that alkalinity is closely related to the charge balance in seawater. This comes from a small excess charge of the conservative cations over anions⁴. This small excess is mainly balanced by $[\text{HCO}_3^-]$, $[\text{CO}_3^{2-}]$, and $[\text{B}(\text{OH})_4^-]$. Therefore these components

⁴"Ions such as Na^+ , K^+ , Ca_2^+ , Mg_2^+ , Cl^- , SO_4^{2-} , and NO_3^- can be regarded as 'conservative' in the sense that their concentrations are unaffected by changes in pH , pressure, or temperature (within the ranges normally encountered near the earth's surface and assuming no precipitation or dissolution of solid phases, or biological transformations)." (Drever, 1982, cited in Zeebe and Wolf-Gladrow (2001): p. 29)

Table 2.3: The six variables of the CO_3 -system (Zeebe and Wolf-Gladrow, 2001)

	Variable	Remarks
1	$[\text{H}^+] =: h$	alternatively: $[\text{OH}^-]$
2	$[\text{CO}_2] =: s$	
3	$[\text{HCO}_3^-]$	
4	$[\text{CO}_3^{2-}]$	
5	TA	$= [\text{HCO}_3^-] + 2[\text{CO}_3^{2-}] + [\text{B}(\text{OH})_4^-] + [\text{OH}^-] - [\text{H}^+]$
6	DIC	

represents the most important contribution to TA. Derived from this fact the following equation can be written:

$$\begin{aligned} & \sum \text{conservative cations} - \sum \text{conservative anions} \\ &= [\text{HCO}_3^-] + 2[\text{CO}_3^{2-}] + [\text{B}(\text{OH})_4^-] + [\text{OH}^-] - [\text{H}^+] \\ & \pm \text{minor compounds} \end{aligned} \quad (2.30)$$

Neglecting the term 'minor compounds' this expression is very similar to practical alkalinity (PA) given by Zeebe and Wolf-Gladrow (2001), which gives a very good approximation for alkalinity of natural seawater for almost all practical purposes at pH values above 8. In this study all calculations will be done by using the practical alkalinity.

$$PA = [\text{HCO}_3^-] + 2[\text{CO}_3^{2-}] + [\text{B}(\text{OH})_4^-] + [\text{OH}^-] \quad (2.31)$$

The typical value for alkalinity in seawater is $2.2 \text{ mmol} \cdot \text{kg}^{-1}$ but varies with salinity. Therefore one can find in hyper saline solutions alkalinity values with more than $5.5 \text{ mmol} \cdot \text{kg}^{-1}$ (see section 4.2) or even above (Gleitz et al., 1995). Additional changes in alkalinity are due to precipitation or dissolution of calcium carbonate. Where alkalinity decreases by two moles when one mole of CaCO_3 precipitates (Wolf-Gladrow et al., 2007). Other processes which influence the alkalinity are the uptake of nitrate (NO_3^-) by algae and remineralization of algae material (Zeebe and Wolf-Gladrow, 2001).

2.3.6 From TA and pH to CO_2 , HCO_3^- , CO_3^{2-} , and DIC

Zeebe and Wolf-Gladrow (2001) consider six variables in the carbonate system (see table 2.3). If any two variables are given, it is possible to calculate all other variables. During this expedition total alkalinity (TA) and pH were measured. Therefore carbon

dioxide, bicarbonate, carbonate, and dissolved inorganic carbon have to be calculated, using following equations (Zeebe and Wolf-Gladrow, 2001, and references therein):

$$s = \left(TA - \frac{K_B^* B_t}{K_B^* + h} - \frac{K_W^*}{h} + h \right) / \left(\frac{K_1^*}{h} + 2 \frac{K_1^* K_2^*}{h^2} \right) \quad (2.32)$$

$$DIC = s \left(1 + \frac{K_1^*}{h} + \frac{K_1^* K_2^*}{h^2} \right) \quad (2.33)$$

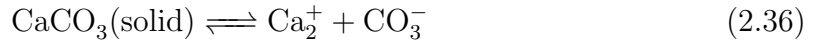
$$[\text{HCO}_3^-] = DIC / \left(1 + \frac{h}{K_1^*} + \frac{K_2^*}{h} \right) \quad (2.34)$$

$$[\text{CO}_3^{2-}] = DIC / \left(1 + \frac{h}{K_2^*} + \frac{h^2}{K_1^* K_2^*} \right) \quad (2.35)$$

where $s = [\text{CO}_2]$, TA = total alkalinity, $h = [\text{H}^+]$, K_B^* = equilibrium constant for the dissociation of $\text{B}(\text{OH})_3$, B_t = total boron concentration, K_W = ion product of water, DIC = dissolved inorganic carbon, K_1 and K_2 = the first and second dissociation constant of carbonic acid

2.4 The polymorphs of CaCO_3

Calcium carbonate (CaCO_3) can be found nearly everywhere in soils, rocks, sediments and oceans (Pauly, 1963; Buchardt, 1997; Nehrke, 2007; Dieckmann et al., 2008). In general, the precipitation of CaCO_3 is written as:



While calcite is the dominant polymorph of calcium carbonate on earth, another five can occur: Vaterite, Aragonite, amorphous carbonate (ACC), monohydrate calcium carbonate (MCC), and hexahydrate calcium carbonate (HCC) (mineral name ikaite). The latter three are hydrated polymorphs, whereas Vaterite and Aragonite are anhydrous crystalline polymorphs. Interested readers are referred to Nehrke (2007). This study will focus on the hydrated phase of CaCO_3 , the mineral ikaite.

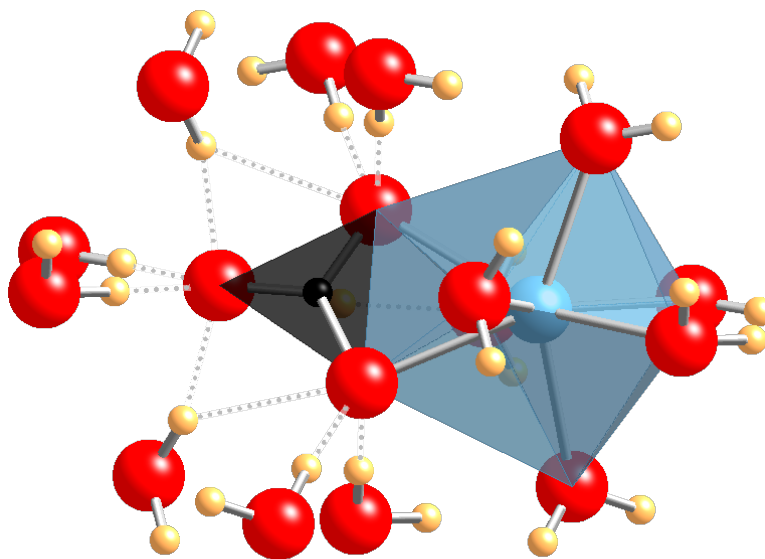


Figure 2.4: Ion pair ($\text{Ca}_2^+\text{CO}_3^{2-}$) and hydration cage. Part of the crystal structure of ikaite. Ca (blue) is in dodecahedral coordination with O atoms (red) of the carbonate (black planar) and water molecules, while hydrogen bonds (dotted) exists between H-atoms (yellow) of the water molecules and the O-atoms of the carbonate ion.

2.5 The mineral ikaite and its natural abundance

Known from laboratory experiments (Johnston et al., 1916, cited in Nehrke (2007)), the CaCO_3 polymorph hexahydrate calcium carbonate (HCC) ($\text{CaCO}_3 \cdot 6\text{H}_2\text{O}$) was first reported in natural environment by Pauly (1963). The mineral is named after the Ikka Fjord in southwest Greenland as ikaite, where it first was found. Other occurrences are reported in organic-rich sediments in the Brainsfield Strait, Antarctica, in Nankai Trough, in a deep-sea fan in Zaire, in Barrow, Arctic Alaska and the Laptev sea (Suess et al., 1982; Stein and Smith, 1986; Jansen et al., 1987; Kennedy et al., 1987, cited in Burchardt et al. (2001)). Furthermore ikaite has been reported in Mono Lake, California, from cold water springs, Hokkaido, Japan (Bischoff et al., 1993b; Ito, 1996, 1998, cited in burchardt2001) and from Expedition Fiord, Canadian High Arctic (Omelson et al., 2001). The most recent occurrence has been reported by Dieckmann et al. (2008) in Antarctic sea ice in the Weddell Sea and throughout fast ice off Adélie Land, Antarctica.

Ikaite is a hydrate of calcium carbonate, where one CaCO_3 molecule is bonded to six water molecules (see figure 2.4). However, the calcium ion is bonded more closely to the six water molecules than to the CO_3^{2-} ion. Dickens and Brown (1970) determined

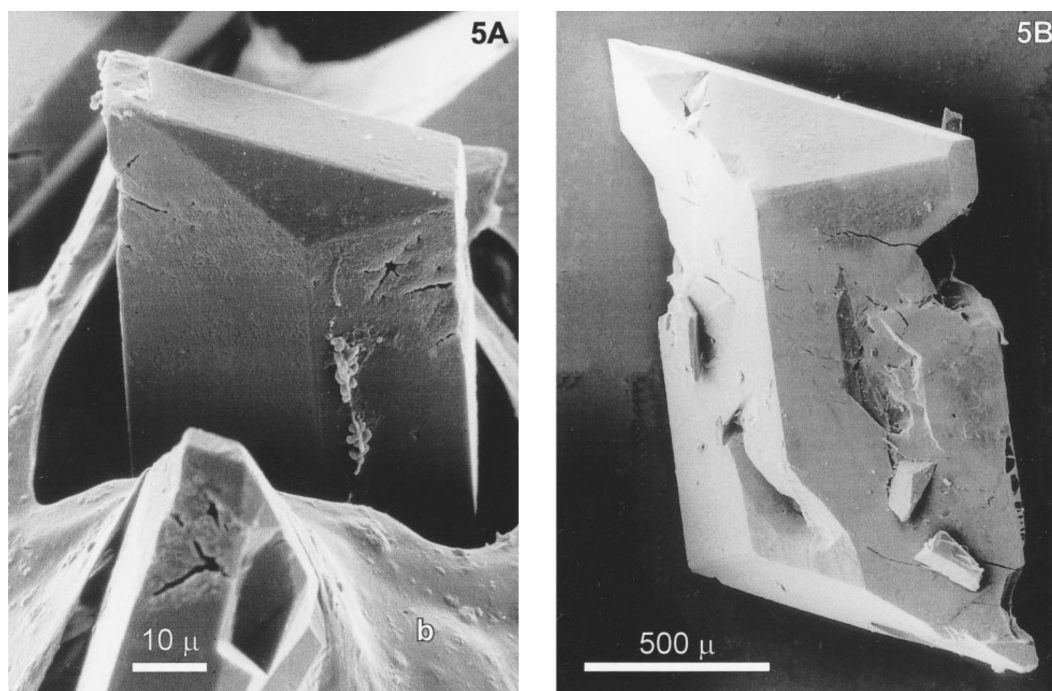


Figure 2.5: Ikaite crystals from tufa columns collected in Ikka Fjord. A) Micrograph of frozen ikaite ($\sim 140^{\circ}\text{C}$) in the cryo-SEM. The photo illustrates nonrecrystallized ikaite crystals with mucilaginous biofilm (b) embedding the crystals. These membranes are suggested to seal the ikaite crystals from the aggressive seawater environment, where ikaite is strongly undersaturated. Photo by O.B. Lyshede. B) Micrograph of a freeze-dried crystal. Freeze drying results in recrystallization of ikaite to calcite but retains the morphology of the original crystals. Photo by B. Buchardt. (Buchardt et al., 2001)

a monoclinic crystal structure. Ikaite has a density of only 1.8 g/cm^3 (Marland, 1975, cited in Bischoff et al. (1993a)). In the literature different descriptions of the crystal structure are provided, depending on the environment, where they were found. Dieckmann et al. (2008) describes beside the idiomorphic shape also shapes constrained by the size of brine pockets and brine channels within sea ice. All of the reported occurrences appear to be anoxic and at low temperatures. Ikaite is a metastable polymorph as it only exists at low temperatures ($T < 5^{\circ}\text{C}$) (Dieckmann et al., 2008) or high pressures (Van Valkenburg et al., 1971). As soon as the mineral is exposed to temperatures above 5°C at atmospheric pressure it decomposes to calcite or Vaterite (Bischoff et al., 1993b). For more details readers are referred to Pauly (1963); Dickens and Brown (1970); Marland (1975); Bischoff et al. (1993a,b); Buchardt (1997); Buchardt et al. (2001); Omelon et al. (2001); Swainson and Hammond (2001); Rickaby et al. (2006); Dieckmann et al. (2008).

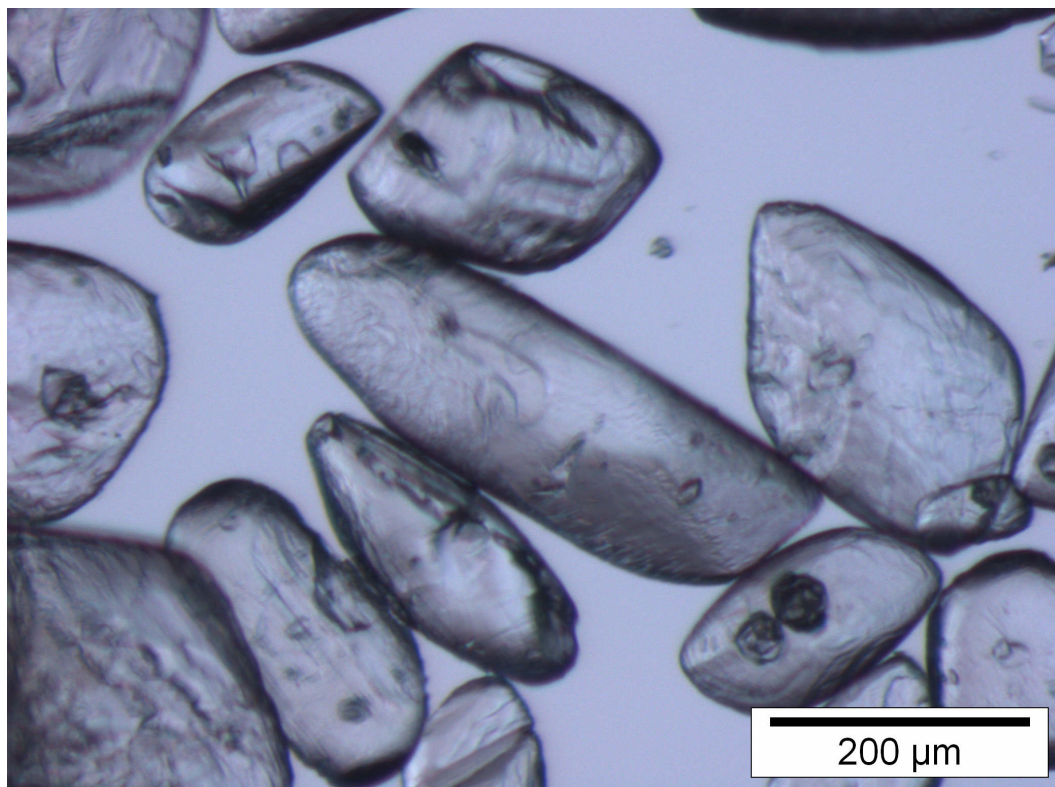


Figure 2.6: Ikaite from Antarctic sea ice (Dieckmann, unpublished data)

Chapter 3

Methodology and study area

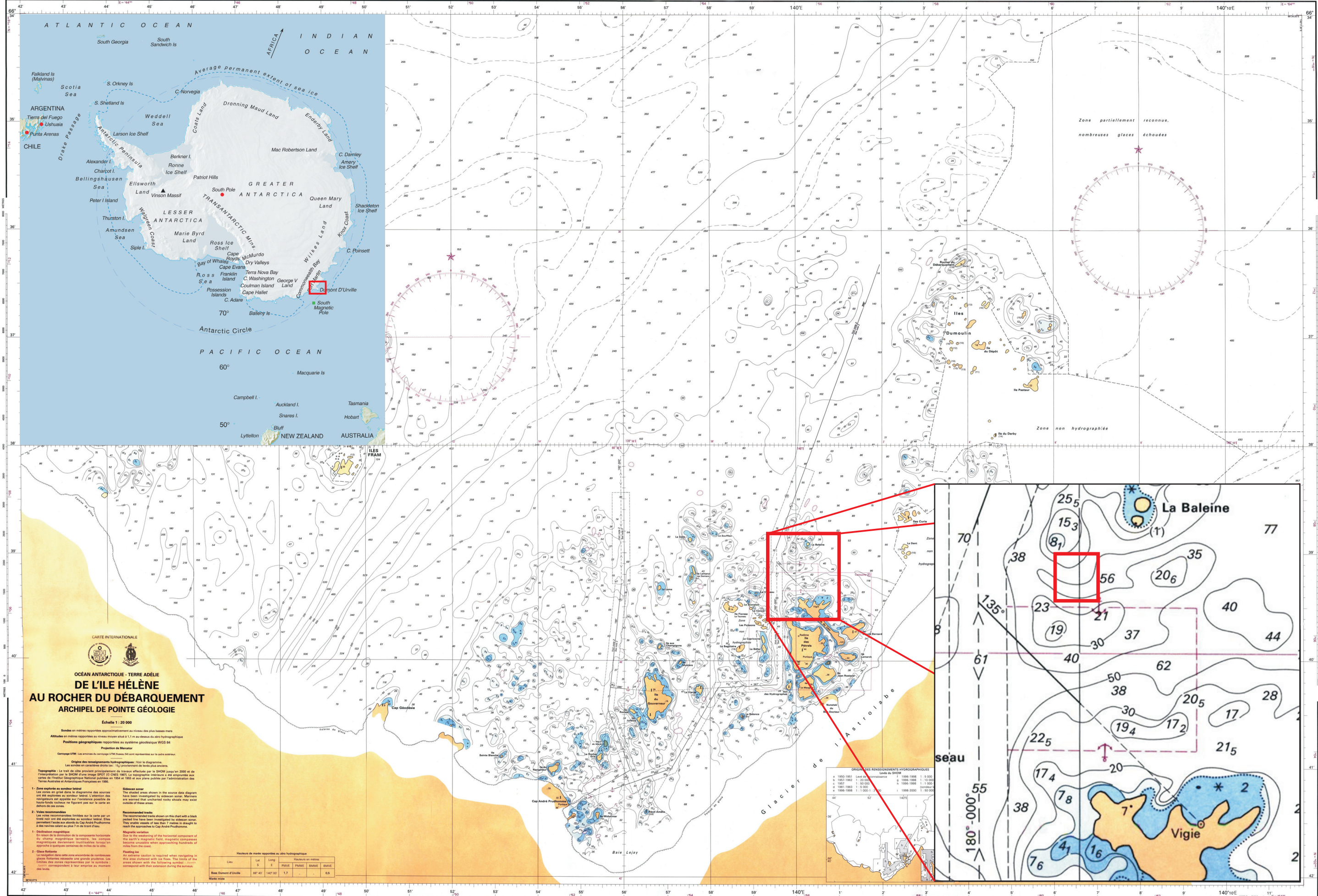
3.1 Study area

The first occurrence of CaCO_3 crystals was reported from East Antarctica off Adélie Land. The second report and at the same time the first evidence of ikaite ($\text{CaCO}_3 \cdot 6 \text{H}_2\text{O}$) has been reported from sea ice from the Weddel Sea, Antarctica in 2006. The first report of CaCO_3 was probably ikaite as well, since some of the crystals had the typical hexagonal and idiomorphic shape of the mineral found in the Weddell Sea. Due to incorrect handling and because ikaite is only stable up to 4°C , these crystals could not be investigated further (Dieckmann et al., 2008). Therefore this expedition was carried out in East Antarctica off Adélie Land again, to investigate if the mineral exists here, and if it does, to determine its mineralogy, its quantity and further chemical properties of the environment in which the mineral occurs.

Antarctica is a continent surrounded by the southern ocean. During winter the ocean is covered with sea ice up to an extent of $19 \cdot 10^6 \text{ km}^2$ (Blümel, 1999), while in summer the minimum extent is reached with $3.6 \cdot 10^6 \text{ km}^2$ (Comiso, 2003). Sea ice has a mean thickness of 0.5 to 0.6m (Wadhams, 2000) and ranges in extent from 55°S to 75°S (Eicken, 2003). The study area is off Adélie Land which is located in East Antarctica between 136°E and 142°E (see figure 3.1 on the following page). The area was chosen due to the accessibility near the french research station Dumont d'Urville. The exact coordinates are $\text{S}66^\circ 39' 13'' \text{ E}140^\circ 00' 05''$.

3.1.1 Climate

Antarctica and therefore the study site is located in a polar climate. According to the climate classification from Köppen this region belongs to group E, which is char-



Les avis de correction publiés dans les Groupes hebdomadaires d'avis aux Navigateurs sont accessibles sur le site Internet www.shom.fr.

SERVICE HYDROGRAPHIQUE ET Océanographique de la Marine - Publication 3002

GARDEZ VOTRE MER PROPRE
KEEP YOUR WATERWAYS CLEAN

INT 9017
7593

Figure 3.1: Map Antarctic Ocean - Terre Adélie, Archipel de pointe géologie

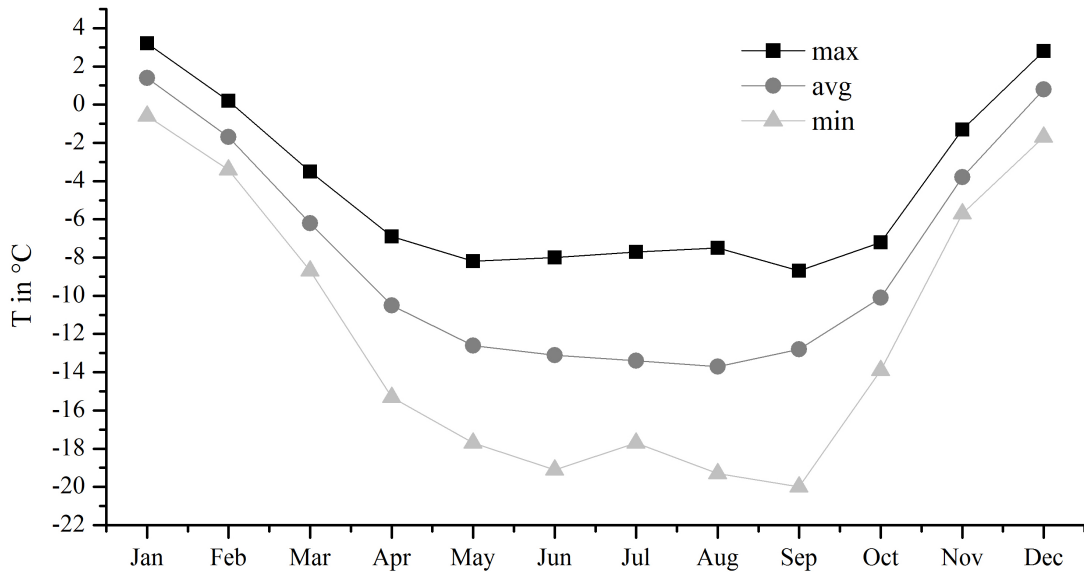


Figure 3.2: Average maximum temperatures at Dumont d'Urville (1956 - 2002) Source: IPEV, Base Dumont d'Urville

acterized by average temperatures below 10°C (50°F) in all twelve months of the year (Blümel, 1999). Since this definition fits for a wide range of polar regions, a more detailed view on the climate at the research station Dumont d'Urville will be given. There are no typical seasons in the sense of temperature, however there are at least seven months when temperatures do not rise above -10°C . From October the temperatures start to rise to a maximum in December and January when temperatures above zero are possible. Data about precipitation are rare. Data of an exact amount of precipitation do not exist, only data of the duration of precipitation events are available (see figure 3.3 on the next page). Even though it is not possible to quantify the precipitation, one can say that there is an increase starting in June with a maximum in July/August followed by a minimum in November.

The seasons are determined by the available light. Since Dumont d'Urville is located almost at the southern polar circle, there is one day with nearly exact 24 hours of light (winter solstice) and one in the year with 24 hours of darkness (summer solstice). Another important factor is the wind. The highest wind speed ever measured at Dumont d'Urville was in June 1972 with a speed of 90 m/s. Due to the high elevation and the profile of the continent, the dominant wind system are catabatic winds. These winds are extremely cold and constitute heavy air masses which result from the high radiation above the Antarctic continent. Following the relief they form fall winds. These winds are important, since they stress the sea ice cover around Antarctica (Blümel, 1999). A recent example happened in the beginning of august 2007 when huge parts of the

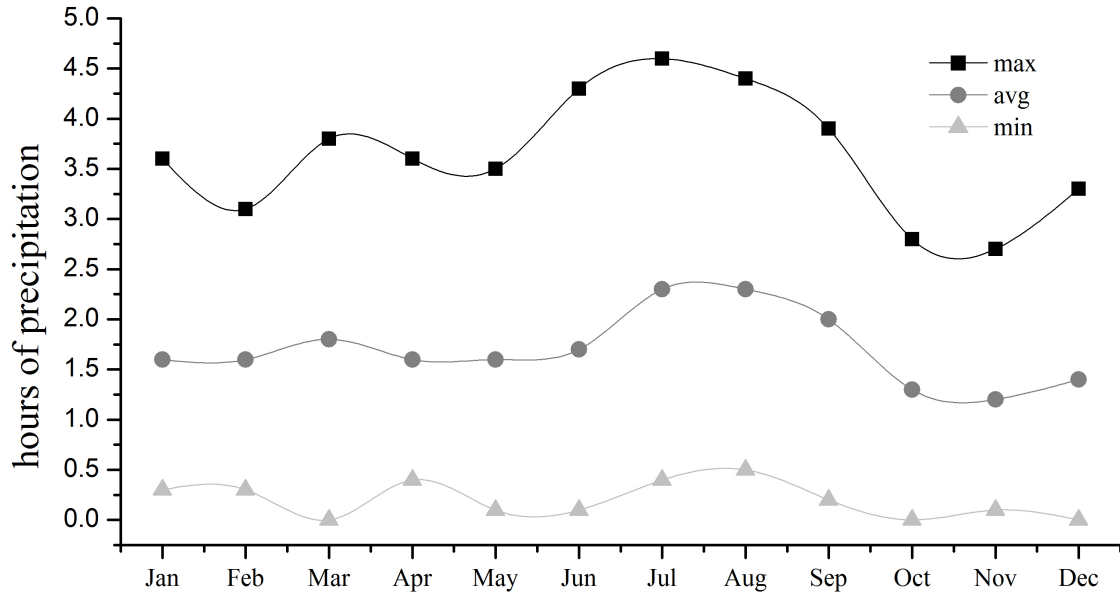


Figure 3.3: Average duration of precipitation in hours at Dumont d'Urville (1956-2002)
Source: IPEV, Base Dumont d'Urville

sea ice cover off Adélie Land broke apart leading to open water (Jaquet, 2007, personal comm.). Two components played a major role. On the one hand, the already mentioned wind with a maximum up to 158 km/h and an average speed of 104 km/h in the first days of August and on the other hand at the same time an increase of the temperatures to a maximum of -1.9°C on 3rd August. After this event a new cover of sea ice started to develop straight away, since the temperatures dropped fast below -10°C and even further down below -25°C with a minimum of -29.2°C just a few days after the break up. Therefore, the average temperature for August was -14.2°C despite the warm temperatures of the first few days. In September the average temperature reached approximately the same value with -14.3°C , but without any significant events. The following October was slightly warmer with -10.5°C but with increasing temperatures at the end of the month when values were around -5°C . This trend continued in November when even positive temperatures were observed around the 10th and the 27th. This resulted in an average temperature of -3.8°C . During the last days of measurements in December the temperature was approximately the same as in November but with an increasing tendency. After the event in August the wind had no significance for the sea ice cover from September to December. A tabular overview about the meteorological data for the sampling period is given in appendix A. For more detail about meteorological data during the sampling period see section 4.1.

Table 3.1: Ice thickness of land fast ice at the beginning of austral spring near Dumont d'Urville on 11/07/2007

Position	Ice depth	Snow depth	Freeboard
S66 39' 13.2" E140 00' 07.7"	72	0	8
S66 39' 10.1" E140 00' 03.4"	74	1	7
S66 38' 59.1" E139 59' 48.3"	64	5	5
S66 38' 45.1" E139 59' 27.3"	75	15	2
S66 38' 31.2" E139 59' 07.1"	60	9	3
S66 38' 17.8" E139 58' 48.5"	56	14	0
S66 38' 03.7" E139 58' 29.4"	53	9	5
S66 37' 48.0" E139 58' 12.0"	62	10	4
S66 37' 33.2" E139 57' 55.8"	67	0	5
N/A	58	11	2
S66 37' 03.5" E139 57' 22.3"	68	2	5
S66 36' 48.8" E139 57' 05.8"	70	10	3

* all values are in cm

3.1.2 Sea ice cover

The typical ice cover in the Géologie Archipelago, Adélie Land, Antarctica is a solid and homogeneous layer of land-fast ice which forms in March/April and lasts until December. The sea ice reaches a thickness of more than one meter (Delille et al., 2007). Multi-year ice is likely to occur in some places near the coast. Due to ice break up in August 2007 (see section above) the ice was only able to regrow to a thickness of ca. 70 cm by October. Therefore the ice was only 3 months old at the beginning of the sampling period. This young ice was a homogeneous layer of land-fast ice, as it typically develops in this region. At the beginning of the sampling period the sea ice was stable but at the end of November the ice was getting thinner. Due to this event, sampling was stopped when the sea ice thickness was less than 40cm, since inferences from the underlying sea water were likely to occur.

3.2 Methodology during the expedition in Terre Adélie

3.2.1 Sampling

During this expedition several sampling techniques were applied. These methods have been described by Horner et al. (1992), Thomas and Papadimitriou (2003), and Dieckmann et al. (2008). The sampling was carried out during austral spring from early November until mid December 2007 in the Géologie Archipelago, Adélie Land, Antarctica. First of all, the ice thickness was measured on a transect of 5 km (see table 3.1) to ensure a safe activity area and to find a suitable site for sampling. The chosen sampling site is close to the described station C from Delille et al. (2007) at S66 39' 13" E140 00' 05" and was accessible by foot and surface vehicles. All samples were taken on an area of $10 \times 10 \text{ m}^2$ to minimize bias from spatial heterogeneity. Depending on the weather conditions, especially wind, samples were taken every two or three days. The sampled sea ice was only three month old. Usually this area is covered by a homogeneous solid layer of land fast ice from March/April to December (Delille et al., 2007). Due to heavy storms there has been a temporary ice break up in august, during the Antarctic winter in 2007, leading to an open sea. After that period sea ice restarted to grow to a thickness of approximately 70 cm (Anne Jacquet, personal commun.). Delille et al. (2007) reported an ice thickness at their station C of 133 cm to 153 cm.



Figure 3.4: 9 cm diameter corer (Photo: Camille Fresser)

At each sampling day two complete ice cores were taken, using an ice corer (see figure 3.4) with a diameter of 9 cm, operated by a cordless electric drill. Both ice cores were then placed in an insulated PVC tube for further processing. The first core was used to determine a temperature profile by inserting a digital thermometer at 5 cm intervals in predrilled holes. While the other core was cut into segments of 10 cm and each piece was then placed into a container for transport to the laboratory where they were stored at -20°C . For reference purposes and to exclude the possibility of CaCO_3 in Antarctic glacier ice, two ice cores were taken on the continent near the logistic station Prud' Homme. The ice cores were one meter long.

3.2.2 Sackhole method

As mentioned in section 2.2 the brine is the interesting part of the sea ice where the geochemistry takes place. The difficulty is to extract the brine from the crystal sea ice matrix for further analyses. There are two different methods for brine sampling described in the literature. The first is using a refrigerated centrifuge. An intact ice core section is centrifuged. Although some of the ions remain in the ice, the so sampled brine retains the salinity, at temperature sampled. This method is very time consuming and material intensive (Horner et al., 1992). Another problem is the ice core sampling for the centrifuge. During this sampling some of the brine may be lost due to drainage from the ice core. The most often applied method is the sackhole method (Gleitz et al., 1995; Papadimitriou et al., 2004, 2007; Delille et al., 2007), which was used during this study as well. The sackhole method is an easily adoptable method for brine sampling. For this purpose an ice corer with a typical diameter of 9 cm is used to drill holes into the sea ice to a depth between 7 and 50 cm. There is no standard depth in the literature, and depth chosen depends on ice thickness and purpose of sample. However, most important is not to drill through the sea ice to the underlying water column and to ensure that the obtained hole has a dead end and there is no interference by seawater from the underlying water column due to the pressure head. During this study, three sackholes (to ensure a basic statistical security) were drilled into the ice to a depth of 30 cm at each sampling day (see figure 3.7b). The corer has been marked at 30 cm to guarantee a uniform depth for each sackhole. The obtained cores (figure 3.7a) from each sackhole were placed into separate clean plastic containers, marked and stored at -20°C . The sackholes were covered with plastic lids, while brine was allowed to accumulate into the holes (figure 3.7c). As soon as enough brine had collected into the hole, sampling commenced. From each sackhole brine was filled into two small plastic bottles for later analyses of pH and alkalinity in the laboratory at the research station.

3.2.3 Brine salinity

Brine salinity was determined twice for each sackhole. The first measurement has been done directly during the field sampling using a handheld refractometer. To confirm these results a second measurement was done in the laboratory, typically less than 2 hours after sampling. A conductivity meter was used. Due to the ability of the conductivity meter to measure the salinity only to a maximum of 45 the sample was diluted with distilled water in a ratio of 1:1. During the whole expedition the values were obtained with both methods.



Figure 3.5: Drilling a sackhole with an ice corer (Photo: Camille Fresser)

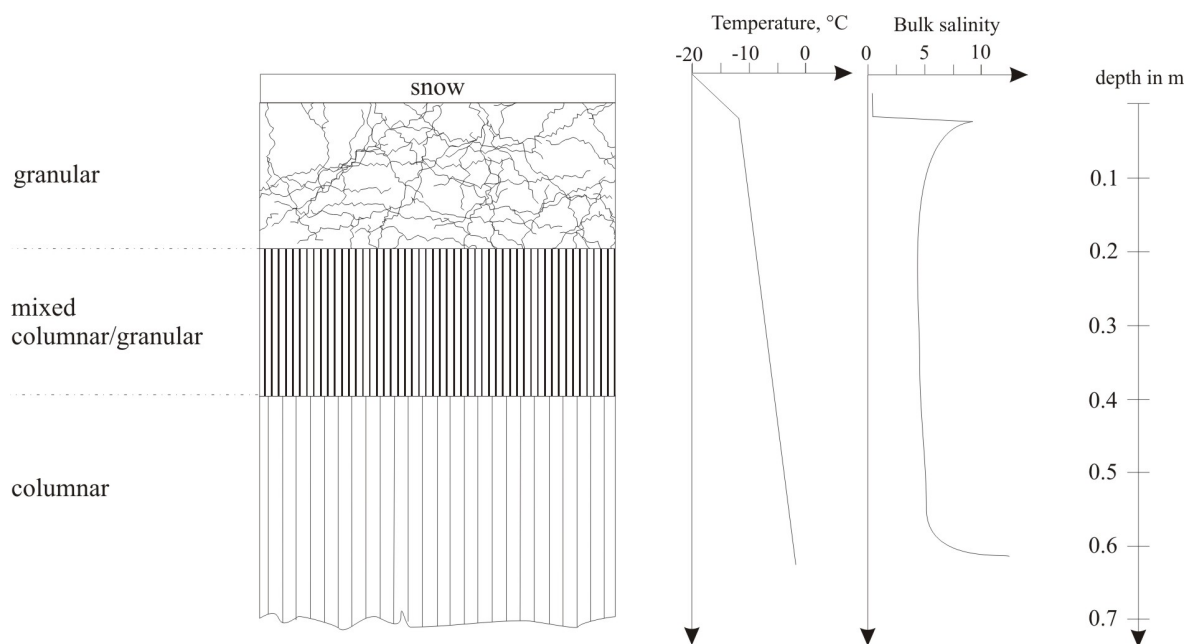


Figure 3.6: Schematic body of sea ice with typically winter temperatures and salinity profiles of first-year sea ice according to Eicken (2003).

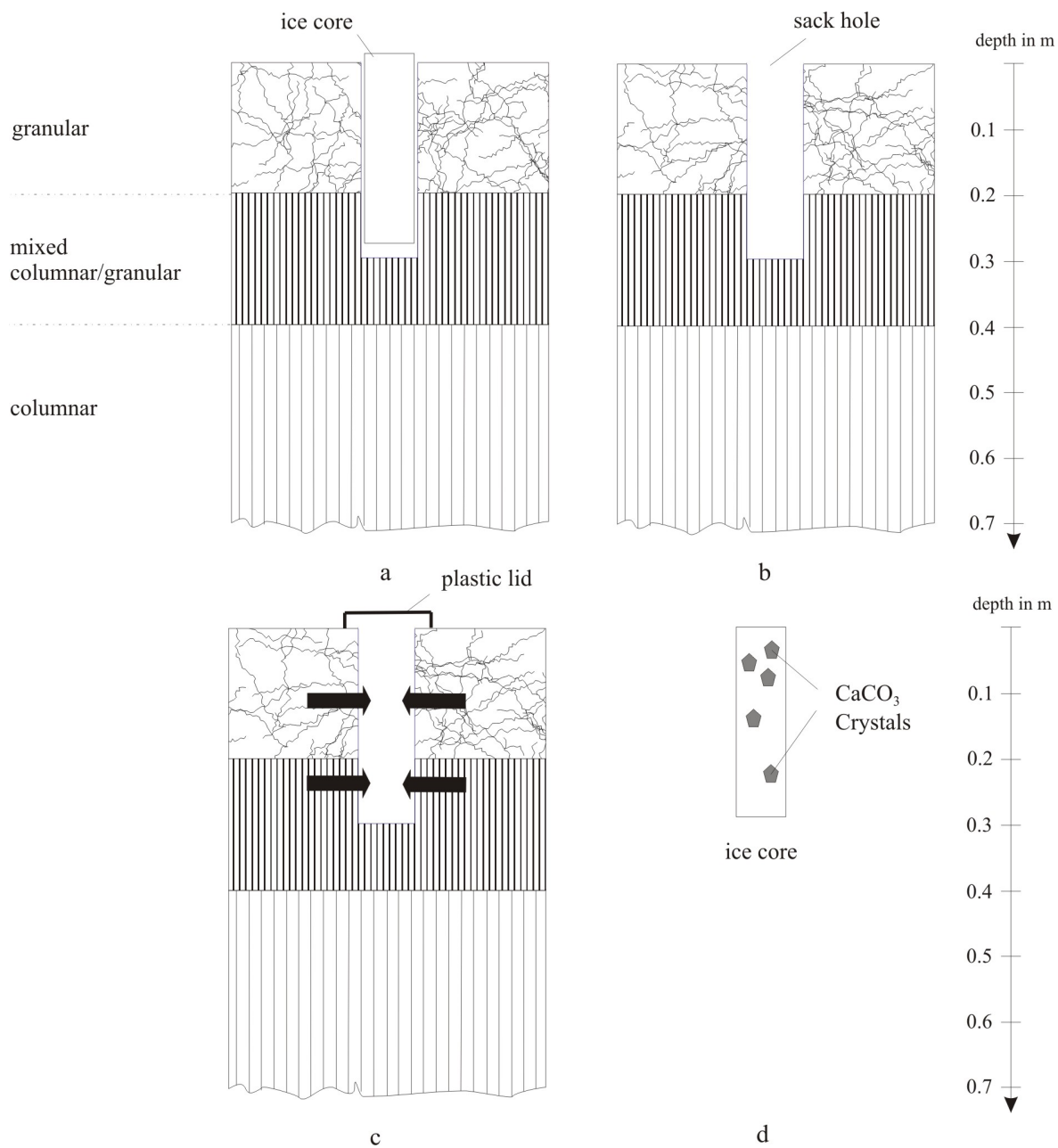


Figure 3.7: A drilled ice core (a), leaving a sack hole (b) which is covered by a plastic lid while brine percolates from the surroundings into the sackhole (c). The ice core (d) contains CaCO_3 crystals and is stored in a clean plastic container for further processing. - Schematic figure. The texture does not necessarily represent the structure of the sea ice during this study.

3.2.4 Extraction of the CaCO_3 crystals from the ice core

The calcium carbonate crystals within the sea ice body are trapped in the brine pockets and channels (Dieckmann et al., 2008). To extract the crystals from the sea ice the obtained ice cores (see section 3.2.2) and the 10 cm sections of the complete sea ice cores (see section 3.2.1) the method described by Dieckmann et al. (2008) were applied. The temperature throughout the sample preparation was maintained below 4°C , since the mineral ikaite is metastable and decomposes to calcite above 5°C . Therefore the ice cores were melted slowly in a climate controlled room where temperatures never exceeded 4°C . Regular monitoring (several times a day) guaranteed a processing of the samples as soon as the cores, or sections were melted. This ensured that the temperature of the melt water never rose much above 0°C .

The melt water was swirled and the particles allowed to settle in the vortex. The crystals were transferred from the vortex on to a GF/F filter. Due to the partly massive accumulation of the crystals onto the filter the filtration was supported by the vacuum pump, which was connected to the Erlenmeyer flask. This procedure was repeated several times to ensure that no crystals remained in the melt water. The filter with the crystal was then placed in a plastic vial containing 75 per cent ethanol and frozen at -18°C for later mineralogical phase identification and quantitative measurements. In several instances before crystals were transferred, they were briefly inspected under the binocular microscope to check for differences in morphology. At the end the filtered melt water and the remaining melt water in the plastic container were measured to get the exact volume of melted sea ice. This is essential for late quantitative determination. This procedure was applied for all ice cores obtained from the sackholes and all 10 cm sections from the complete cores from each sampling day. The latter was necessary to obtain a stratigraphic profile of the distribution of CaCO_3 within the sea ice.

3.2.5 pH in brine solution

Measurement of pH in highly saline solution is never a simple task (see section 2.3.3), especially if salinity is varying between 35 and more than 100 and is not predictable. Salinity in sea ice brine is directly related to temperature, thus it drops with increasing temperature and vice versa. For the calculation of $[\text{CO}_2]$ according to the equations in section 2.3.6 one needs values on the pH_{SWS} scale. There are different approaches for the determination of pH in highly saline solution. The simplest way seems to be the calculation of pH_{SWS} if values for dissolved inorganic carbon (DIC) and total alkalinity (TA) exist (Papadimitriou et al., 2007). The most typical approach used in the determination of pH in brine solution in sea ice is the measurement of pH using a

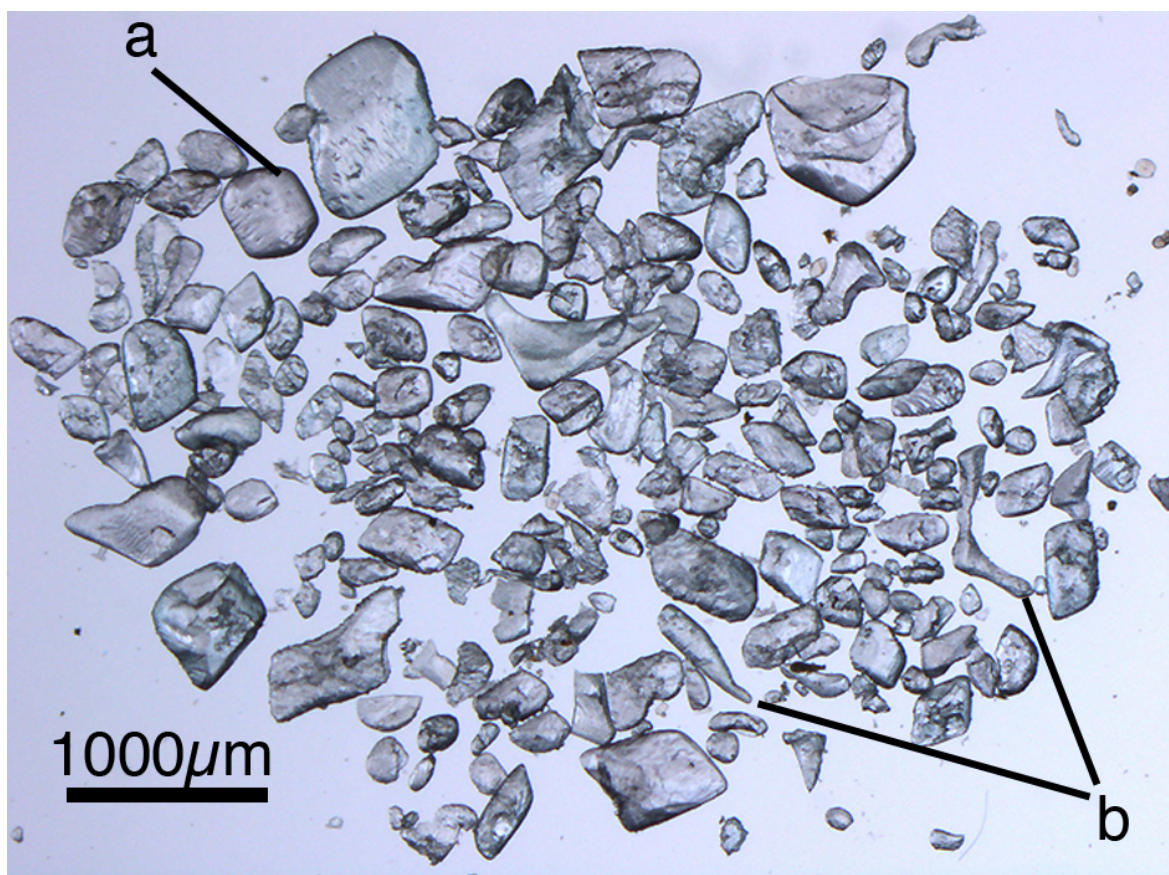


Figure 3.8: Photograph of ikaite crystals taken from a single bulk sea ice sample showing various crystal shapes and sizes: a) idiomorphic; and b) shape of brine pockets or channels (Dieckmann et al., 2008).

combination glass / reference electrode connected to a voltmeter (Gleitz et al., 1995; Papadimitriou et al., 2004; Delille et al., 2007). But even for this approach different setups can be found in the literature. The first difference is the used pH scale. While Gleitz et al. (1995) and Papadimitriou et al. (2004) used the pH_{NBS} scale (calibrated with standard NIST buffers), Delille et al. (2007) used the pH_{SWS} ¹ scale (calibrated on the total hydrogen ion scale using TRIS (2-amino-2-hydroxymethyl-1,3-propanediol) and AMP (2-aminopyridine buffers). To avoid errors they prepared buffers at different values at salinities of 30, 35, 40, and 80, according to the formulations proposed by the DOE (1994). The problem which occurs here is a huge variation of the salinities in relation to brine temperature. The values vary between 35 and more than 100. Therefore one would need more buffers than used by Delille et al. (2007) to minimize

¹It has to be noted that there is not a clear utilization of the term pH_{SWS} in Delille et al. (2007). Since they are calibrating on the total hydrogen ion scale, they get values on the pH_T scale (compare section 2.3.3) and not on the pH_{SWS} scale. Even the differences between these scales are small it may result in further errors

errors in the determination of pH_{SWs} .

If one uses the pH_{NBS} scale one has to calculate the pH_{SWs} using following equation:

$$10^{-pH(NBS)} = f_H[H]_{sws} \quad (3.1)$$

Gleitz et al. (1995) converted their pH values using a calculated apparent activity coefficient (f_H). They calculated f_H for each salinity. In contrast Papadimitriou et al. (2004) used the average of the reported values of the apparent hydrogen ion activity coefficient at $S = 34.6$ and $S = 43.7$ and 25°C in Culberson and Pytkowicz (1973), $f_H = 0.709$ and 0.730 for the under-ice seawater and sea ice brine respectively. Both did not include temperature in their calculations.

Due to the named uncertainties in the determination of pH in a highly saline solution, this study used NIST Buffers for calibration and took the temperature into account to minimize errors in the determination of pH_{SWs} . The pH was measured with the pH meter Metrohm 713. This contains a combination glass / reference electrode and a voltmeter with a sensitivity of $\pm 0.1\text{mV}$ or $\pm 0.001\text{pH}$ units respectively. The pH was measured immediately after return to the laboratory (less than one hour after sampling). Before every measurement, a three point calibration with standard NIST buffers (with pH values at 4, 7, and 9) was carried out. Every sample was measured twice and the differences between both measurements never rose above 0.05 units. Then all values were transferred to pH_{SWs} . For the transfer from pH_{NBS} to pH_{SWs} one needs the apparent hydrogen ion activity coefficient. The coefficient was calculated according to Dickson and Millero (1987) by interpolating the experimental data of Mehrbach et al. (1973) using a quadratic function of salinity and temperature. Due to measurements of subzero temperatures, this study determines f_H as a function of salinity and temperatures according to the experimental data of Mehrbach et al. (1973) using the following equation:

$$f_H = 1.8460 - 0.0042(T + 273.15) + 0.0031S \quad (3.2)$$

(Wolf-Gladrow, 2008, personal comm.)

3.2.6 Total alkalinity

Because total alkalinity (TA) is not affected by CO_2 exchange between sample and air, it has not to be the first drawn. Furthermore it is possible to use an open titration vessel (Grasshoff et al., 2002). Alkalinity was measured according to methods described in DOE (1994) and Grasshoff et al. (2002) by titration of the brine sample with hydrochloric acid. The titration is followed with an electrochemical cell. The same

pH meter as in section 3.2.5, the Metrohm 713, was applied for this. Additionally a "Dosimat" was used. This device consists of a motor-driven burette (reproducible to 0.001 cm^3 in the delivered volumes) which was interfaced to a magnetic stirrer and to a microcomputer which controlled the titrated volumes. Thus the solution was stirred during the titration. The solution was titrated with 0.02 mol/l hydrochloric acid. The acid was given to the sample over a free movable acid injection tip, since the volume in the titration vessel changed. The start volume (V_0) of the sample was always 40 ml . The sample was then titrated to an end point of a pH value of 3.3 to 3.5 . For each sample the total alkalinity was calculated with the following equation:

$$TA = \frac{V_{HCl} * [HCl] * 1000 - 10^{-pH_{end}} * (V_0 + V_{HCl}) * 1000 / f_{H^+}}{V_0} \quad (3.3)$$

(Schlüter, 2007, personal communication)

where V_{HCl} is the volume of hydrochloric acid, which has been added to the sample during the titration, $[HCl]$, the concentration of the hydrochloric acid, V_0 , the start volume of the sample and f_H the hydrogen ion activity coefficient.

3.2.7 Examining spatial distribution of ikaite with the help of Kriging

Since all other values described above are single point measurements, it is not possible to derive spatial information of the distribution of the mineral ikaite. Therefore, an extra experiment was carried out at the end of the study using a grid with the size of 20m by 20m . Every 5 m an ice core was drilled in x and y direction. The first 10 cm of the ice core was then cut off and placed into a plastic container for further processing. At each sampling point the ice thickness was determined.

Using the geostatistical method of ordinary Kriging (or punctual Kriging) with the program Surfer 8 from Golden Software, a contour map of the distribution of ikaite and the ice thickness was calculated.

3.3 Methodology during the SIPEX expedition in the southern ocean

The sampling at the "Sea Ice Physics and Ecosystem eXperiment" (SIPEX) has been carried out by Andreas Krell from the Alfred Wegener Institute for Polar and Marine Research during September and October 2007. Ice cores were taken at different locations, using standard techniques (Horner et al., 1992) as described above. The samples from the SIPEX cruise were taken between the latitude $S64^{\circ}13'$ and $S65^{\circ}36'$

and the longitude E116°49' and E128°04'. The sea ice was between 51 and 187 cm thick. Complete ice cores were not always taken and differ between 40 and 109 cm in length.

3.4 ICP OES

While quantifying the collected ikaite within the sea ice samples it is necessary to ensure that only the calcium carbonate has to be measured and not any impurities. To achieve this an optical emission spectrometry has been adopted. Thus it is possible to measure the pure calcium and hence to calculate the quantity of the mineral ikaite. The technique of the Inductively-Coupled Plasma Optical Emission Spectrometry (ICP OES) that has been applied, offers a wide range of advantages. Recommended by many European countries it is established throughout science and environmental analysis as well (Nölte, 2002). The advantages of the ICP OES are a higher range of concentrations which can be measured compared to other spectroscopic methods and a better reproducibility of the atomizing conditions. Due to the very high temperatures (4000 – 6000°C) there is a smaller disturbance of the single elements to each other and one obtains good spectra (Skoog and Leary, 1992). For an introduction to method of ICP OES the interested reader is referred to Skoog and Leary (1992) and Nölte (2002). The frozen samples of the ikaite ² (see subsection 3.2.4 on page 34) were stored in plastic caps. These plastic caps were rinsed in the home laboratory with highly concentrated ethanol and the content was transferred to larger vials. The transferred samples were then put in an oven and dried at 60°C until all ethanol was evaporated. The remaining material was mixed with 5 ml highly concentrated HNO₃ to dissociate all molecules to get free ions. Finally the liquid samples were then analyzed in the ICP OES, measuring the amount of calcium within the sample.

Based on the amount of the measured calcium the amount of CaCO₃·6H₂O was calculated since all minerals were ikaite (see above). Therefore the following equations were used:

$$[\text{CaCO}_3 \cdot 6\text{H}_2\text{O}] = [\text{Ca}^{2+}] + [\text{CO}_3^{2-}] + 6[\text{H}_2\text{O}] \quad (3.4)$$

$$[\text{Ca}^{2+}] = \textit{measured with ICP OES} \quad (3.5)$$

²The samples of the extracted minerals were analyzed by means of X-ray diffraction using synchrotron radiation (X-ray beamline of the Synchrotron Laboratory for Environmental Studies SUL-X at the synchrotron radiation source ANKA, Forschungszentrum Karlsruhe) by Nehrke, G., Göttlicher, J., and Steininger, R. This methods were also used when Dieckmann et al. (2008) found the first ikaite in sea ice. The analyses showed 100% ikaite in the samples taken off Adélie Land, Antarctica (Nehrke, 2008, personal comm.)

$$[\text{CO}_3^{2-}] = [\text{Ca}^{2+}] \cdot \frac{\text{molecular weight of CO}_3^{2-}}{\text{atomic weight weight of Ca}^{2+}} \quad (3.6)$$

$$6[\text{H}_2\text{O}] = \frac{([\text{Ca}^{2+}] + [\text{CO}_3^{2-}]) \cdot 6 \cdot \text{molecular weight of H}_2\text{O}}{(\text{molecular weight of CO}_3^{2-}) + (\text{atomic weight weight of Ca}^{2+})} \quad (3.7)$$

in cases where a dilution of the sample due to high concentration was necessary for the measurement the result was multiplied by the factor the sample was diluted. Finally the values were set in relation to the volume of melted ice to calculate the amount of ikaite in one liter melted sea ice.

3.5 Calculation of the concentrations in the carbonate system

For the calculation of the concentrations of the species in the carbonate system two sets of constants according to section 2.3.2 were used within the equations of 2.3.6. The constants are those of Mehrbach et al. (1973) as refitted by Dickson and Millero (1987) and those of Millero et al. (2006). This should result in a better accuracy or gives at least the possibility to compare the values with each other and with those from other workers such as Delille et al. (2007).

Chapter 4

Results

4.1 Meteorological data during the sampling period at Dumont d'Urville

Since there is a meteorology station at the research station at Dumont d'Urville with regular observations, detailed climate data are available. The Station is situated at S66°39'5 and E140°00'3 at an altitude of 43 meter. Thus, the station is very close to the sampling site giving the opportunity to plot meteorological data of the same time when the sampling took place.

The average temperature in November 2007 was -3.8°C . This is exactly the average temperature usually observed in November. The average temperature of the sampling period was -3.5°C , since the first days of December were also taken into account. Two remarkable peaks were observed on 9th and 28th November when temperatures reached 0°C . These events alternated with colder periods when the maximum temperatures dropped below -4°C and -5°C respectively. The average global radiation reached 2679.43 J/cm^2 during November. The average of the sampling period was slightly less with 2628.13 J/cm^2 . A steady increase in global radiation can be seen in November with a maximum at the end of the month when values were far beyond 3000 J/cm^2 . These values were observed over several days. However, two sudden drops have to be noted. The first around the 18th November when only less than 2000 J/cm^2 were measured and the second at the beginning of December with a value of 2157 J/cm^2 . This is in accordance with the cloudiness. The wind did not affect the sea ice, even though maximums of more than 18.1 m/s were observed. The average was 8.7 m/s . For the complete data set see appendix A.

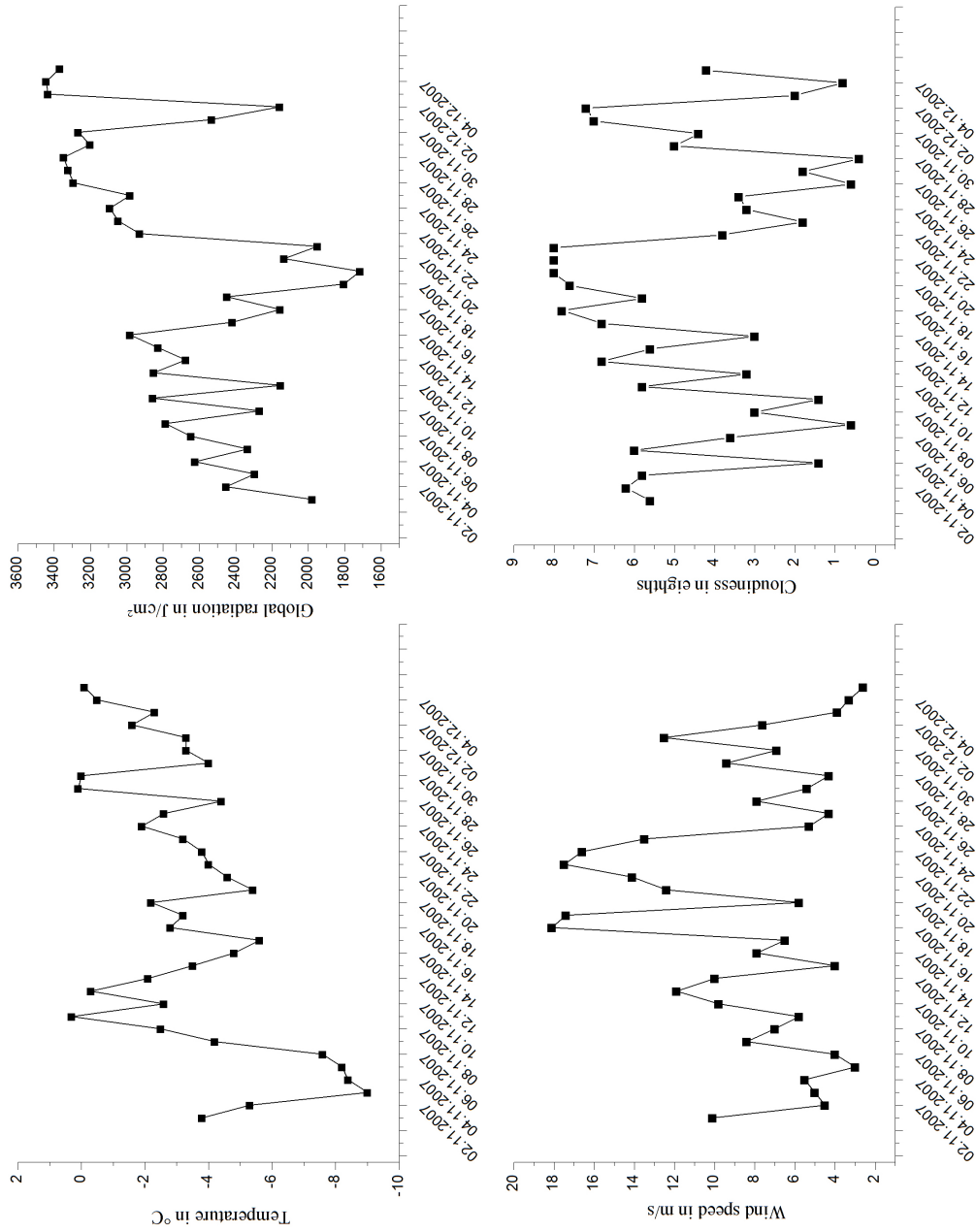


Figure 4.1: Meteorological data at Dumont d'Urville, Ile des Petrels, Terre Adélie - Antarctica (S66°39.5' / E140°00.3', 41m a.s.l.) during the sampling period focusing on temperature, global radiation, wind speed, and cloudiness

4.2 Geochemistry of sea ice brine

4.2.1 Salinity and temperature of sea ice brine

The maximum salinity was measured right at the beginning of the sampling period with 87 psu, while the minimum was measured in the middle and at the end of the period with values around 40 psu. Temperature values were the opposite with the minimum of -4.8°C at the beginning, the maximum in the middle and at the end with around $-2/-2.5^{\circ}\text{C}$. The relation between salinity and brine temperature is shown in table B.1 and figure 4.2. The salinity decreases with increasing temperatures. The relation is almost linear. Although there is a linear relation between temperature of the brine

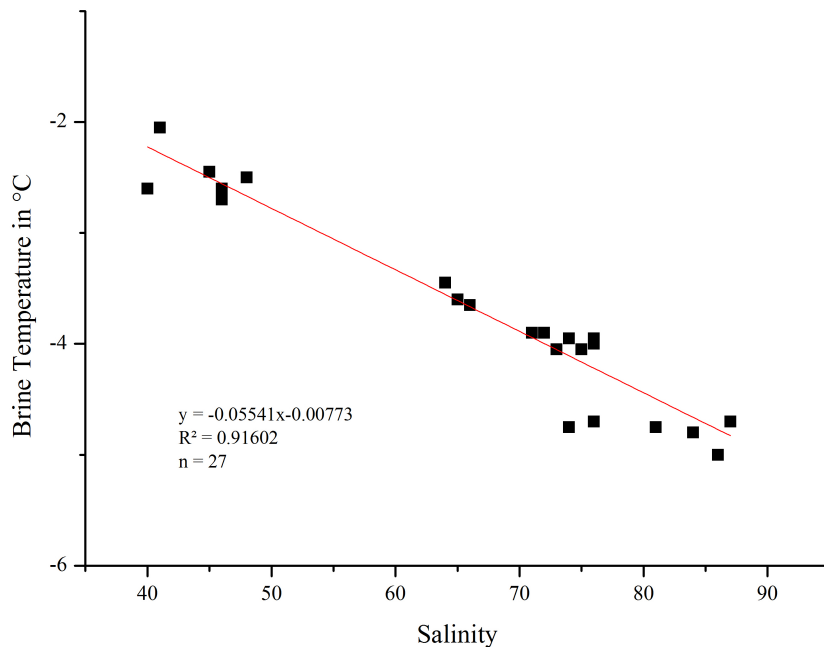


Figure 4.2: Relation of salinity and temperature in sea ice brine

and salinity the values did not develop linearly with time. They oscillated over the sampling period. The salinity with its maximum at the beginning was followed by a steady decrease until the 5th sampling day. On the 6th sampling day the salinity dropped even further to values below 50 psu. Ionic strength then rose again for a short period until it dropped again. The temperature of the brine behaved indirectly proportional (see figure 4.3). The relation between salinity and temperature of brine are shown in figure 4.2 and 4.3.

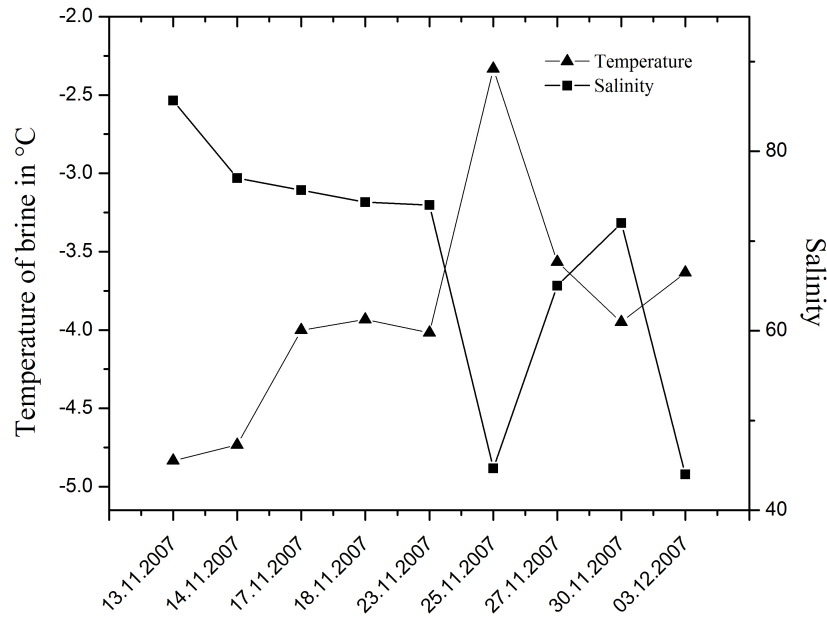


Figure 4.3: Salinity and temperature of the brine during the sampling period

4.2.2 pH values in the brine solution

Since the pH values were measured on the NBS scale using standard NIST buffers, they had to be converted to the seawater scale. Thus the hydrogen ion activity coefficient was calculated first (see table 4.1) from a quadratic function of salinity and temperature:

$$f_H = 1.8460 - 0.0042(T + 273.15) + 0.0031S \quad (4.1)$$

(Wolf-Gladrow, 2008, personal comm.)

Table 4.1: Calculated total hydrogen ion activity coefficient as function of temperature and salinity

Sample Name	Date	Brine temperature in °C	Salinity	$f_H(S, T)$
ROV2 #1	13.11.07	-5	86	0.986
ROV2 #2	13.11.07	-4.7	87	0.988
ROV2 #3	13.11.07	-4.8	84	0.979
ROV3 #1	14.11.07	-4.75	81	0.970
ROV3 #2	14.11.07	-4.7	76	0.954
ROV3 #3	14.11.07	-4.75	74	0.948
ROV4 #1	17.11.07	-4.05	75	0.948

Sample Name	Date	Brine temperature in °C	Salinity	$f_H(S, T)$
ROV4 #2	17.11.07	-4	76	0.951
ROV4 #3	17.11.07	-3.95	76	0.951
ROV5 #1	18.11.07	-3.9	71	0.935
ROV5 #2	18.11.07	-3.95	76	0.951
ROV5 #3	18.11.07	-3.95	76	0.951
ROV6 #1	23.11.07	-4.05	73	0.942
ROV6 #2	23.11.07	-3.95	74	0.945
ROV6 #3	23.11.07	-4.05	75	0.948
ROV8 #1	25.11.07	-2.05	41	0.834
ROV8 #2	25.11.07	-2.45	45	0.849
ROV8 #3	25.11.07	-2.5	48	0.858
ROV9 #1	27.11.07	-3.6	65	0.915
ROV9 #2	27.11.07	-3.65	66	0.919
ROV9 #3	27.11.07	-3.45	64	0.912
ROV11 #1	30.11.07	-3.9	71	0.935
ROV11 #2	30.11.07	-3.9	72	0.938
ROV11 #3	30.11.07	-4.05	73	0.942
ROV13 #1	03.12.07	-3.6	40	0.838
ROV13 #2	03.12.07	-3.7	46	0.857
ROV13 #3	03.12.07	-3.6	46	0.856

Using the calculated values of f_H and the measured data of pH_{NBS} , the concentration of $[H^+]$ is directly calculated according to the equation:

$$[H^+_{sws}] = \frac{10^{-pH(NBS)}}{f_H} \quad (4.2)$$

The pH values are between 8 and 10. The average is 8.773 with the highest value of 9.4 in the middle of the sampling period. A mean value out of the three samples was calculated for each sampling day. Only for the last sample were the first two samples used, since the last one is obviously an outlier. If one calculates H^+_{sws} from these values and plots them one can see a clear pattern (see figure 4.4). The concentration of hydrogen ions drops continuously until 25th November and rises suddenly to values which are even above those from the beginning of the sampling period. But after the penultimate sampling day the pH again dropped to a mean value of 8.72 on 3rd December. A detailed view on the calculated values can be found in appendix B.

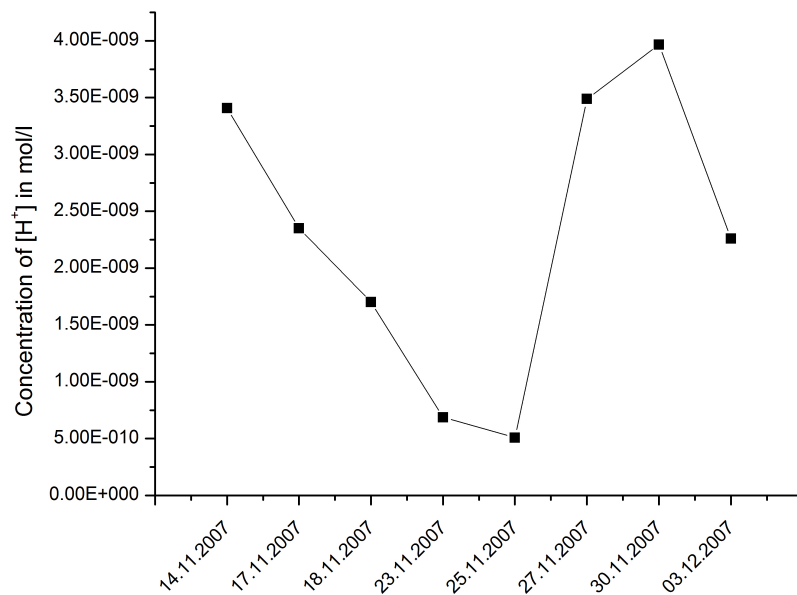


Figure 4.4: Concentration of H^+_{SWS}

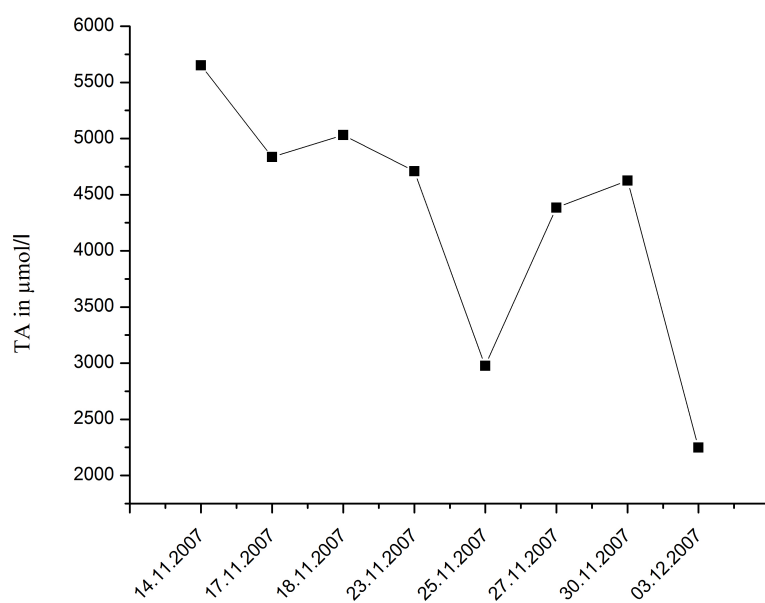


Figure 4.5: Total alkalinity in $\mu\text{mol/kg}$

4.2.3 Total Alkalinity

The total alkalinity almost follows the same pattern as the pH values. They drop from the beginning to the middle of the sampling period, but then start to rise, followed by another decrease at the end. But there are differences. The highest value is not just after the increase on 27th November, but right at the beginning with $5672 \mu\text{mol}/\text{kg}$. The average is $4311 \mu\text{mol}/\text{kg}$ and the minimum was measured on 3rd December with less than $2000 \mu\text{mol}/\text{kg}$. Another interesting aspect is, that the total alkalinity does not drop continuously like the pH values. There is a light increase on 18th November up to more than $5000 \mu\text{mol}/\text{kg}$ again. The values after the second increase do not exceed those from the beginning like the pH values do.

At the end of the sampling a reference sample of the underlying water column was taken and measured as well. The obtained value was $2218 \mu\text{mol}/\text{kg}$. This is slightly below the typical values found in the oceans (Edmond, 1970; Dickson et al., 2003).

4.2.4 Concentration of the species in the carbonate system in sea ice brine

The concentrations of carbon dioxide, dissolved inorganic carbon, bicarbonate, and carbonate in the carbonate system in sea ice brine are calculated with the equations from section 2.3.6. According to section 2.3.2 and section 3.5 two sets of constants are used. The results using the dissociation constants of Mehrbach et al. (1973) refitted by Dickson and Millero (1987) will be described first. Secondly the results using the dissociation constants of Millero et al. (2006) will be described at the end of the section.

Calculations with dissociation constants of Dickson and Millero

The concentrations of carbon dioxide, bicarbonate, carbonate ions, and dissolved inorganic carbon fluctuate over a wide range during the sampling period. The concentration of carbon dioxide varies between 0.55 and $32.23 \mu\text{mol}/\text{kg}$. The values of DIC and bicarbonate develop in a similar way but different to the concentration of $[\text{CO}_2]$. The minima are reached at ROV8 with $906.67 \mu\text{mol}/\text{kg}$ for DIC and $459.18 \mu\text{mol}/\text{kg}$ for $[\text{HCO}_3^-]$ respectively. In contrast to $[\text{CO}_2]$ the maxima are reached at the very beginning of the sampling period. While the maximum of DIC is $4172.30 \mu\text{mol}/\text{kg}$ the maximum of bicarbonate does not exceed $3593.30 \mu\text{mol}/\text{kg}$. The concentration of the carbonate ions seems to develop in a totally different way, since the minimum is reached at the end of the sampling period and the maximum is in between at ROV6 with $721.48 \mu\text{mol}/\text{kg}$. After the last sampling day a sea water sample was taken showing a value

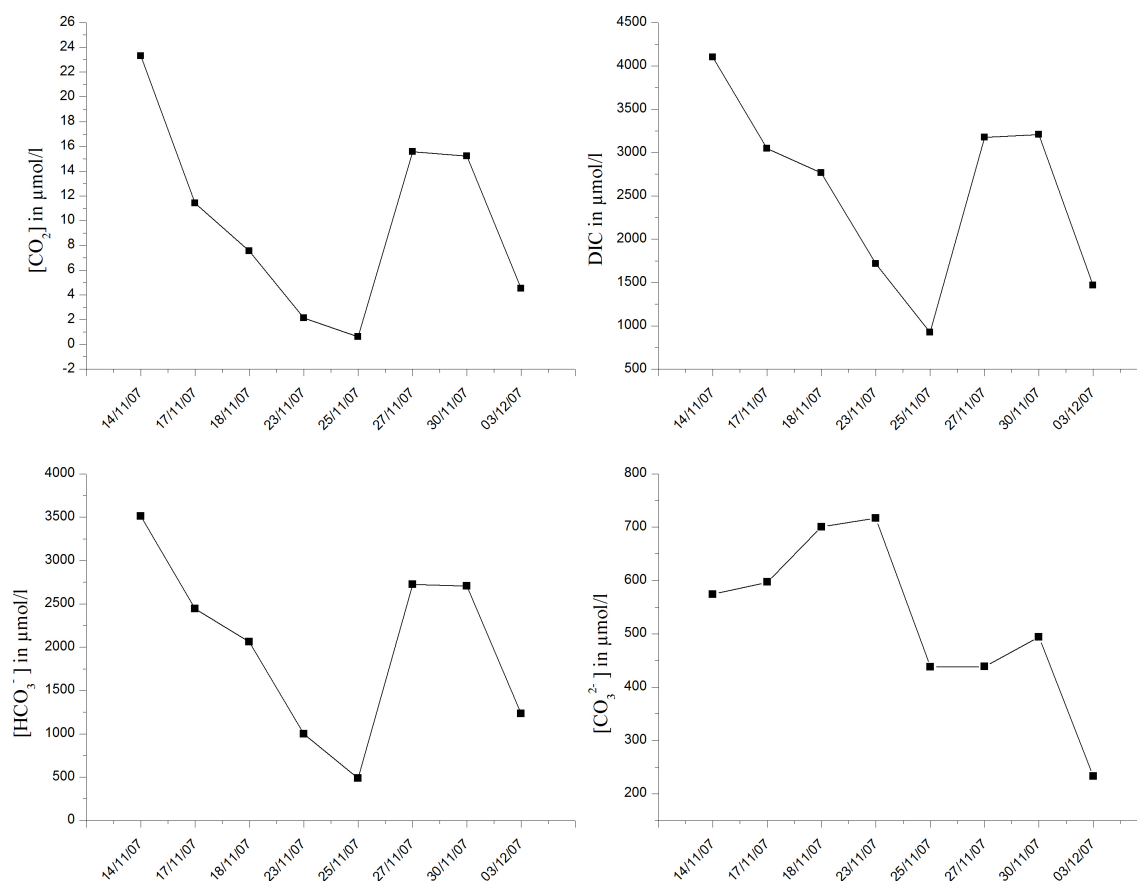


Figure 4.6: Concentration of the species of the carbonate system calculated with the dissociation constants of Dickson and Millero (1987)

of $48.41 \mu\text{mol}/\text{kg}$ for $[\text{CO}_2]$ and $2147.51 \mu\text{mol}/\text{kg}$ for DIC, which is slightly above typically measured values in sea water (compare <http://andrew.ucsd.edu/co2qc/>).

Except for the concentration of the carbonate ions all other values drop over time to the end of November. Followed by a sudden remarkable increase by a factor of 5. On 25th November there is a comparable decrease of the concentrations of HCO_3^- , DIC, and CO_2 . The concentration of the carbonate ions change more diversely. Starting with a slight increase, the concentration grows stronger to mid November. In contrast to the increase of the concentration of the other species, there is a sudden decrease of $[\text{CO}_3^{2-}]$. The decrease is not as strong as the increase of the other concentrations and occurs one sampling day earlier. Since all values change the other way around than the values of bicarbonate one would expect an increase at the end of the sampling period. Instead there is only a slight increase in the concentration of $[\text{CO}_3^{2-}]$ followed by a strong decrease.

Table 4.2: Calculated concentrations of the species in the carbonate system in sea ice brine, using pK_1 and pK_2 according to Dickson (1987)

Sample Name	Date	T of brine	S	TA	[CO ₂]	DIC	[HCO ₃ ⁻]	[CO ₃ ²⁻]
ROV3 #1	14.11.07	-4.75	81	5616.13	25.08	4093.85	3513.38	561.79
ROV3 #2	14.11.07	-4.7	76	5671.62	24.37	4172.30	3593.30	560.72
ROV3 #3	14.11.07	-4.75	74	5672.03	20.45	4041.04	3426.80	599.39
ROV4 #1	17.11.07	-4.05	75	4802.84	10.77	2993.52	2386.37	600.27
ROV4 #2	17.11.07	-4	76	4875.94	11.99	3104.65	2501.47	595.35
ROV4 #3	17.11.07	-3.95	76	4825.49	11.50	3044.39	2442.35	594.59
ROV5 #1	18.11.07	-3.9	71	4948.90	4.90	2447.24	1712.41	732.43
ROV5 #2	18.11.07	-3.95	76	5105.02	10.45	3095.07	2427.34	661.26
ROV5 #3	18.11.07	-3.95	76	5042.44	7.30	2752.54	2040.93	707.58
ROV6 #1	23.11.07	-4.05	73	4746.13	0.88	1202.45	544.71	657.57
ROV6 #2	23.11.07	-3.95	74	4744.25	2.23	1750.38	1028.14	721.48
ROV6 #3	23.11.07	-4.05	75	4709.42	2.06	1678.81	965.92	712.20
ROV8 #1	25.11.07	-2.05	41	2732.23	0.63	909.13	501.38	407.56
ROV8 #2	25.11.07	-2.45	45	3068.32	0.55	906.67	459.18	447.35
ROV8 #3	25.11.07	-2.5	48	3128.12	0.65	960.06	501.00	458.88
ROV9 #1	27.11.07	-3.6	65	4484.54	16.80	3290.74	2840.40	437.71
ROV9 #2	27.11.07	-3.65	66	4283.98	15.92	3121.72	2689.11	420.69
ROV9 #3	27.11.07	-3.45	64	4383.50	13.98	3110.41	2643.51	456.72

Sample Name	Date	T of brine	S	TA	[CO ₂]	DIC	[HCO ₃ ⁻]	[CO ₃ ²⁻]
ROV11 #1	30.11.07	-3.9	71	4653.12	15.12	3240.25	2729.08	500.36
ROV11 #2	30.11.07	-3.9	72	4659.36	32.26	3776.18	3403.72	345.82
ROV11 #3	30.11.07	-4.05	73	4565.30	15.34	3178.51	2679.46	488.05
ROV13 #1	03.12.07	-3.6	40	1987.98	4.81	1400.36	1205.49	191.28
ROV13 #2	03.12.07	-3.7	46	2405.69	4.21	1538.68	1261.44	274.40
ROV13 #3	03.12.07	-3.6	46	2350.35	26.90	2121.29	2002.70	94.01
SW Sample	04.12.07	-1	34	2218.39	48.41	2147.51	2054.35	46.82

all concentrations are in $\mu\text{mol}/\text{kg}$ Temperature in $^{\circ}\text{C}$, Salinity in ‰

Table 4.3: Calculated concentrations of the species in the carbonate system in sea ice brine, using pK_1 and pK_2 according to Millero (2006)

Sample Name	Date	T of brine	S	TA	[CO ₂]	DIC	[HCO ₃ ⁻]	[CO ₃ ²⁻]
ROV3 #1	14.11.07	-4.75	81	5616.13	5.76	3580.65	3080.72	1791.07
ROV3 #2	14.11.07	-4.7	76	5671.62	8.16	3884.70	3352.42	1562.65
ROV3 #3	14.11.07	-4.75	74	5672.03	7.48	3886.48	3301.02	1545.01
ROV4 #1	17.11.07	-4.05	75	4802.84	3.32	2988.24	2384.78	1495.74
ROV4 #2	17.11.07	-4	76	4875.94	3.51	3036.54	2449.63	1528.93
ROV4 #3	17.11.07	-3.95	76	4825.49	3.35	2988.95	2400.78	1521.21
ROV5 #1	18.11.07	-3.9	71	4948.90	1.69	2888.55	2022.12	1642.78
ROV5 #2	18.11.07	-3.95	76	5105.02	2.92	3100.22	2433.95	1665.07

Sample Name	Date	T of brine	S	TA	[CO ₂]	DIC	[HCO ₃ ⁻]	[CO ₃ ²⁻]
ROV5 #3	18.11.07	-3.95	76	5042.44	1.88	2911.60	2160.56	1736.40
ROV6 #1	23.11.07	-4.05	73	4746.13	0.20	2267.90	1027.47	1834.16
ROV6 #2	23.11.07	-3.95	74	4744.25	0.54	2437.35	1432.04	1763.38
ROV6 #3	23.11.07	-4.05	75	4709.42	0.46	2375.35	1367.05	1773.08
ROV8 #1	25.11.07	-2.05	41	2732.23	0.59	1625.11	896.24	760.71
ROV8 #2	25.11.07	-2.45	45	3068.32	0.49	1749.01	885.78	922.88
ROV8 #3	25.11.07	-2.5	48	3128.12	0.55	1780.18	929.00	936.90
ROV9 #1	27.11.07	-3.6	65	4484.54	10.00	3423.10	2957.72	867.94
ROV9 #2	27.11.07	-3.65	66	4283.98	9.08	3225.92	2781.93	858.84
ROV9 #3	27.11.07	-3.45	64	4383.50	8.49	3296.37	2803.92	876.66
ROV11 #1	30.11.07	-3.9	71	4653.12	6.57	3242.84	2734.74	1169.17
ROV11 #2	30.11.07	-3.9	72	4659.36	15.46	3618.57	3270.22	899.51
ROV11 #3	30.11.07	-4.05	73	4565.30	5.96	3110.31	2625.76	1208.71
ROV13 #1	03.12.07	-3.6	40	1987.98	4.69	1607.54	1383.87	234.93
ROV13 #2	03.12.07	-3.7	46	2405.69	3.85	1832.02	1502.04	373.18
ROV13 #3	03.12.07	-3.6	46	2350.35	25.55	2201.51	2079.34	114.00
SW Sample	04.12.07	-1	34	2218.39	48.85	2193.45	2097.82	49.16

all concentrations are in $\mu\text{mol}/\text{kg}$, Temperature in $^{\circ}\text{C}$, Salinity in ‰

Calculations with dissociation constants of Millero

Using the constants of Millero et al. (2006) one gets different results. The minimum concentration of carbon dioxide is $0.2 \mu\text{mol}/\text{kg}$ while the maximum is $15.46 \mu\text{mol}/\text{kg}$. The highest values of dissolved inorganic carbon are at the beginning of the study. The lowest values around $1600 \mu\text{mol}/\text{kg}$ are in middle and the end of the sampling period. In sample ROV8#2 the smallest amount of $[\text{HCO}_3^-]$ occurs with $885.78 \mu\text{mol}/\text{kg}$. The highest value of bicarbonate can be found in sample ROV3#2 with $3352.42 \mu\text{mol}/\text{kg}$. The concentration of the carbonate ions varies only slightly around 1600 to $1800 \mu\text{mol}/\text{kg}$ in the first samples but then suddenly drop to half and even lower to a minimum of $234.93 \mu\text{mol}/\text{kg}$.

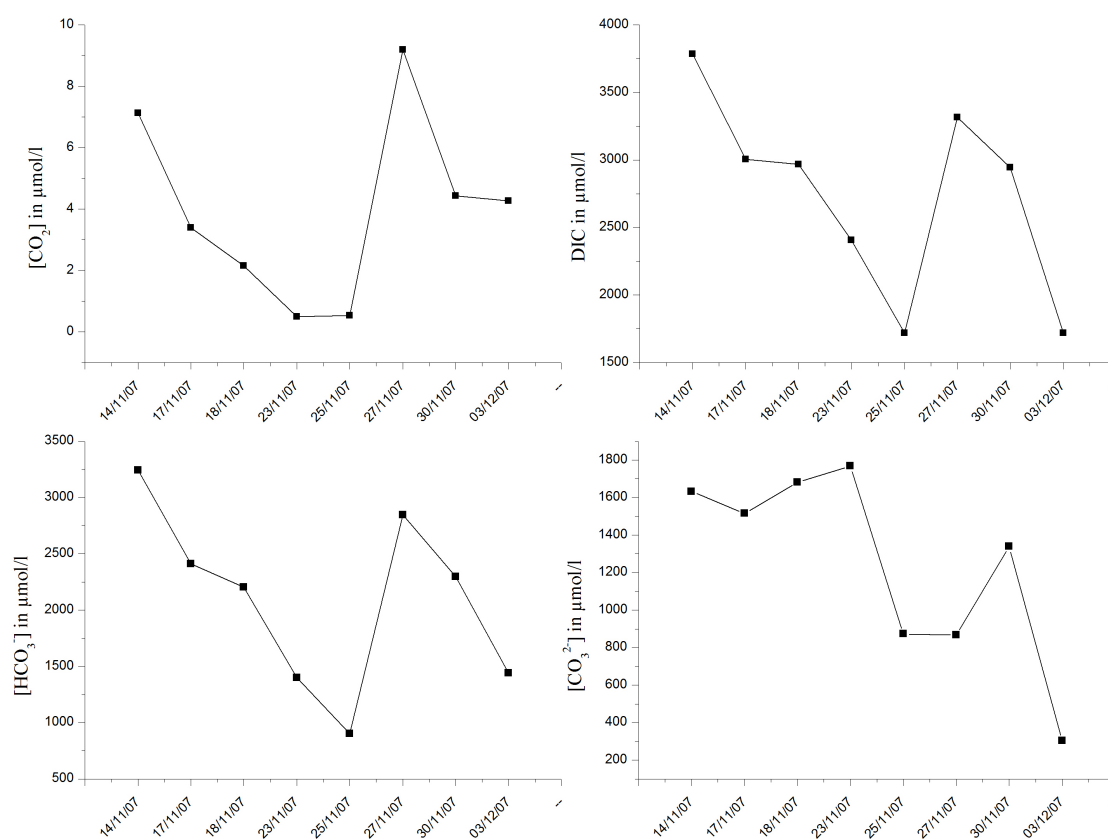


Figure 4.7: Concentration of the species of the carbonate system calculated with the dissociation constants of Millero et al. (2006)

The values of DIC, $[\text{CO}_2]$, and $[\text{HCO}_3^-]$ drop within the first 4 samples. The concentration of carbon dioxide stays on this level and rises with the values of DIC and bicarbonate. This increase is followed by another decrease until the end of the sampling period. The carbonate ions do not fluctuate over a wide range at the beginning, there is only a slight increase in the concentration. Remarkably here is a decrease of the values in sample ROV8. Staying on a constant level in sample ROV9 and ROV11

the concentration starts to increase again and results in a decrease to the lowest value at the end of the sampling period.

4.3 Distribution of ikaite

4.3.1 Total amount of ikaite in sea ice

The following data represent the second quantitative report of ikaite in sea ice. Providing even a larger number of samples this gives a more detailed view on the amount of the mineral which can be found in Antarctic sea ice. The samples represent values on different scales, since different volumes were taken. The typical thickness of one sample is 10 cm. But there are two other variations. First the samples have a thickness of 30 cm, because they were taken from the sackholes described in section 3.2.2. Second, due to field observations also samples on a smaller scale were taken. These samples were 2 cm thick. For an easier understanding these different scales will be described according to Neumeister (2007) as pico ($< 10\text{cm}$) and nano (0.1 to 1 m) scale.

Because of the sampling method (see section 3.2.1) the typical unit is mass per volume of melted sea ice in which the ikaite crystals are found. Additionally the absolute amount is provided in table D.1 on page 96.

The maximum absolute and the maximum relative amount of ikaite was found in samples from station ROV15 which is situated on 'old' ice only several hundred meters from the study site away at S66°39.276, E140°00.486. Remarkable 52.89 mg of the mineral were found in the bulk sample and 125.56 mg/liter melted sea ice from a 2 cm section from this station. Three samples show a concentration above 100 mg/liter melted sea ice. All of these samples are on the pico scale and were found in land-fast ice off Adélie Land. There are another thirteen samples with values of 10 mg of ikaite per liter melted sea ice and beyond. All of these samples are from the top layer of the sea ice body. The highest relative amount of ikaite within the samples from the SIPEX cruise is 9.49 mg/liter melted sea ice and does not reach the values from land-fast ice. But, this is also a value measured in the top layer.

However in most samples the amount of ikaite is less than 1 mg/liter melted sea ice and sometimes even lower than 0.1 mg/liter melted sea ice. The highest amounts were measured in first year land-fast ice. The young (≈ 3 month) ice did not contain such high amounts of ikaite.

4.3.2 Stratigraphic distribution of ikaite in land-fast ice off Adélie Land on the scale 0.1 – 1 m

During this study six complete ice cores, which were cut into 10 cm sections, provide an overview over the stratigraphic distribution of ikaite in the sea ice body in land-fast ice off Adélie Land. Figures 4.8, 4.9, 4.10, 4.11, 4.12, and 4.13 show that the values of ikaite in the top 10 cm of the sea ice body are by far the highest. Only in ice core ROV13 was the highest value measured in the section between 10-20 cm. However, the amount of ikaite in the top 10 cm of sample ROV13 (Figure 4.13) is almost still as high as in the section below. Therefore generally one can say that most of the mineral found in the top layer of sea ice. The values in this layer fluctuate between 1.2 and 93.03 mg/liter melted sea ice. Most of the cores have values lower or equal to 5 mg/liter melted sea ice. In the first three cores values in the lower part of the ice cores do not differ so much from each other. In ice core ROV7 (Figure 4.11) one can see a slightly higher value in the section between 10 and 20 cm than in the sections below. In ice core ROV9 (Figure 4.12) an increase of the amount of ikaite additionally occurs in the section between 20 and 30 cm. As already mentioned, ice core ROV13 (Figure 4.13) differs from the other ice core with respect to the stratigraphic distribution. The highest value was found in the first top layers between 0 and 20 cm. Furthermore the values in the lower parts behave differently as well. Showing an increase in the amount in the section between 30 and 40 cm after a strong decrease between the second and the third section in this ice core. The temperatures in the sea ice cores show a typical top down increase.

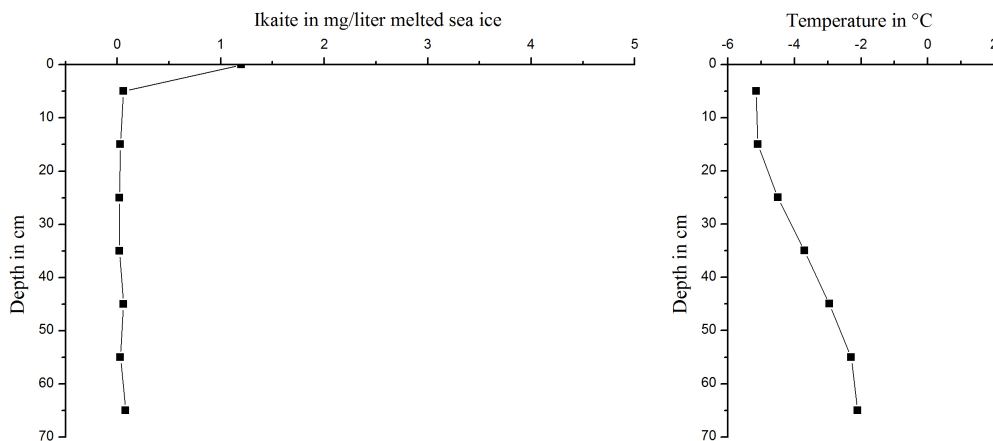


Figure 4.8: Ice core ROV3, $T_{air} = -4.8^{\circ}\text{C}$, land-fast ice

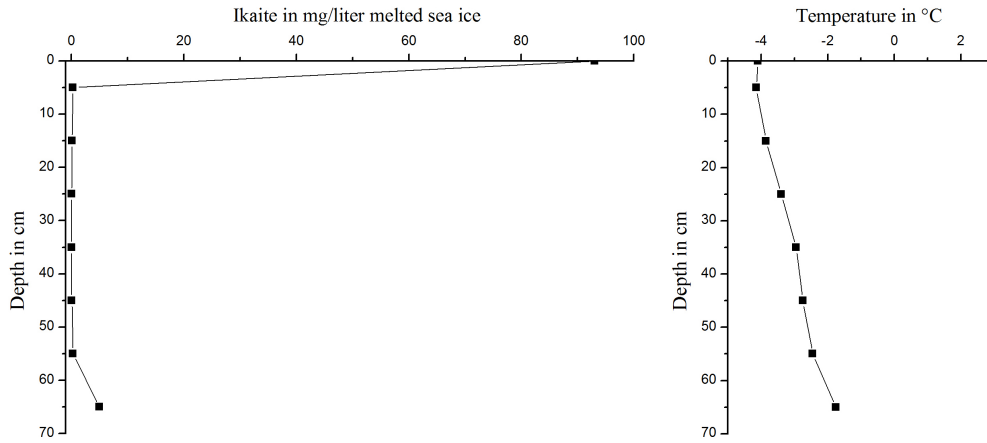


Figure 4.9: Ice core ROV4, $T_{air} = -3.2^{\circ}\text{C}$, land-fast ice

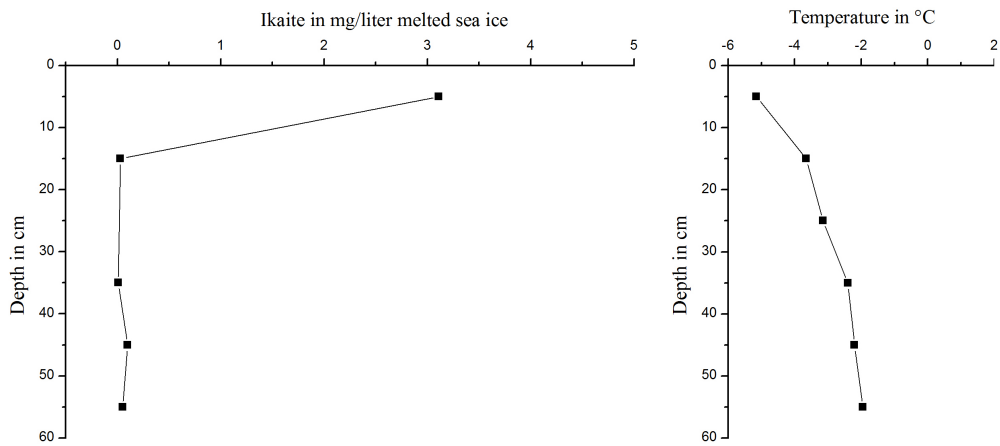


Figure 4.10: Ice core ROV6, $T_{air} = -3.1^{\circ}\text{C}$, land-fast ice

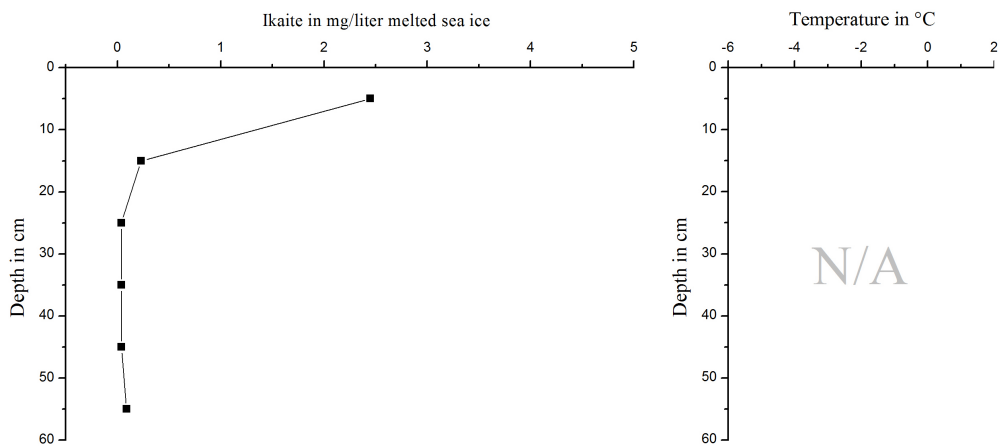
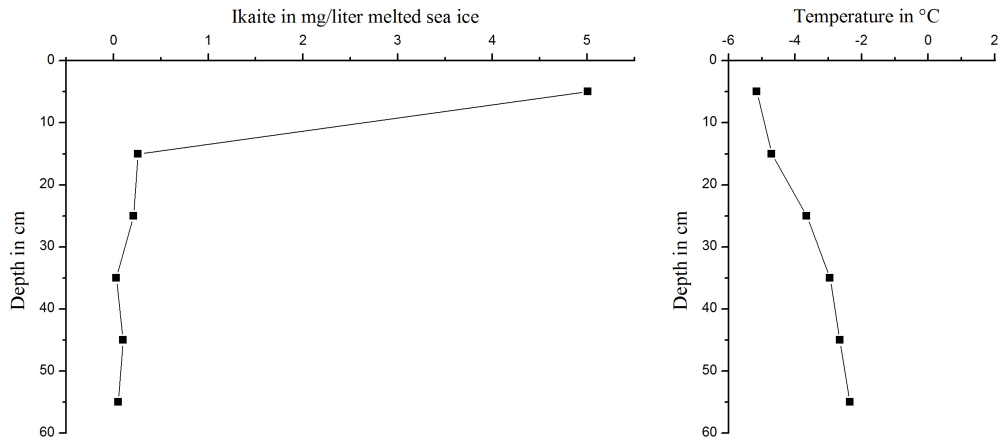
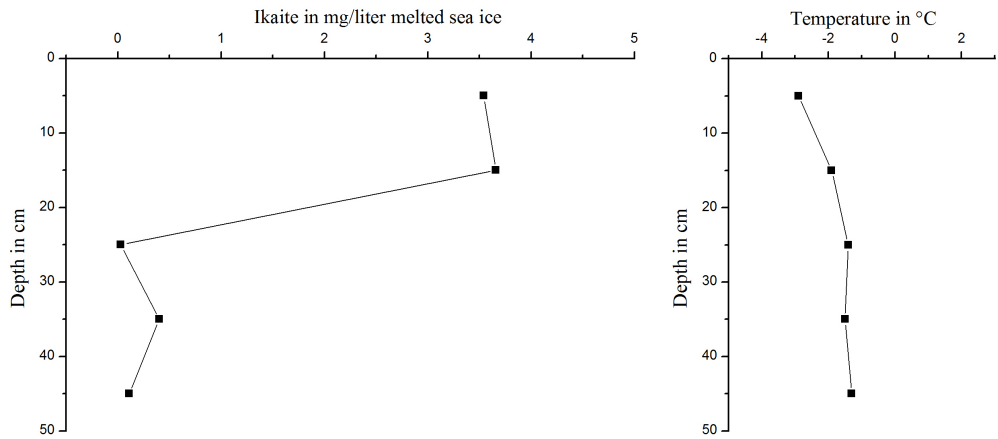


Figure 4.11: Ice core ROV7, $T_{air} = -1.9^{\circ}\text{C}$, land fast ice

Figure 4.12: Ice core ROV9, $T_{air} = 0.1^{\circ}\text{C}$, land-fast iceFigure 4.13: Ice core ROV13, $T_{air} = -2.3^{\circ}\text{C}$, land-fast ice

4.3.3 Stratigraphic distribution of ikaite in sea ice on the SIPEX cruise on the scale 0.1 – 1 m

From the SIPEX expedition data from 14 ice cores are available. Equal to the data from sea ice off Adélie Land the ice cores are divided in 10 cm sections providing the opportunity to compare the data between both sampling sites.

Even the stratigraphic distribution of the mineral ikaite is different to those from Adélie Land, one can say that most of the highest amounts of ikaite were also found in upper layer of the sea ice. However, it has to be noted that there are ice cores where the highest values are found in the lower layers. This is the case in SIPEX cores 3,5, 6 and 14 (Figure 4.16, 4.18, 4.19, and 4.27). In core 3 the highest amount of ikaite is higher than 2 mg/liter melted sea ice and was measured in the section between 30 and

40 cm. Due to missing values it is not possible to say if there might be higher values in the upper layer of this ice core. Core 5 (Figure 4.18) also has the highest values in a lower layer. With more than 4 mg ikaite per liter melted sea ice the highest value is in the section between 20 and 30 cm. Core 6 has two high values in the section between 0-10 cm and in the section between 20-30 cm. Interesting is core 14, since it shows generally the same pattern as the ice cores from Adélie Land. Although it is not very high, the section between 40 and 50 cm contains a slightly higher amount of ikaite than the layers above and below.

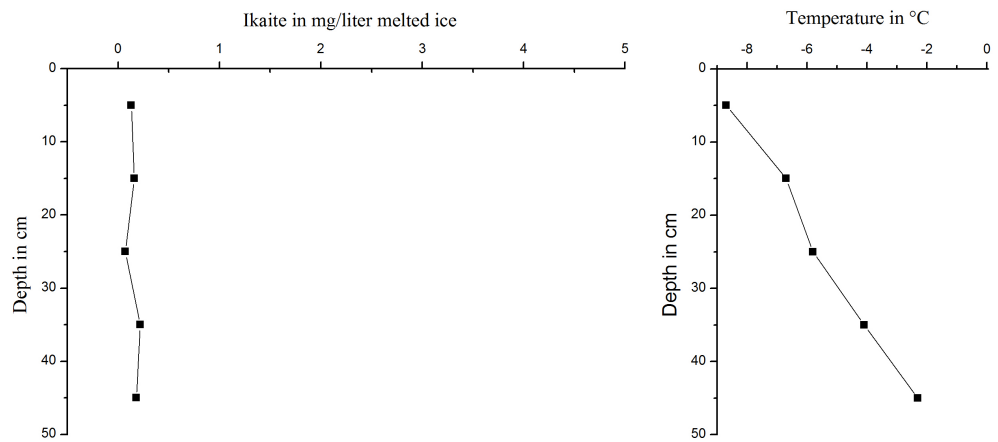


Figure 4.14: SIPEX ice core 1 at S64°13.773 E127°57.132, $T_{air} = -15.6^{\circ}\text{C}$, total ice thickness: 51 cm

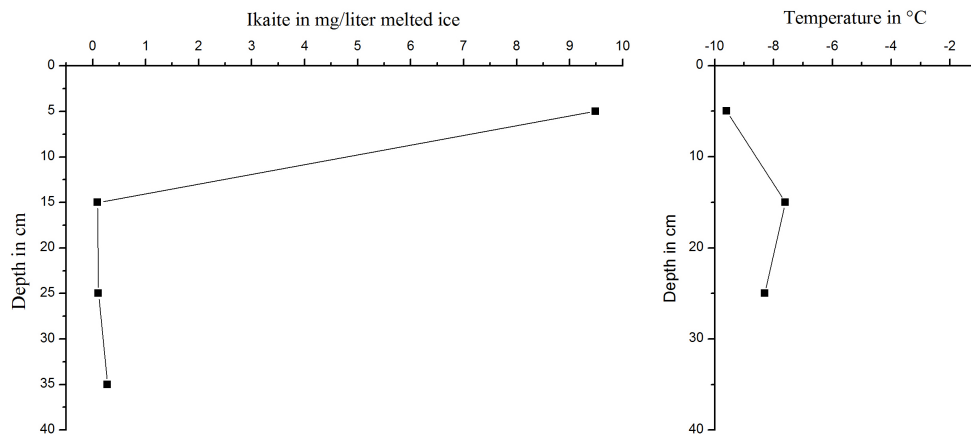


Figure 4.15: SIPEX ice core 2 at S64°29.42 E128°03.29, $T_{air} = -18.6^{\circ}\text{C}$, total ice thickness: 98 cm

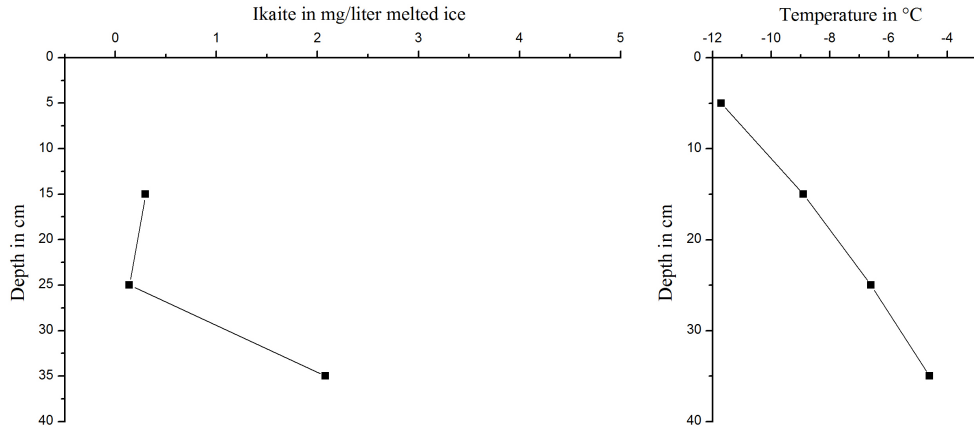


Figure 4.16: SIPEX ice core 3 at S64°23.390 E127°11.293, $T_{air} = -20.1^{\circ}\text{C}$, total ice thickness: 49 cm

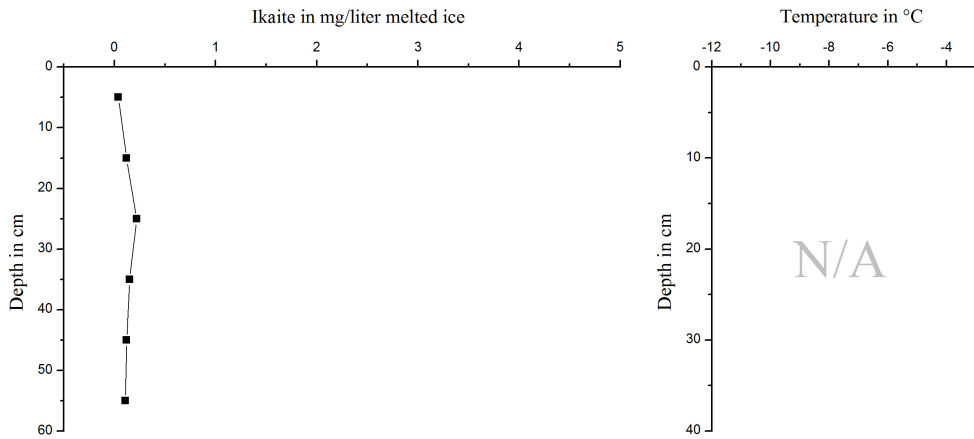


Figure 4.17: SIPEX ice core 4, position = N/A, $T_{air} = \text{N/A}$

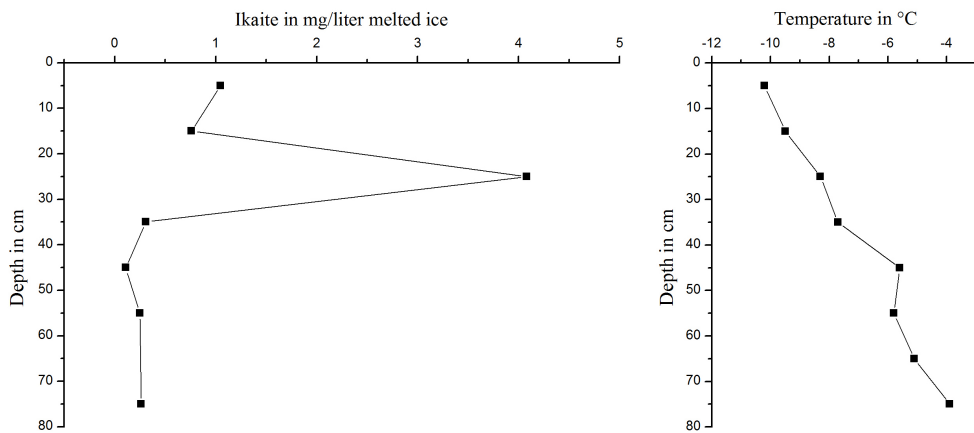


Figure 4.18: SIPEX ice core 5 at S65°31.465 E124°45.121, $T_{air} = -18^{\circ}\text{C}$, total ice thickness: 85 cm, more or less fast ice station between grounded icebergs

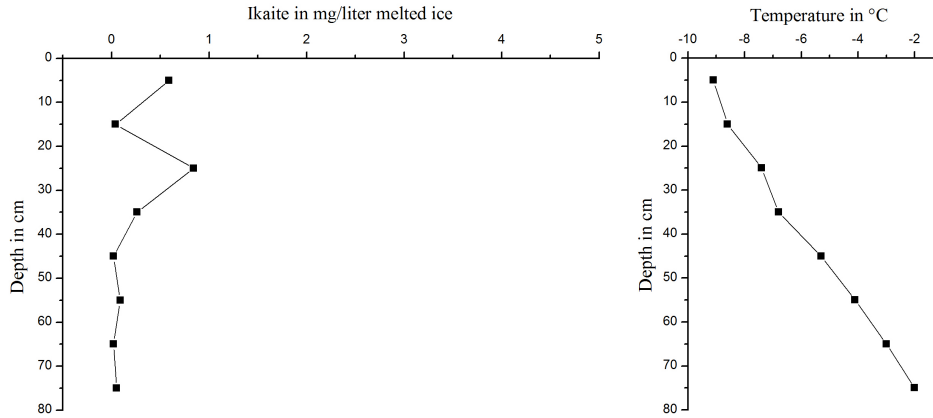


Figure 4.19: SIPEX ice core 6 at S65°35.304 E122°35.043, $T_{air} = -11.7^{\circ}\text{C}$, total ice thickness: 81 cm, heavily rafted floes, very fragile skeletal layer at bottom

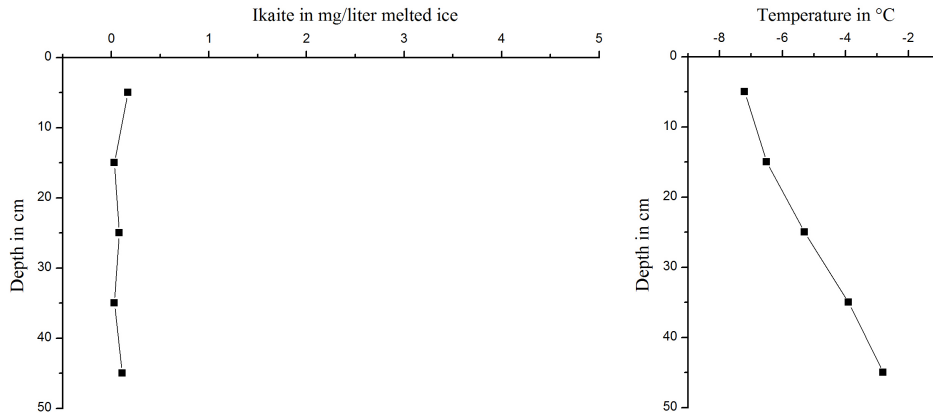


Figure 4.20: SIPEX ice core 7 at S65°33.492 E121°31.640, $T_{air} = -12.3^{\circ}\text{C}$, total ice thickness: 53 cm

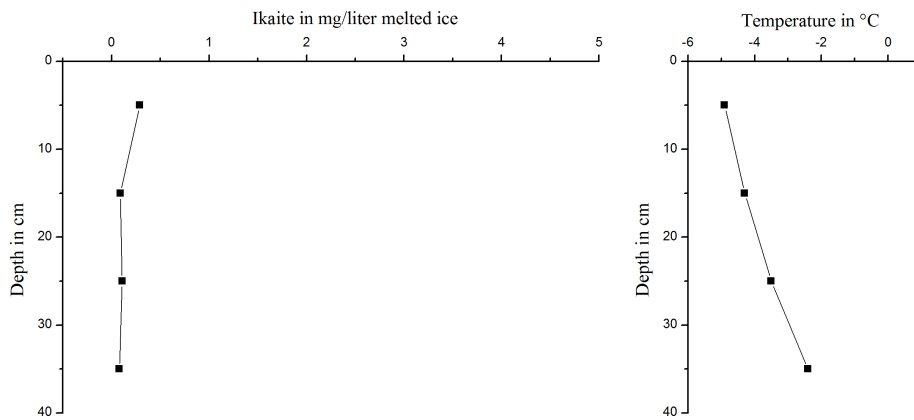


Figure 4.21: SIPEX ice core 8 at S65°33.281 E118°52.480, $T_{air} = -7^{\circ}\text{C}$, total ice thickness: 37 cm

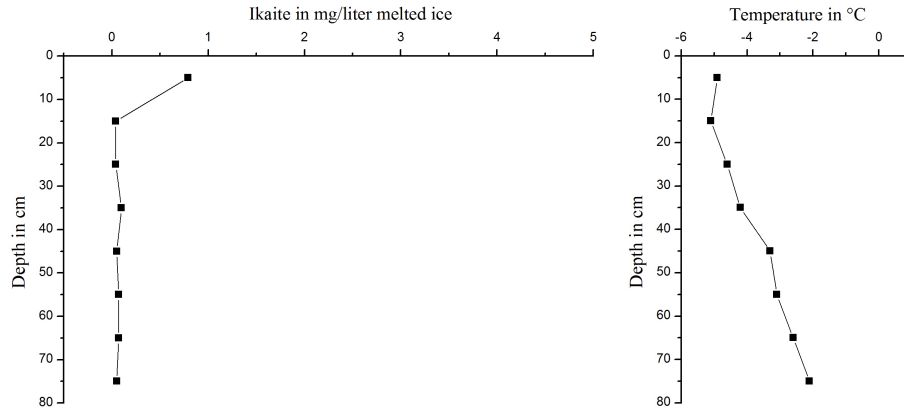


Figure 4.22: SIPEX ice core 9 at S65°20.612 E118°33.809, $T_{air} = -11.1^{\circ}\text{C}$, total ice thickness: 98 cm, region of heavily rafted and deformed ice

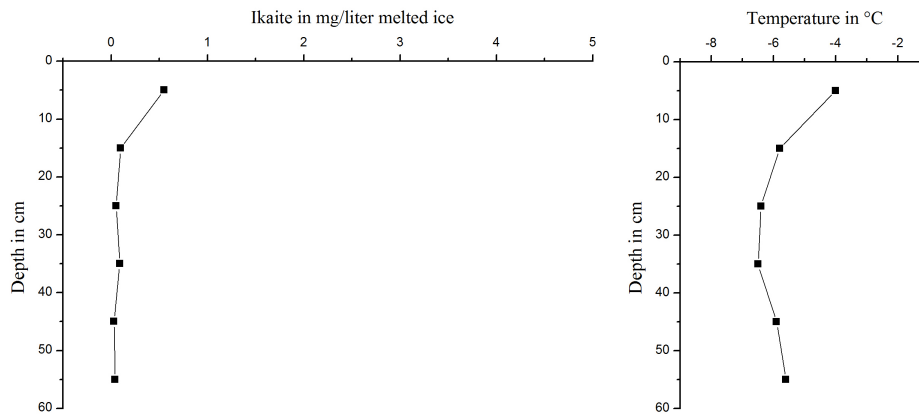


Figure 4.23: SIPEX ice core 10 at S64°56.549 E119°07.976, $T_{air} = -14.8^{\circ}\text{C}$, total ice thickness: 133 cm, coring site on an adjacent rafted area, negative freeboard

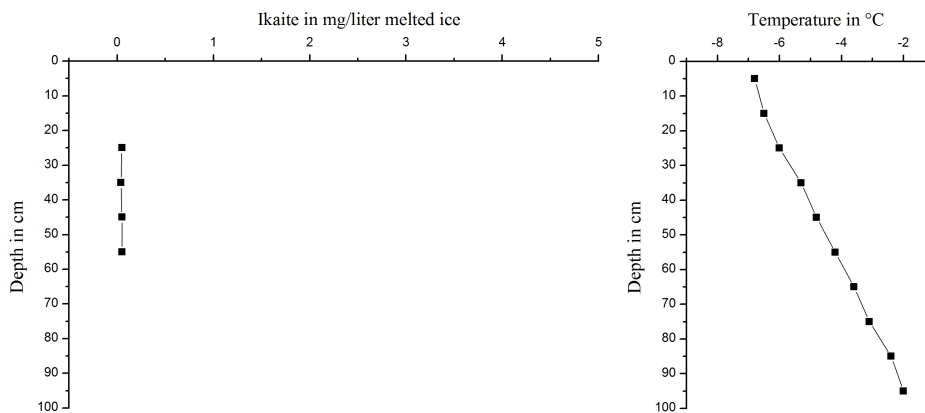


Figure 4.24: SIPEX ice core 11 at S65°01.496 E117°42.015, $T_{air} = -7.3^{\circ}\text{C}$, total ice thickness: 101 cm, rafted floe, ice surface very rough

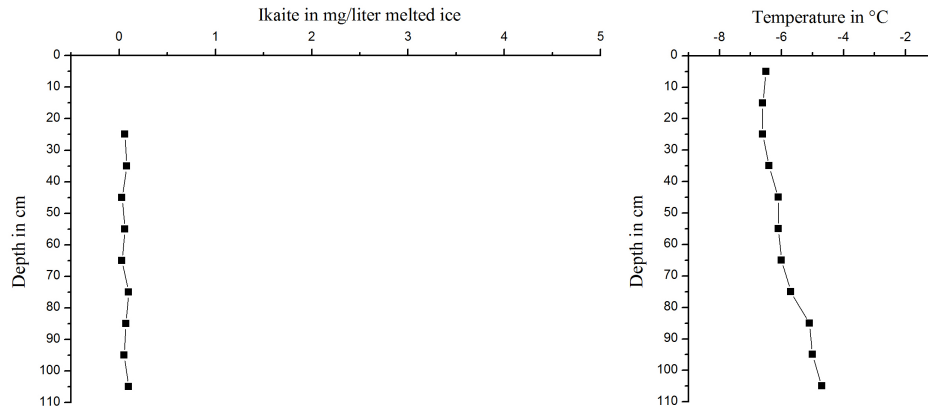


Figure 4.25: SIPEX ice core 12, $T_{air} = -6.9^{\circ}\text{C}$, total ice thickness: 187 cm, close to station 11 (1.5 nm)

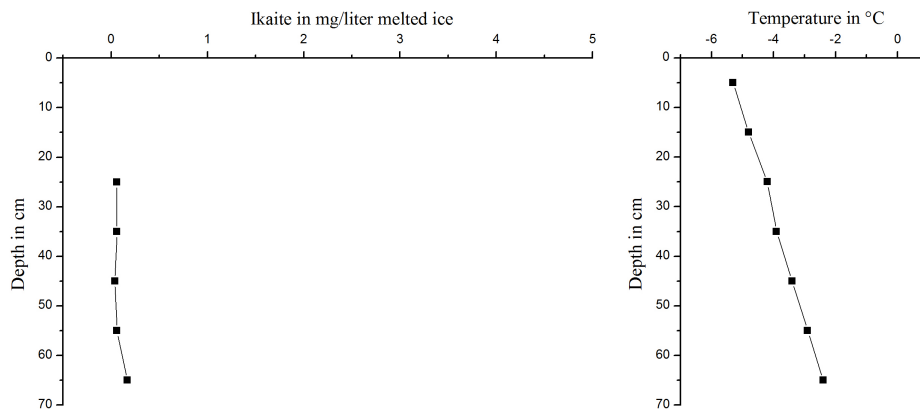


Figure 4.26: SIPEX ice core 13 at $S64^{\circ}44.436$ $E116^{\circ}49.274$, $T_{air} = -7.8^{\circ}\text{C}$, total ice thickness: 78 cm, rafted floes

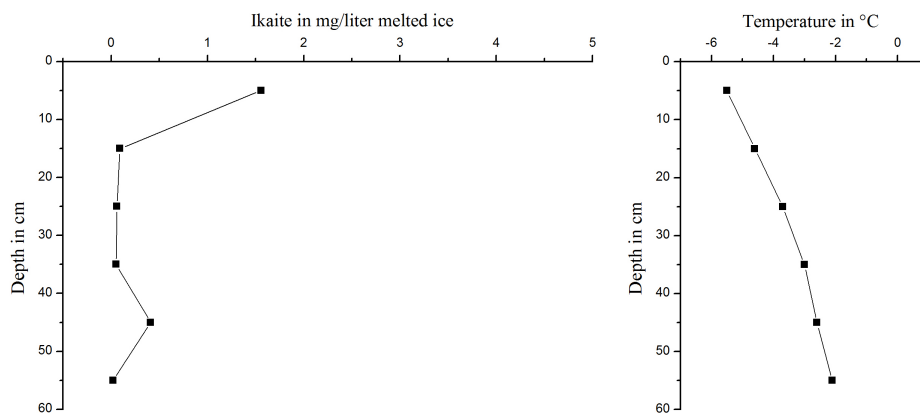


Figure 4.27: SIPEX ice core 14 at $S64^{\circ}18.483$ $E116^{\circ}49.594$, $T_{air} = -10^{\circ}\text{C}$, total ice thickness: 64 cm

Apart from the described outliers the samples from the SIPEX expedition show a similar behavior as those from Adélie Land. The values in the lower parts do not differ much from each other and are less than 0.5 mg ikaite per liter melted sea ice. The temperature profiles are similar and increase from the top down to the lower layer of the column. Only sample 10 is different. The higher temperature at the top results from the flooding of the ice floe.

4.3.4 Stratigraphic distribution of ikaite in land-fast ice off Adélie Land on the scale ≤ 10 cm

Due to the observations on field it was decided to reduce the sample sections to 2 cm instead of 10 cm. According to Neumeister (2007) this scale will be referred as pico scale (≤ 10 cm). Looking on the figures below we can see a massive increase in the relative amount of ikaite in the sample. The amounts exceed in some samples 100 mg ikaite per liter melted sea ice. Since these values are on a smaller scale, one can say that ikaite is definitively found in the very top layer of sea ice. The occurrence of the mineral tend to pile up in the top layer on the pico scale similar as on the nano scale.

Figure 4.28a is interesting. Here a complete core was taken including a layer snow on top. The values in the snow are also high. However, in the section between 6 and 8 cm where the transitions zone between snow and sea ice is located, the value suddenly increases by a factor of 2, followed by a decrease of the amount of ikaite. Figure 4.28b shows a high value in the top 2 cm with a decrease to low values similar to those from lower layers on the nano scale. This sample was taken on blank ice with no snow on top. Both samples were taken on the same date from young sea ice (≈ 3 month) and are from the same sampling site as ROV6 (see figure 4.29). The accumulation of the mineral occurs here in the first 4 cm and values then drop to low levels. Figure 4.29b shows a sample from first year ice which is older than 3 months. The ice thickness at this sampling point was 133 cm. The values are much higher than those from young sea ice and are constantly high down to the section between 8 and 10 cm. But also in layers below, ikaite was measured.

4.3.5 Temporal distribution of ikaite in land-fast ice off Adélie Land

In the study of Dieckmann et al. (2008) only single amounts of ikaite were measured. This study is the first to provide data about the amount of ikaite in sea ice over a certain time scale. Even though only six measuring points are available, this gives a first idea of the temporal distribution of ikaite in sea ice during austral spring. All

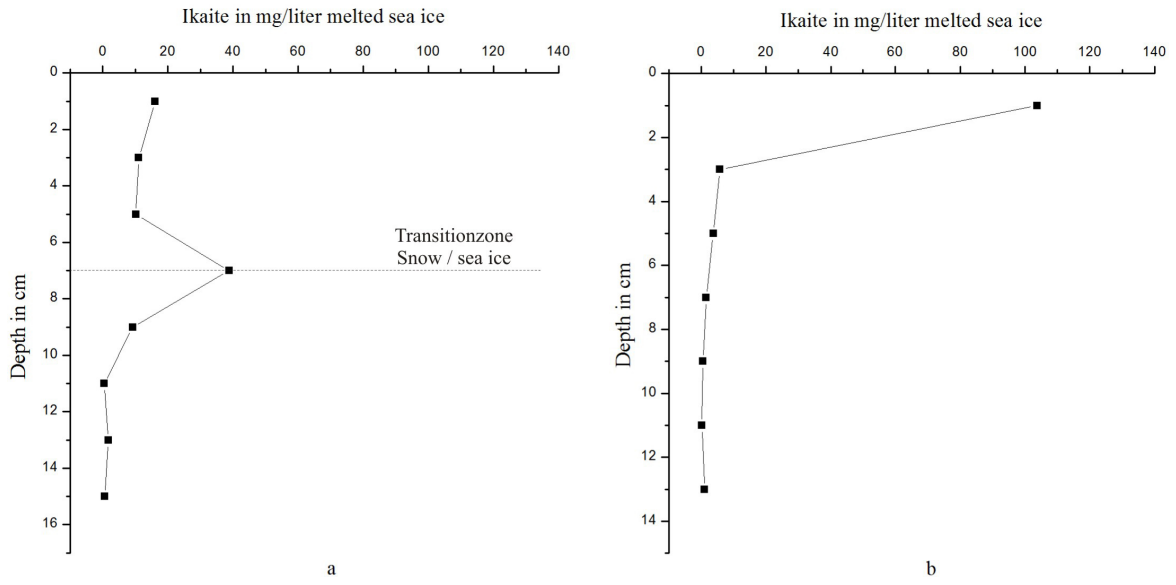


Figure 4.28: Ikaite on the pico scale a) ROV7 with snow on top, b) ROV7 without snow on top

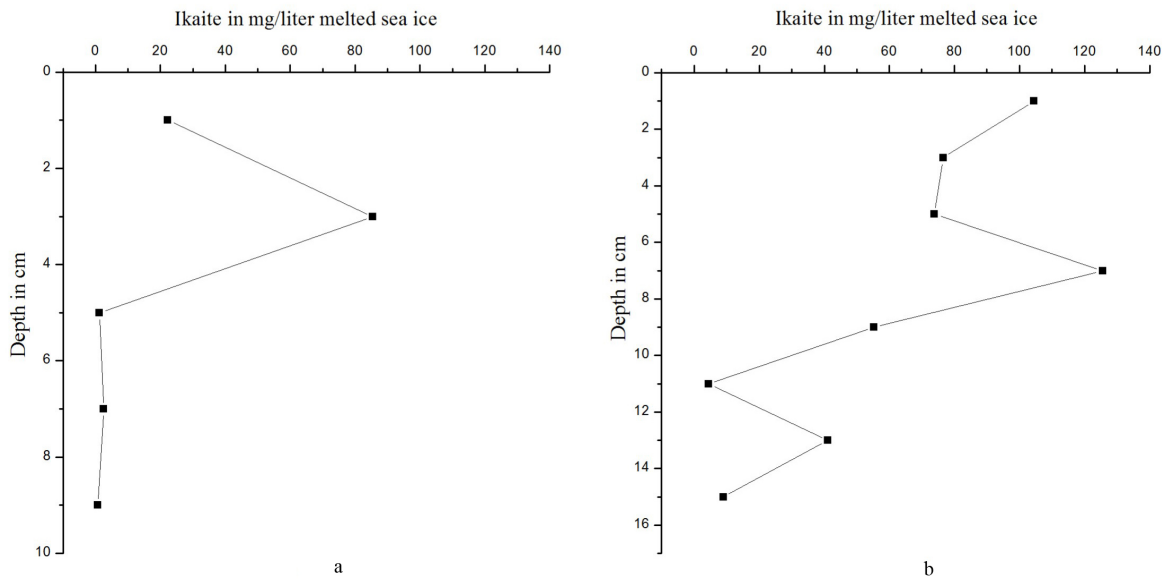


Figure 4.29: Ikaite on the pico scale a) ROV6 sample from young ice (≤ 3 month), and b) ROV15 sample from single year ice but older than the sea ice from the stations ROV3 to ROV13

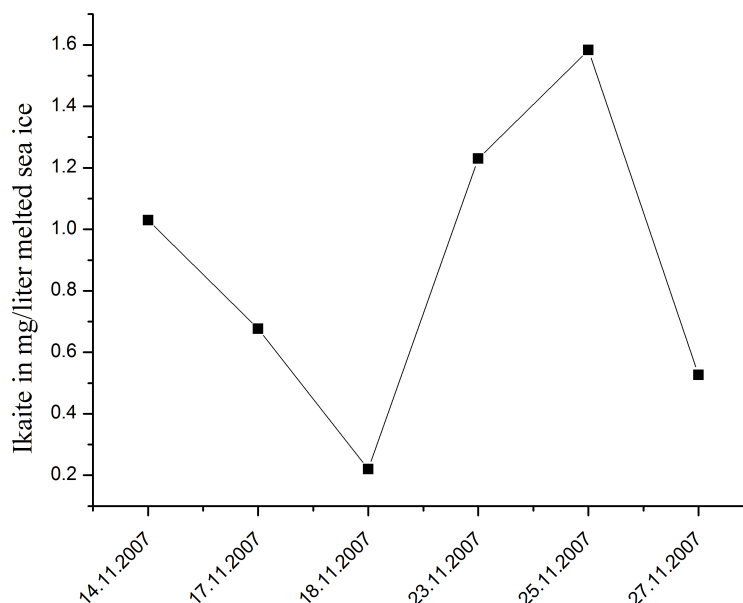


Figure 4.30: Temporal distribution of ikaite during Austral spring - sum parameter from sack hole ice cores

values are from 30 cm thick ice cores taken from the sack holes. Therefore these bulk samples refer to a different scale than the data from the sections above. Figure 4.30 shows that there is not a constant amount of ikaite over time. The values fluctuate. Starting with 1 mg ikaite per liter melted sea ice the values drop down to approximately 0.2 mg/liter melted sea ice. Followed by a strong increase up to 1.6 mg/liter melted sea ice which results in a repeated decrease down to approximately 0.5 mg/liter melted sea ice.

4.3.6 Spatial distribution of ikaite

The data of the amount of ikaite are from the first 10 cm of the sea ice body to minimize interferences by sea water, since the ice thickness was reduced to 30 cm due to thawing and rising temperatures. The sampling site was just 50 meter away from the site where the sack holes were drilled. The values are not as high as in the first top 10 cm of the complete ice cores which were taken at the beginning of the sampling period. Figure 4.31 shows a contour map of the distribution of the mineral ikaite in the first 10 cm of land-fast sea ice on a field with a size of 20m by 20m. This contour map is an interpolation of the point data described in section 3.2.7 using the method of punctual Kriging. The interpolation was calculated with the help of the software "Surfer 8".

The figure shows 4 "hot spots" with up to 4 mg ikaite per liter melted sea ice. However, a wide area seem to be homogeneous with respect to the distribution of ikaite, showing similar amounts of the mineral.

Additionally, the ice thickness was measured at each sampling point where the amount of ikaite was determined. Using the same method of punctual Kriging the ice thickness of the same area was interpolated. Figure 4.32 shows a homogeneous ice thickness of around 30 cm with one exception where the ice thickness exceeded 40 cm. This exception is at the same location where the highest values of the mineral ikaite are. For the other hot spots with high values of ikaite no similar hot spot with respect to ice thickness was found.

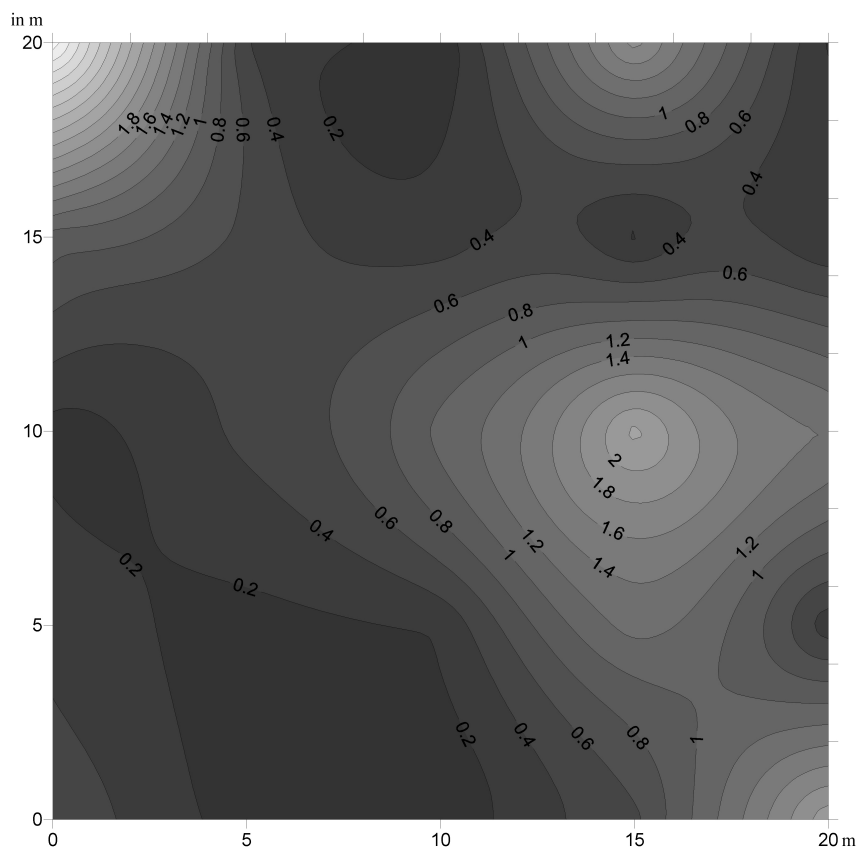


Figure 4.31: Contour map of the distribution of ikaite in the first 10 cm of land-fast ice in an area of 20m^2 , amount of ikaite in mg/liter melted sea ice

4.3.7 Additional measurements of ikaite

Due to first field observations some extra measurements were carried out. For example several snow samples and a scratch sample from the top of the sea ice were taken. The snow samples contain between 0.02 and 4.95 mg ikaite per liter melted snow depending on the depth of the snow. The snow sample from ROV9 where the snow depth was 40 cm the amount is very small, whereas a sample from a location with less snow shows the highest amount of ikaite in snow. The scratch sample from the top of the ice shows

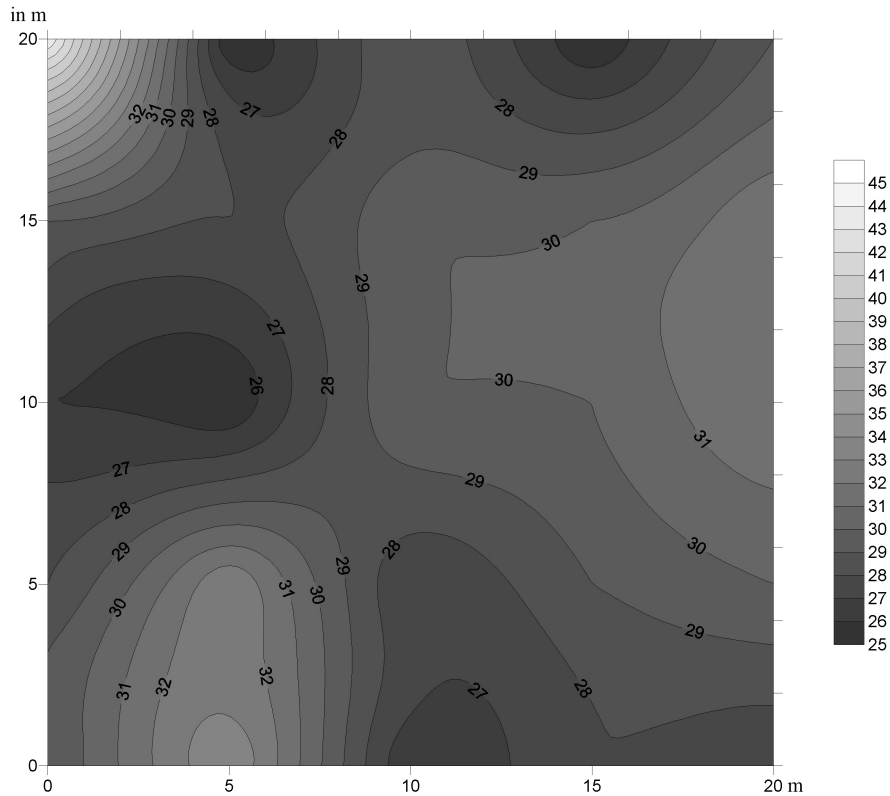


Figure 4.32: Contour map of sea ice thickness of a 20m², sea ice thickness in cm

a remarkable amount of almost 40 mg ikaite per liter melted sea ice. See Appendix D.1.

4.3.8 Ikaite in continental firn ice

After the sampling period an ice core was drilled in firn ice on the continent near Prud'homme. The ice core was 1 m long and cut into three equal sections for further processing. Despite the expected non existence of ikaite in firn ice, small amounts of the mineral were found. The values are between 0.07 and 0.12 mg/liter melted ice. There is no significant stratification, since the values are close together.

Chapter 5

Discussion and conclusion

5.1 Discussion of methodology

5.1.1 Sampling techniques

The applied sampling techniques are standard techniques described by Horner et al. (1992) and are used in most studies (Gleitz et al., 1995; Delille et al., 2007; Papadimitriou et al., 2007, Dieckmann, G.S. personal communication 2007). Critical points of the applied techniques will be discussed in this section.

Ice core sampling is simple and often done using an ice corer with a diameter of 9 cm. However, using this technique, the ice core should be processed quickly. Delays in processing will lead to inaccurate data. For example a delay may causes incorrect temperature profiles due to warming of the ice core. Using an ice core for determination of CaCO_3 crystals, a delay could lead to a loss of minerals due to rejection of brine from the ice core. Therefore two ice cores where taken close to each other to reduce such source of errors. In contrast to the described use of a gasoline motor in other studies, a battery driven drill was used, allowing quicker processing and easier handling while taking the ice cores. However, it has to be remembered that the ice was quite warm and this technique has not yet been tested in cold sea ice with temperatures below -10°C .

Brine sampling was carried out as described by Gleitz et al. (1995); Papadimitriou et al. (2007) and Delille et al. (2007). Beside this widely used method the only known alternative method is centrifuging the ice core in a refrigerated centrifuge (Horner et al., 1992). However, this method is not appropriate since it is time consuming and requires a larger logistic effort. Although, the method of collecting sea ice brine in predrilled sackholes is used in all studies analyzing sea ice brine some problems are left. The brine which penetrates into the sackhole is not from the core itself, which is taken

from this location, but from the surroundings. Therefore looking on a smaller scale the analyzed brine is not in direct relation to the precipitated calcium carbonate which was found in these cores. Strictly seen, this is a bulk sample since the brine penetrates over the whole 30 cm and even from the bottom into the sack hole. This makes it impossible to draw direct conclusions on the relation of the precipitation of CaCO_3 and carbonate chemistry on the pico scale or even smaller. Therefore other methods should be developed to understand the precipitation of calcium carbonate in sea ice. Such a method for reconstructing temperatures at which the mineral precipitates could use for example stable isotope fractionation as suggested by Kennedy (personal comm.) based on methodologies outlined by Romanek et al. (1992); Rickaby et al. (2006) and Kim et al. (2007). Up to now it is only possible to provide bulk data on the cm scale whereas brine pockets and calcium carbonate minerals are on the μm or mm scale.

5.1.2 Measured chemical values

In this study, pH , total alkalinity and salinity were measured at the research station within a short time after sampling. Calcium for quantitative determination of ikaite was measured in the home laboratory using ICP-OES (see section 3.4).

According to Gleitz et al. (1995) pH and total alkalinity were measured to calculate $[\text{CO}_2]$, DIC and other values of the carbonate system in sea ice brine at in-situ temperatures. Measuring pH in sea ice brine has shown several problems. First of all brine is a highly saline solution. Even though there are solutions for measuring pH in saline solutions like seawater (see section 2.3.3), sea ice brine reaches higher salinities which also alter in relation to temperature. Salinities between 35 and beyond 100 are possible. Delille et al. (2007) tried to solve this problem by preparing pH -buffers at different salinities up to 80 psu. This is an option to reduce uncertainties but buffers at a certain salinity might be missing since salinities in brine could not be predicted. To avoid this, pH was measured on the NBS scale and then transferred to pH_{SWS} by using the activity coefficient f_H (see section 3.2.5). However, f_H was determined using empiric data. Thus, this might be another source of error.

Another problem measuring pH occurred during the sampling. The measurement of pH was carried out in the laboratory within a short time after sampling. However, even using gas tight tubes, this short time could be enough to change pH due to degassing of CO_2 . The pH -meter was calibrated at low temperatures similar to Delille et al. (2007), but still not at temperatures as found in sea ice. Resulting from these findings alternative, more accurate methods for determining carbonate chemistry within highly saline solutions should be discussed. For example one could use the measurement of DIC and alkalinity to calculate all other species of the carbonate system.

The measurement of total alkalinity is not affected by CO₂ exchange between air and sample. Therefore this method does not suffer from the sampling method like the measurement of *pH*. The calculation of alkalinity using equation 3.3 on page 37 needs only one measuring point. This allows a fast processing of the samples. However, in the literature a potentiometric titration is recommended using the Gran method (Edmond, 1970; Dickson, 1981; DOE, 1994). Since this method provides more accurate data it should be applied when only a few samples exist.

The measurement of calcium with the optical emission spectroscopy (see section 3.4 on page 38) for indirect quantitative determination of the mineral ikaite emerged as a suitable method. This method is easy to apply and gives accurate values. However, this method is only possible when 100% of the same mineral is found. As soon as there are different minerals like vaterite, calcite, ikaite, and aragonite this method is no longer adoptable. However, this method allows the calculation of the quantity of carbonate which is bound in precipitated calcium carbonates.

5.2 Discussion of results

5.2.1 Species in the carbonate system

Dissociation constants and calculated values

In section 2.3.2 the difficulties of the applied dissociation constants are already highlighted. Hence, two different sets of constants were used in this study. The dissociation constants from Mehrbach et al. (1973) refitted by Dickson and Millero (1987) and the constants from Millero et al. (2006) were chosen. The former were used in the latest study on the dynamics of the carbonate system within natural sea ice by Delille et al. (2007) and the latter are the youngest determination of the dissociation constants. Although these constants of Millero et al. (2006) have never been used for calculations of the carbonate system in highly saline solutions, they are the only ones which drop with increasing salinity (see figure 2.3.2 on page 13 and 2.3.2 on page 14) as described by Zeebe and Wolf-Gladrow (2001).

According to the large differences between the different sets of constants at high salinities the values of the species of the carbonate system vary as well. Figure 5.1 shows the difference between the the calculated values using the constants of Dickson and Millero (1987) and Millero et al. (2006), respectively. The largest variation occur in the concentrations of carbon dioxide and carbonate ions. However, also the other species show differences, though they are not as large. The concentration of carbon dioxide varies by up to a factor of 3.

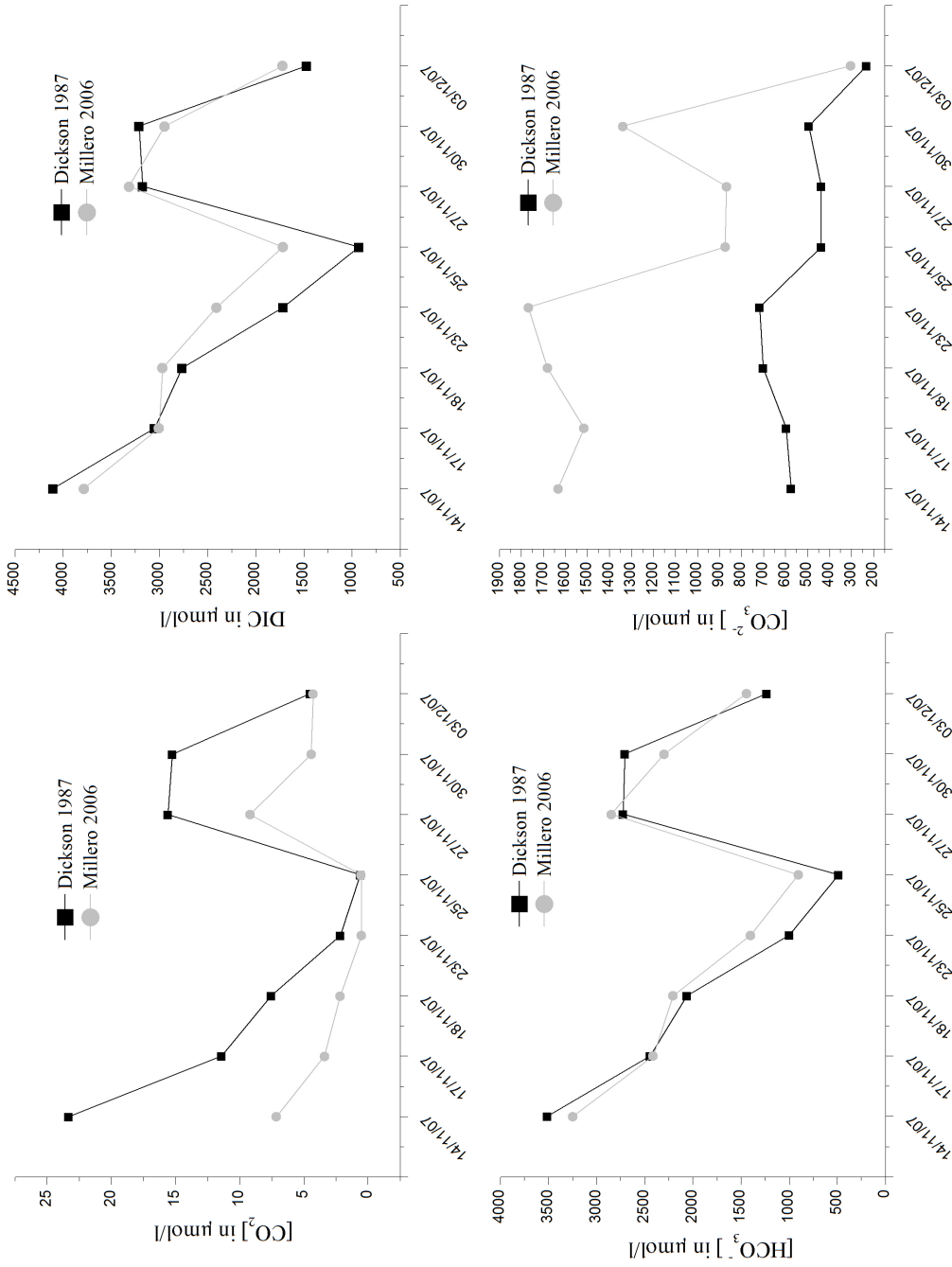


Figure 5.1: Comparison of the calculated concentrations of the species in the carbonate system using the dissociation constants of Dickson and Millero (1987) and Millero et al. (2006)

The concentration of $[\text{CO}_2]$ at the beginning of the sampling period is about $7.5 \mu\text{mol}/l$ calculated with the constants of Millero et al. (2006) and almost $25 \mu\text{mol}/l$ calculated with the constants of Dickson and Millero (1987). This difference reduces over time down to almost zero in the middle of the sampling period. Followed by an increase the difference reduces again at the end of the period. The same pattern occurs for the concentration of the carbonate ions but the other way around. Here the values calculated with the constants of Millero et al. (2006) are much higher than those calculated with those of Dickson and Millero (1987). The variations are up to $1100 \mu\text{mol}/l$ and reduce down to approximately $500 \mu\text{mol}/l$. The difference here does not drop to zero but reduces also over time and reincreases at the end of the sampling period. The difference within the concentrations of dissolved inorganic carbon and $[\text{HCO}_3^-]$ are small but noticeable.

The variations correlate with the salinity of sea ice brine. The higher the salinity the higher the differences within the concentration. This effect can be expected, since the differences between the dissociation constants occur at salinities above 50 psu (see section 2.3.2). Figure 5.1 on the preceding page shows a obvious problem with respect to the dissociation constants in high saline solutions. All dissociation constants provided in the literature are valid to a maximum salinity of 50, sometimes even less. Though the dissociation constants for carbonic acid of Millero et al. (2006) are the only constants which drop with increasing salinity as described by Zeebe and Wolf-Gladrow (2001) they are not valid for salinities above 50. The same occurs with the constants of Dickson and Millero (1987) which are not valid for such high salinities found in sea ice brine. Hence the values of the carbonate system which are calculated with these constants should be handled with care. This has also be taken into account if one looks on values provided in the literature (i.e. Gleitz et al. (1995)). Also other values from studies which use dissociation constants for carbonic acid mentioned in section 2.3.2 have the same problem, since their used dissociation constants also increase with the increase of salinity. This leads to data which can not be classified. Even, if I assume that the dissociation constants of Millero et al. (2006) are the proper constants, it is not sure if the calculated values are accurate enough. Since the values of $[\text{CO}_2]$ differ between $7.5 \mu\text{mol}/l$ and $25 \mu\text{mol}/l$, the difference is to big to use these values for further calculations (i.e. the budget calculation of carbon dioxide in sea ice or polar regions respectively). Resulting from these findings there is a definitively demand for dissociation constants for carbonic acid in highly saline solutions such as sea ice brine. The constants should be valid for salinities far beyond 100 psu, since brine salinity easily rises up to such values. Furthermore these constants should be validated for subzero temperatures.

Due to these huge uncertainties it is not possible, in reasonable bounds of this diploma thesis, to determine a relation between the concentration of the carbonate species and the precipitation of calcium carbonate before a valid set of dissociation constants for carbonic acid exist.

Comparison with data from various workers

Three studies on sea ice brine biogeochemistry exist in the literature. Gleitz et al. (1995) and Papadimitriou et al. (2007) investigated sea ice brine in the Weddell Sea, whereas Delille et al. (2007) have done research on brine in land-fast sea ice off Adélie Land. Those studies provide data on different values, such as salinity, temperature, nutrients, O_2 , DOC, DON, silicic acid, TA, pH, and dimethylsulfide (DMS). Furthermore they determined the carbonate system but they do not provide data for all species mentioned above.

The values of the carbonate system provided by Gleitz et al. (1995), Papadimitriou et al. (2007), Delille et al. (2007), and this study are difficult to compare. They all use different sets of dissociation constants for carbonic acid. Only this study uses two sets of dissociation constants whereas one set is the same as used by Delille et al. (2007). However, Delille et al. (2007) provide only data on pCO_2 . All other authors provide $[CO_2]$ in sea ice brine. Since the exact values for salinity and temperature are missing in the study of Delille et al. (2007) it is not possible to calculate the concentration of carbon dioxide from pCO_2 and thus to compare the data with values of Gleitz et al. (1995), Papadimitriou et al. (2007), and this study.

It is for example possible to discuss the data of Gleitz et al. (1995) and this study. Focusing on the concentration of carbon dioxide the values of Gleitz et al. (1995) are similar to this study at low salinities. However, at high salinities Gleitz et al. (1995) report values of CO_2 up to $87 \mu mol/l$ which are much higher than those values calculated in this study. According to section 5.2.1 these high values of Gleitz et al. (1995) should be seen with reservations. This results from the used dissociation constants of Roy et al. (1993), as they behave in a similar way like the constants of Dickson and Millero (1987) where pK_1 and pK_2 rise with increasing salinities, starting from 50 psu (see figure 2.3.2 on page 13 and 2.3.2 on page 14). Therefore, these values should be recalculated when a proper set of constants exists which is valid for highly saline solutions at subzero temperatures. However, a comparison of the temporal distribution is not possible, since they do not provide such data. Even though Papadimitriou et al. (2007) provide 36 measurements over 22 days these values do not come from the same location. Hence, also this data can not be compared on a temporal scale. The values of carbon dioxide are very similar to the values calculated in section 4.2.4. The salinities

in the study of Papadimitriou et al. (2007) are only up to 63, therefore there is not such a problem with the concentrations like in the study of Gleitz et al. (1995) and this work. Comparing the values of carbon dioxide one can say that the concentrations fluctuate between 1 and approximately $15 \mu\text{mol}/\text{l}$ at low salinities. If the salinity rises beyond 50 or so, yet there is no clear data, since no valid dissociation constants exist. However, I assume that the values calculated with the constants other than those of Millero et al. (2006) are too high.

Only the work of Delille et al. (2007) provide data on the temporal distribution of carbon dioxide. More precisely the partial pressure of CO_2 . In contrast to this study the values of CO_2 drop all the time and no oscillation occurs. This originates from the continuous rising of the temperatures of the brine.

Other calculated values of the carbonate system are not provided in the literature. Only data of dissolved inorganic carbon and total alkalinity are provided. But these values coincide with the data of this study and no significant differences were found.

5.2.2 Distribution of ikaite

Different amounts of ikaite in sea ice were found. Samples exist from young land-fast sea ice (≈ 3 month), single year land-fast ice (> 3 month), and pack ice. The samples in land-fast ice were taken in November 2007 and the samples in pack ice in September and early October 2007. The highest value of ikaite was found in old land-fast sea ice whereas the smallest values occurred in pack ice. The small amounts in pack ice might result from the continuous movement of the ice floes which leads to an enhanced drainage of sea ice brine and therefore to a reduction of the mineral since it follows the path of the brine. However, this depends on the temperature. Sea ice as moved by the wind and tides causes breakage and occasionally forces parts of the floe below freeboard, flooding the ice surface with sea water. Similarly, heavy snow cover can also force the ice floe below freeboard, resulting in surface flooding. Hence, the brine is diluted changing the thermodynamic equilibrium and leading to smaller precipitation of calcium carbonate. Also time seems to play an important role in the precipitation of CaCO_3 . Since in the Antarctic more than twice as much first-year ice develops in contrast to the Arctic (Arrigo, 2003) the pack ice is young and this seems to result in a reduced precipitation of CaCO_3 . But even in land-fast ice differences were found. In young land-fast ice less ikaite was found than in older single-year ice. This shows that the precipitation of calcium carbonate seems to be a continuous development over time.

Precipitation of calcium carbonate is not homogeneous within the sea ice body. In land-fast ice the highest amount of CaCO_3 was found in the top layer of sea ice.

More precisely these high values occur in the first few centimeters from the top. This phenomenon can be explained with the observations of Rysgaard et al. (2007), when DIC is rejected together with brine from the sea ice. Following Arrigo (2003) that land-fast ice is mostly columnar ice this favors the drainage of brine to the underlying water column. Hence also ikaite crystals might be transported downwards as well. However, this evidence is inconclusive and further investigation is needed. On the other hand when dissolved inorganic carbon is rejected together with brine to the water column the thermodynamic equilibrium is not exceeded, thus leading to an undersaturation with respect to CaCO_3 and no precipitation takes place.

Though most ice cores from the SIPEX expedition show the same pattern as the ice cores from sea ice off Adélie Land, in some ice cores this pattern is not observed. Analyses of the figures in section 4.3.3 shows that the highest values of ikaite in some cores are found in deeper layers within the sea ice. The ice cores in which the highest values are not in the top, were taken from locations with rafted ice floes. The explanation for this phenomenon is trivial and simple. Ice floes with high concentrations with respect to CaCO_3 in the top layer raft over each other, thus creating two layers where high concentrations of calcium carbonate exist.

However, a temporal oscillation is observed during the sampling period (see section 4.3.5 on page 61). The maximum value¹ of ikaite was measured on 25th November. Analyzing the development of total alkalinity (TA), dissolved inorganic carbon (DIC) and the amount of ikaite between 18th and 25th November shows a significant relation. Focusing on the data calculated with the dissociation constants of Dickson and Millero (1987) one gets a ratio of $TA : DIC \approx 1$. This shows a degassing of the produced CO_2 as predicted by Papadimitriou et al. (2007). However, if one considers the values calculated with the constants of Millero et al. (2006) the ratio $TA : DIC$ changes to ≈ 1.6 . This would result in a fractional degassing and accumulation of CO_2 in solution respectively (Lazar and Loya, 1991, cited in Papadimitriou et al. (2007)). These two different results show, obviously, the demand for valid dissociation constants for carbonic acid to determine whether CO_2 is degassing or not. However, analyses of the values between 14th and 18th November does not show any significant relations. Due to sea ice warming ikaite could be rejected to deeper levels (see figure 4.9) and CO_2 values were dropping probably following the same pattern or carbon dioxide is consumed due to primary production. But this remains inconclusive.

Obviously there are additional processes controlling the precipitation of CaCO_3 , but those are not known and can not be fully assessed yet. For the precipitation of

¹It has to be considered that these values were measured in a 30 cm ice core. Therefore these values can not be compared with values from 2 cm or 10 cm sections

ikaite inhibitors such as phosphate are suggested to be responsible (Gal et al., 1996). This and other possible biogeochemical processes have to be analyzed in further studies to unravel the precipitation of the mineral ikaite and its impact on the CO₂ cycle in polar regions.

5.2.3 Ikaite in firn ice

Primarily the ice cores in continental firn-ice were taken to provide evidence that ikaite only develops within sea ice in polar regions. However, small amounts of ikaite were found. Since there is no carbonate system in Antarctic firn ice like in sea ice or brine in which chemical processes take place there must be another source of the mineral. These findings support the hypothesis of Sala et al. (2008) that calcium carbonates derive from sea ice surface. The minerals seem to be transported by aeolian processes to the continent. Even events of air mass advection from the sea ice surface to the continent are rare but likely to occur (Sala et al., 2008). This hypothesis is furthermore supported by the finding of ikaite in snow samples from the sea ice. This snow can easily be "eroded" by aeolian processes and transported to firn ice.

Considering the main wind direction and events of catabatic winds from inland and the finding of ikaite in the top layer of sea ice and in snow samples, I assume that most of the precipitated calcium carbonate will be transported to the open sea. But this too remains inconclusive.

5.2.4 Spatial distribution

In section 4.3.6 a almost homogeneous distribution of ikaite in sea ice is shown. However, this is interrupted by several spots where significantly higher values of the mineral were observed. Since the sea ice was more than 70 cm thick at the beginning of the study, the thickness reduced to a value of around 30 cm. This shows a massive thawing and that sea ice can be considered as rotten at this stage. Therefore this experiment should be repeated, since this one determination could only be seen as snapshot at this special time. In sections of lower values, ikaite might have been transported already to the underlying water column, thus falsifying this experiment.

5.2.5 Significance for the CO₂ cycle in polar regions

Jones and Coote (1981) describe CO₂ fluxes from the near surface to deeper regions of the ocean due to preferential precipitation of salt from brines formed during the production of sea ice. Similar to Rysgaard et al. (2007) the described fluxes represent a

Table 5.1: Amount of ikaite in selected types of sea ice

	Type of ice	mg ikaite	mmol/m ² ikaite
ROV3	young fast-ice	0.168	0.0127
ROV4	young fast-ice	0.995	0.0751
ROV6	young fast-ice	1.217	0.0918
ROV7	young fast-ice	1.394	0.1052
ROV9	young fast-ice	2.137	0.1614
ROV13	young fast-ice	3.372	0.2546
ROV15	single-year ice	49.427	3.7330
SIPEX1	pack ice	0.455	0.03440
SIPEX2	pack ice	5.667	0.4280
SIPEX4	pack ice	0.422	0.03187
SIPEX5	pack ice	3.963	0.2993
SIPEX6	pack ice	1.123	0.0848

CO₂ "pump", where in summer CO₂ is transferred from the atmosphere into the ocean, and in winter it is transferred from the surface of the ocean to deeper regions. Since they could not rely on any measurements, they used laboratory data to calculate the annual flux of CO₂ in regions with sea ice. They calculated $6 \cdot 10^3 \text{ mol}\cdot\text{a}^{-1}$ CO₂ for both the arctic and the antarctic regions. However, they stated that their laboratory results which they used in their calculation may not be entirely representative of natural conditions. Therefore, this study represents the first calculation which bases on measurements on natural sea ice.

The amount of ikaite in sea ice is calculated from the values obtained in section 4.3 and the area of the ice corer. The area of the ice corer is 63.62 cm^2 . Table 5.1 shows the concentrations of ikaite in different types of sea ice. The concentration of CO₂, which is produced during the precipitation of CaCO₃·6H₂O, is the same as the concentration of ikaite. When one mol calcium carbonate precipitates, one mol CO₂ is produced (Papadimitriou et al., 2004). Obviously there are huge variations among the values. However, the values for CO₂ assumed by Jones and Coote (1981) can not be verified. If one would assume a homogeneous distribution of ikaite within the sea ice and take the area of the maximum arctic and antarctic ice cover of about $28.5 \cdot 10^6 \text{ km}^2$ (Comiso, 2003) into account, the calculated values are smaller than those of Jones and Coote (1981). The calculated values of CO₂ range between $9.08 \cdot 10^8 \text{ mol}\cdot\text{a}^{-1}$ and $1.06 \cdot 10^{11} \text{ mol}\cdot\text{a}^{-1}$. If one assumes that in the entire sea ice column the same amount of

CaCO_3 precipitates as in the first 10 cm of the sea ice (see section 4.3.2) and only due to the structure of sea ice large amounts of the mineral are transferred to the underlying water column, one would get much higher values. Taking the highest amount of ikaite which was found in sea ice one would get $1.93 \cdot 10^{12} \text{ mol}\cdot\text{a}^{-1} \text{ CO}_2$. Even this value would be less than 1 per cent of the total carbon dioxide entering the ocean (Jones and Coote, 1981). However, to calculate reliable values of the CO_2 flux it is necessary to fully assess the processes leading to the precipitation of calcium carbonate within sea ice. Especially if one considers that there is an additional temporal variation of the amount of ikaite. This variation could eventually lead to further production of CO_2 which is then released to the ocean.

5.3 Conclusion

This study presents the amount of ikaite in young land-fast ice off Adélie Land and pack ice in the Southern Ocean. A spatial and temporal distribution of the mineral within Antarctic sea ice is provided. At the same location off Adélie Land and at the same time as the occurrence of precipitated CaCO_3 was investigated, this study analyses the carbonate chemistry within brine solution.

Supporting the assumptions of Rysgaard et al. (2007) (see section 1) the study also shows difficulties in the calculation of the species of the carbonate system within hypersaline solutions. Therefore dissociation constants for carbonic acid, which are valid on a large range between 35 and beyond 100 psu as well as at subzero temperatures, need to be determined before a true appreciation of the role of CaCO_3 precipitation towards a sea ice driven carbon pump can be assessed. Furthermore I assume that during sea ice warming when the ice gets porous CO_2 also might be released to the atmosphere. However, this question needs further investigation.

Regarding the mineral ikaite, the study is the first to give an overview on the spatial distribution in Antarctic sea ice. Presenting the surprising occurrence of the mineral within samples of the snow cover of sea ice, this supports the assumptions of Sala et al. (2008) that ikaite in firn ice originates from sea ice when the mineral is transported as aerosol due to atmospheric processes. Therefore, additional to the recommended replication of the determination of the spatial distribution of CaCO_3 (see section 5.2.4), this should be studied on a larger scale. This enables modelers to include quantitative data when modeling the occurrence and frequency of air mass trajectories capable of transporting particles from the sea ice surface to Antarctic inland. Furthermore, the quantitative data of the spatial distribution of ikaite throughout polar regions would allow an appreciation to which extent calcium carbonate contributes to the polar and

global carbon cycle and ikaite could act as a proxy for sea ice cover.

The study highlights on several occasions that the observed data are measured at different scales causing problems in comparability among the data sets. Existing data and data provided in this study with respect to the biogeochemical composition of sea ice present a high degree of spatial and temporal heterogeneity. A large part of this variability is caused by the difference in abundance, size, and shape of brine pockets, as well as their degree of connectivity within the ice column. The used sampling protocol in this study using the sackhole method describes brine properties, but provides integrations of these properties over an unknown spatial scale within the ice column (see also Gleitz et al. (1995); Papadimitriou et al. (2007), and Kennedy and Thomas, personal comm.). This does not offer a satisfactory resolution of sea ice brine properties over small and known spatial scales. Kennedy and Thomas (personal comm.) suggest a novel method providing data on the scale of brine pockets (μm to mm) using ikaite crystals which grow in these brine pockets. Using the isotopic composition of oxygen ($\delta^{18}O$) and carbon ($\delta^{13}C$) of carbonate minerals one could reconstruct different features of the chemistry within sea ice. Thereby one could for example determine the ocean temperature at which ikaite precipitates using the $\delta^{18}O$ of carbonate minerals ($\delta^{18}O_{CaCO_3}$) (Kim et al., 2007) or the $\delta^{13}C$ of the DIC in the ambient brine ($\delta^{13}C_{brine}$) (Romanek et al., 1992). Following from these parameters one can investigate the processes that have influenced the carbon chemistry of the brine at a scale representative of natural features in the ice (Kennedy and Thomas, personal comm.). However, this shows once more that the importance of small-scale processes extends far beyond the obvious well studied problems (Eicken, 2003). Much work is needed in the future for the assessment of the chemical properties of sea ice and the mechanisms leading to the precipitation of ikaite. One major question is whether $CaCO_3$ is precipitated in Arctic sea ice?

Bibliography

- Anderson, L. G. and Jones, E. P. (1985). Measurement of total alkalinity, calcium, and sulfate in natural sea ice. *Journal of Geophysical Research*, 90:9194 – 9198.
- Arrigo, K. R. (2003). Primary Production in Sea Ice. In Thomas, D. N. and Dieckmann, G. S., editors, *Sea Ice: An introduction to its physics, chemistry, biology and geology*, chapter 5, pages 143 – 183. Blackwell.
- Assur, A. (1958). Composition of sea ice and its tensile strength. In *Arctic Sea Ice*, volume 598, pages 106 – 138. National Academy of Sciences - National Research Council.
- Bischoff, J. L., Fitzpatrick, J. A., and Rosenbauer, R. J. (1993a). The solubility and stabilization of ikaite $\text{CaCO}_3 \cdot \text{H}_2\text{O}$ from 0° to 25°C : Environmental and paleoclimatic implications for thynolite tufa. *The Journal of Geology*, 101:21 – 33.
- Bischoff, J. L., Scott, S., Rosenbauer, R. J., Fitzpatrick, J. A., and Stafford, T. W. J. (1993b). Ikaite precipitation by mixing of shoreline springs and lake water, Mono Lake, California, USA. *Geochimica et Cosmochimica Acta*, 57:3855 – 3865.
- Blümel, W. D. (1999). *Physische Geographie der Polargebiete*. B. G. Teubner.
- Buch, K., Harvey, H., Wattenberg, H., and Gripenberg, S. (1932). Über das Kohlen-säuresystem im Meerwasser. *Conseil Permanent International pour L'Exploration de la Mer. Rapports et Proces-Verbeaux des Reunions*, 79:1 – 70.
- Buchardt, B. (1997). Submarine columns of ikaite tufa. *Nature*, 390:129 – 130.
- Buchardt, B., Israelson, C., Seaman, P., and Stockmann, G. (2001). Ikaite tufa towers in Ikka Fjord, Southwest Greenland: Their formation by mixing of seawater and alkaline spring water. *Journal of Sedimentary Research*, 71:176 – 189.
- Campbell, D. M., Millero, F., Roy, R., Roy, L., Lawson, M., Vogel, K. M., and Moore, C. (1993). The standard potential for the hydrogen-silver, silver chloride electrode in synthetic seawater. *Marine Chemistry*, 44:221 – 233.

- Comiso, J. C. (2003). Large-scale Characteristics and Variability of the Global Sea Ice Cover. In Thomas, D. N. and Dieckmann, G. S., editors, *Sea Ice: An introduction to its physics, chemistry, biology and geology*, chapter 4, pages 112 – 142. Blackwell.
- Culberson, C. and Pytkowicz, R. (1973). Ionization of water in seawater. *Marine Chemistry*, 1:309 – 316.
- Del Valls, T. A. and Dickson, A. G. (1998). The pH of buffers based on 2-amino-2-hydroxymethyl-1,3-propanediol ('tris') in sytnhetic sea water. *Deep-Sea Research*, 45:1541 – 1554.
- Delille, B., Jourdain, B., Borges, A. V., Tison, J.-L., and Delille, D. (2007). Biogas (CO₂, O₂, dimethylsulfide) dynamics in spring Antarctic fast ice. *Limnol. Oceanogr*, 52(4):1367 – 1379.
- Dickens, B. and Brown, W. B. (1970). The crystal structure of calcium carbonate hexahydrate at $\sim -120^\circ$. *Inorganic Chemistry*, 9(3):480 – 486.
- Dickson, A., Afghan, J., and Anderson, G. (2003). Reference materials for oceanic CO₂ analysis: a method for the certification of total alkalinity. *Marine Chemistry*, 80:185 – 197.
- Dickson, A. G. (1981). An exact definition of total alkalinity and a procedure for the estimation of alkalinity and total inorganic carbon from titration data. *Deep-Sea Research*, 28A(6):609 – 623.
- Dickson, A. G. (1984). pH scales and proton-transfer reaction in saline media such as sea water. *Geochimica et Cosmochimica Acta*, 48:2299 – 2308.
- Dickson, A. G. (1990). Thermodynamics of the dissociation of boric acid in synthetic seawater from 273.15 to 318.15 K. *Deep-Sea Research*, 37(5):755 – 766.
- Dickson, A. G. and Millero, F. J. (1987). A comparison of the equilibrium constants for the dissociation of carbonic acid in seawater media. *Deep-Sea Research*, 34(10):1733 – 1743.
- Dickson, A. G. and Riley, J. P. (1979). The estimation of acid dissociation constants in seawater media from potentiometric tritrations with strong base. *Marine Chemistry*, 7:89 – 99.
- Dieckmann, G. S. and Hellmer, H. (2003). The importance of Sea Ice: An Overview. In Thomas, D. N. and Dieckmann, G. S., editors, *Sea Ice: An introduction to its physics, chemistry, biology and geology*, chapter 1, pages 1 – 21. Blackwell.

- Dieckmann, G. S., Nehrke, G., Papadimitriou, S., Göttlicher, J., Steininger, R., Kennedy, H., Wolf-Gladrow, D., and Thomas, D. N. (2008). Calcium carbonate as ikaite crystals in Antarctic sea ice. *Geophys. Res. Lett.*, 35:L08501.
- DOE (1994). *Handbook of Methods for the Analysis of the Various Parameters of the Carbon Dioxide System in Sea Water*. DOE.
- Drever (1982). *The Geochemistry of Natural Waters*. Prentice hall.
- Edmond, J. M. (1970). High precision determination of titration alkalinity and total carbon dioxide content of sea water by potentiometric titration. *Deep-Sea Research*, 17:737 – 750.
- Eicken, H. (2003). From the microscopic, to the macroscopic, to the regional scale: Growth, microstructure and properties of sea ice. In Thomas, D. N. and Dieckmann, G. S., editors, *Sea Ice: An introduction to its physics, chemistry, biology and geology*, chapter 2, pages 22–81. Blackwell.
- Fedotov, V. I., Cherepanov, N. V., and Tyshko, K. P. (1998). Some features of the growth. structure and metamorphism of East Antarctic landfast ice. In *Antarctic Sea Ice: Physical Processes, Interactions and Variability*. American Geophysical Union.
- Gal, J.-Y., Bollinger, J.-C., Tolosa, H., and Gache, N. (1996). Calcium carbonate solubility: a reappraisal of scale formation and inhibition. *Talanta*, 43:1497 – 1509.
- Gitterman, K. E. (1937). Thermal analysis of seawater. *CRREL TL*, 287.
- Gleitz, M., Rutgers v.d. Loeff, M., Thomas, D. N., Dieckmann, G. S., and Millero, F. (1995). Comparison of summer and winter inorganic carbon, oxygen and nutrient concentrations in Antarctic sea ice brine. *Marine Chemistry*, 51:81 – 91.
- Goyet, C. and Poisson, A. (1989). New determination of carbonic acid dissociation constants in seawater as function of temperature and salinity. *Deep-Sea Research*, 36:1635 – 1654.
- Grasshoff, K., Kremling, K., and Ehrhardt, M. (2002). *Methods of seawater analysis*. Wiley-VCH Verlag GmbH.
- Hansson, I. (1973a). A new set of acidity constants for carbon acid and boric acid in sea water. *Deep-Sea Research*, 20:461 – 478.
- Hansson, I. (1973b). A new set of ph-scales and buffers for sea water. *Deep-Sea Research*, 20:479 – 491.

- Horner, R., Ackley, S. F., Dieckmann, G. S., Gulliksen, Hoshiai, T., Legendre, L., Melnikov, I. A., Reeburgh, W. S., Spindler, M., and Sullivan, C. W. (1992). Ecology of sea ice biota. *Polar Biology*, 12:417 – 427.
- Ito, T. (1996). Ikaite from cold spring water at Shiowakka, Hokkaido, Japan. *Journal of Mineralogy Petrology and Economic Geology*, 91:209– 219.
- Ito, T. (1998). Factors controlling the transformation of natural ikaite from Shiowakka, Japan. *Geochemical Journal*, 32:267 – 273.
- Jansen, J. H. F., Woensdregt, C. F., Kooistra, M. J., and van der Gaast, S. J. (1987). Ikaite pseudomorphs in the Zaire deep sea fan: An intermediate between calcite and porous calcite. *Geology*, 15:245 – 248.
- Johnston, J., Merwin, H. E., and Williamson, E. D. (1916). The several forms of calcium carbonate. *American Journal of Science*, 41:473 – 512.
- Jones, E. P. and Coote, A. R. (1981). Oceanic CO₂ Produced by the Precipitation of CaCO₃ From Brines in Sea Ice. *Journal of Geophysical Research*, 86:11,041 – 11,043.
- Kennedy, G. L., Hopkins, D. M., and Pickthorn, W. J. (1987). Ikaite, the glendonite precursor, in estuarine sediments at Barrow, Arctic Alaska (abstract). In *Geological Society of America, Annual Meeting, Abstracts with Program*, volume 19, page 725.
- Killawee, J. A., Fairchild, I. J., Tison, J.-L., Janssens, L., and Lorrain, R. (1998). Segregation of solutes and gases in experimental freezing of dilute solutions: Implications for natural glacial systems. *Geochimica et Cosmochimica Acta*, 62(23/24):3637 – 3655.
- Kim, S.-T., O’Neil, J. R. ., Hillaire-Marcel, C., and Mucci, A. (2007). Oxygen isotope fractionation between synthetic aragonite and water: Influence of temperature and Mg²⁺ concentration. *Geochimica et Cosmochimica Acta*, 71:4704 – 4715.
- Lazar, B. and Loya, Y. (1991). Bioerosion of coral reefs -A chemical approach. *Limnol. Oceanogr.*, 36:377 – 383.
- Lee, K., Millero, F., Byrne, R. H., Feely, R. A., and Wanninkhof, R. (2000). The recommended dissociation constants for carbonic acid in seawater. *Geophys. Res. Lett.*, 27:229 – 232.
- Lueker, T. J., Dickson, A., and Keeling, C. D. (2000). Ocean pCO₂ calculated from dissolved inorganic carbon, alkalinity, and equations for K₁ and K₂: validation based

- on laboratory measurements of CO_2 in gas and seawater at equilibrium. *Marine Chemistry*, 70:105 – 119.
- Lyman, J. (1956). *Buffer mechanism of seawater*. PhD thesis, Univ. Calif., Los Angeles.
- Marion, G. M. (2001). Carbonate mineral solubility at low temperatures in the Na–K–Mg–Ca–H–Cl– SO_4 –OH– HCO_3 – CO_3 – CO_2 – H_2O system. *Geochimica et Cosmochimica Acta*, 65(12):1883 – 1896.
- Marland, G. (1975). The stability of $\text{CaCO}_3 \cdot 6 \text{H}_2\text{O}$ (ikaite). *Geochimica et Cosmochimica Acta*, 39:83 – 91.
- Mehrbach, C., Culberson, C., Hawley, J., and Pytkowicz, R. (1973). Measurement of the apparent dissociation constants of carbonic acid in seawater at atmospheric pressure. *Limnol. Oceanogr.*, 18:897 – 907.
- Millero, F. J. (1979). The thermodynamics of the carbonate system in seawater. *Geochimica et Cosmochimica Acta*, 43:1651 – 1661.
- Millero, F. J. (1995). Thermodynamics of the carbon dioxide system in the oceans. *Geochimica et Cosmochimica Acta*, 59(4):661 – 677.
- Millero, F. J., Byrne, R. H., Wanninkhof, R., Feely, R. A., Clayton, T., Murphy, P., and Lamb, M. (1993). The internal consistency of CO_2 measurements in the equatorial Pacific. *Marine Chemistry*, 44:269 – 280.
- Millero, F. J., Graham, T. B., Huang, F., Bustos-Serrano, H., and Pierrot, D. (2006). Dissociation constants of carbonic acid in seawater as a function of salinity and temperature. *Marine Chemistry*, 100:80 – 94.
- Millero, F. J., Pierrot, D., Lee, K., Wanninkhof, R., Feely, R. A., Sabine, C. L., Key, R. M., and Takahashi, T. (2002). Dissociation constants for carbon acid determined from field measurements. *Deep-Sea Research*, 49:1705 – 1723.
- Mojica-Prieto, F. J. M. and Millero, F. J. (2002). The values of $pK_1 + pK_2$ for the dissociation of carbon acid in seawater. *Geochimica et Cosmochimica Acta*, 66(14):2529 – 2540.
- Morel, F. M. M. and Hering, J. G. (1993). *Principles and Applications of Aquatic Chemistry*. Wiley and Sons.
- Morin, S., Marion, G. M., von Glasow, R., Voisin, D., Bouchez, J., and Savarino, J. (2008). Precipitation of salts in freezing seawater and ozone depletion events: a status report. *Atmos. Chem. Phys.*, 8:7317 – 7324.

- Nehrke, G. (2007). Calcite precipitation from aqueous solution: Transformation from vaterite and role of solution stoichiometry. *Geologica Ultraiectina*, 273:1 – 133.
- Neumeister, H. (2007). Das universelle "Geo-Öko" verständnis. In "GEO-ÖKO" - *Lehrkonzept - Das System: Speicher - Grenzflächen - Prozesse für Energie und Stoffe im erdoberflächennahen Bereich*. Institut für Geophysik und Geologie Universität Leipzig.
- Nölte, J. (2002). *ICP Emissionsspektrometrie für Praktiker*. Wiley-VCH Verlag GmbH.
- Omelon, C. R., Pollard, W. H., and Marion, G. M. (2001). Seasonal formation of ikaite ($\text{CaCO}_3 \cdot 6\text{H}_2\text{O}$) in saline spring discharge at Expedition Fiord, Canadian High Arctic: Assessing conditional constraints for natural crystal growth. *Geochimica et Cosmochimica Acta*, 65(9):1429 – 1437.
- Papadimitriou, S., Kennedy, H., Kattner, G., Dieckmann, G. S., and Thomas, D. N. (2004). Experimental evidence for carbonate precipitation and CO_2 degassing during sea ice formation. *Geochimica et Cosmochimica Acta*, 68(8):1749 – 1761.
- Papadimitriou, S., Thomas, D. N., Kennedy, H., Haas, C., Kuosa, H., Krell, A., and Dieckmann, G. S. (2007). Biogeochemical composition of natural sea ice brines from the Weddell Sea during early austral summer. *Limnol. Oceanogr*, 52(5):1809 – 1823.
- Pauly, H. (1963). Ikaite a new mineral from Greenland. *Arctic*, 16:263 – 264.
- Rickaby, R. E. M., Shaw, S., Bennitt, G., Kennedy, H., Zabel, M., and Lennie, A. (2006). Potential of ikaite to record the evolution of oceanic $\delta^{18}\text{O}$. *Geology*, 34(6):497 – 500.
- Romanek, C. S., Grossmann, E. L., and Morse, J. W. (1992). Carbon isotopic fractionation in synthetic aragonite and calcite: Effects of temperature and precipitation rate. *Geochimica et Cosmochimica Acta*, 56:419 – 430.
- Roy, R. N., Roy, L. N., Vogel, K. M., Porter-Moore, C., Pearson, T., Good, C. E., Millero, F. J., and Campbell, D. M. (1993). The dissociation constants of carbonic acid in seawater at salinities 5 to 45 and temperatures 0 to 45°C. *Marine Chemistry*, 44:249 – 267.
- Rysgaard, S., Glud, R. N., Sejr, M. K., Bendtsen, J., and Christensen, P. B. (2007). Inorganic carbon transport during sea ice growth and decay: A carbon pump in polar seas. *Journal of Geophysical Research*, 112:C03016.

- Sala, M., Delmonte, B., Frezzotti, M., Proposito, M., Scarchilli, C., Maggi, V., Artioli, G., M, D., Marino, F., Ricci, P., and De Giudici, G. (2008). Evidence of calcium carbonates in coastal (Talos Dome and Ross Sea area) East Antarctica snow and firm: Environmental and climatic implications. *Earth Planet. Sci. Lett.*, 271(1):43 – 52. in Press.
- Sander, R., Burrows, J., and Kaleschke, L. (2006). Carbonate precipitation in brine - a potential trigger for tropospheric ozone depletion events. *Atmos. Chem. Phys.*, 6:4653 – 4658.
- Skoog, D. A. and Leary, J. J. (1992). *Principles of Instrumental Analysis*. Fort Worth, Saunders College Publ., 4th edition.
- Sørensen, S. P. L. (1909). Enzymstudien. II. Mitteilung. Über die Messung und die Bedeutung der Wasserstoffkonzentrationen bei enzymatischen Prozessen. *Biochem. Z.*, 21:131 – 304.
- Stein, C. L. and Smith, A. J. (1986). Authigenic carbonate nodules in the Nankai Trough. In Kagami, H., Karig, D. E., and Coulbourn, W. T., editors, *Initial Reports Deep Sea Drilling Project*, volume 87, pages 659 – 668.
- Suess, E., Balzer, W., Hesse, K. F., J., M. P., and Wefer, G. (1982). Calcium carbon hexahydrate from organic-rich sediments of the Antarctic Shelf: Precursor of glendonites. *Science*, 216 (#4550):1128 – 1131.
- Swainson, I. P. and Hammond, R. P. (2001). Ikaite, $\text{CaCO}_3 \cdot 6\text{H}_2\text{O}$: Cold comfort for glendonites as paleothermometers. *American Mineralogist*, 86:1530 – 1533.
- Thomas, D. N. and Dieckmann, G. S. (2003). *Sea Ice An Intorduction to its Physics, Chemistry, Biology and Geology*. Blackwell Publishing.
- Thomas, D. N. and Papadimitriou, S. (2003). Biogeochemistry of sea ice. In Thomas, D. N. and Dieckmann, G. S., editors, *Sea Ice. An introduction to its physics, chemistry, biology and geology*. Blackwell Publishing.
- Tison, J. L., Haas, C., Gowing, M. M., Sleewaegen, S., and Bernard, A. (2002). Tank study of physico-chemical controls on gas content and composition during growth of young sea ice. *Journal of Glaciology*, 48:177 – 191.
- Van Valkenburg, A., Mao, H. K., and Bell, P. M. (1971). Ikaite ($\text{CaCO}_3 \cdot 6\text{H}_2\text{O}$), a phase more stable than calcite and aragonite (CaCO_3) at high water pressure. *Carnegie Inst. Geophysical Laboratory, Annual Report*, pages 233 – 237.

- Wadhams, P. (2000). *Ice in the Ocean*. Breach Science Publishers.
- Wanninkhof, R., Lewis, E., Feely, R. A., and Millero, F. (1999). The optimal carbonate dissociation constants for determining surface water pCO₂ from alkalinity and total inorganic carbon. *Marine Chemistry*, 65:291 – 301.
- Wedborg, M., Turner, D. R., Anderson, L. G., and Dyrssen, D. (1999). Determination of pH. In Grasshoff, K., Kremling, K., and Erhardt, M., editors, *Methods of seawater analysis*, chapter 7, pages 109 – 125. Wiley-VCH Verlag GmbH.
- Weeks, W. F. and Ackley, S. F. (1986). The Growth, Structure, and Properties of Sea Ice. In Untersteiner, N., editor, *The geophysics of sea ice*. Martinus Nijhoff Publ.
- Wolf-Gladrow, D., Zeebe, R. E., Klaas, C., Körtzinger, and Dickson, A. (2007). Total alkalinity: The explicit conservative expression and its application to biogeochemical processes. *Marine Chemistry*, 106:287 – 300.
- Zeebe, R. E. and Wolf-Gladrow, D. (2001). *CO₂ in seawater: equilibrium, kinetics, isotopes*, volume 65 of *Elsevier Oceanography Series*. Elsevier Science B.V., first edition.

Appendix A

Meteorological data

Table A.1: Meteorological data during the sampling period

Date	Pressure in hPa	T in °C	Duration of Insulation	Global radiation in J/cm ²	avg. Cloudiness in eighths	Wind speed in m/s
01.11.2007	985.51	-3.8	09:19	1979	5.6	10.1
02.11.2007	981.33	-5.3	12:33	2452	6.2	4.5
03.11.2007	979.99	-9	12:12	2295	5.8	5
04.11.2007	990.63	-8.4	15:37	2625	1.4	5.5
05.11.2007	987.4	-8.2	11:26	2335	6	3
06.11.2007	990.4	-7.6	13:49	2645	3.6	4
07.11.2008	989.56	-4.2	17:08	2786	0.6	8.4

Date	Pressure in hPa	T in °C	Duration of Insulation	Global radiation in J/cm ²	avg. Cloudiness in eighths	Wind speed in m/s
08.11.2007	993.95	-2.5	08:49	2270	3	7
09.11.2007	985.51	0.3	17:26	2856	1.4	5.8
10.11.2007	983.69	-2.6	04:53	2153	5.8	9.8
11.11.2007	989.94	-0.3	17:43	2852	3.2	11.9
12.11.2007	993.66	-2.1	14:50	2676	6.8	10
13.11.2007	986.84	-3.5	16:47	2828	5.6	4
14.11.2007	984.33	-4.8	16:51	2981	3	7.9
15.11.2007	987.96	-5.6	09:54	2418	6.8	6.5
16.11.2007	974.95	-2.8	02:19	2155	7.8	18.1
17.11.2007	970.65	-3.2	06:37	2449	5.8	17.4
18.11.2007	985.79	-2.2	00:00	1805	7.6	5.8
19.11.2007	982.16	-5.4	00:00	1716	8	12.4
20.11.2007	970.5	-4.6	00:42	2134	8	14.1
21.11.2007	967.73	-4	00:00	1950	8	17.5
22.11.2007	971.05	-3.8	14:05	2930	3.8	16.6
23.11.2007	973.54	-3.2	17:27	3048	1.8	13.5
24.11.2007	975.59	-1.9	16:53	3094	3.2	5.3
25.11.2007	974.1	-2.6	13:32	2982	3.4	4.3
26.11.2007	978.7	-4.4	19:24	3293	0.6	7.9
27.11.2007	987.46	0.1	19:34	3322	1.8	5.4
28.11.2007	984.85	0	19:43	3347	0.4	4.3

Date	Pressure in hPa	T in °C	Duration of Insulation	Global radiation in J/cm ²	avg. Cloudiness in eighths	Wind speed in m/s
29.11.2007	977.04	-4	19:31	3201	5	9.4
30.11.2007	975.29	-3.3	17:18	3267	4.4	6.9
01.12.2007	975.06	-3.3	04:29	2532	7	12.5
02.12.2007	982.38	-1.6	03:21	2157	7.2	7.6
03.12.2007	978.38	-2.3	20:16	3434	2	3.9
04.12.2007	981.54	-0.5	20:20	3444	0.8	3.3
05.12.2007	985.28	-0.1	16:47	3369	4.2	2.6

Appendix B

Data from the sampling site off Adélie Land

B.1 Air temperature, salinity and temperature of sea ice brine

Table B.1: Salinity and temperature of sea ice brine and air temperature

Sample Name	Date	T_{air} maximum °C	T_{Brine} in °C	Salinity
ROV2 #1	13/11/07	-3.5	-5	86
ROV2 #2	13/11/07	-3.5	-4.7	87
ROV2 #3	13/11/07	-3.5	-4.8	84
ROV3 #1	14/11/07	-4.8	-4.75	81
ROV3 #2	14/11/07	-4.8	-4.7	76
ROV3 #3	14/11/07	-4.8	-4.75	74
ROV4 #1	17/11/07	-3.2	-4.05	75
ROV4 #2	17/11/07	-3.2	-4	76
ROV4 #3	17/11/07	-3.2	-3.95	76
ROV5 #1	18/11/07	-2.2	-3.9	71
ROV5 #2	18/11/07	-2.2	-3.95	76
ROV5 #3	18/11/07	-2.2	-3.95	76
ROV6 #1	23/11/07	-3.2	-4.05	73
ROV6 #2	23/11/07	-3.2	-3.95	74
ROV6 #3	23/11/07	-3.2	-4.05	75
ROV8 #1	25/11/07	-2.6	-2.05	41

Sample Name	Date	T_{air} maximum °C	T_{Brine} in °C	Salinity
ROV8 #2	25/11/07	-2.6	-2.45	45
ROV8 #3	25/11/07	-2.6	-2.5	48
ROV9 #1	27/11/07	0.1	-3.6	65
ROV9 #2	27/11/07	0.1	-3.65	66
ROV9 #3	27/11/07	0.1	-3.45	64
ROV11 #1	30/11/07	-3.3	-3.9	71
ROV11 #2	30/11/07	-3.3	-3.9	72
ROV11 #3	30/11/07	-3.3	-4.05	73
ROV13 #1	03/12/07	-2.3	-2.6	40
ROV13 #2	03/12/07	-2.3	-2.7	46
ROV13 #3	03/12/07	-2.3	-2.6	46

B.2 Calculated concentration of H^+_{SWs}

Table B.2: Calculated concentration of H^+_{SWs} using f_H from section 4.2.2

Sample Name	Date	pH_{NBS}	$f_H(S,T)$	$[H^+]_{SWs}$ in mol/l
ROV3 #1	14/11/07	8.472	0.970	$3.47783412 \cdot 10^{-9}$
ROV3 #2	14/11/07	8.467	0.954	$3.57603328 \cdot 10^{-9}$
ROV3 #3	14/11/07	8.522	0.948	$3.17056523 \cdot 10^{-9}$
ROV4 #1	17/11/07	8.666	0.948	$2.27542963 \cdot 10^{-9}$
ROV4 #2	17/11/07	8.639	0.951	$2.41402551 \cdot 10^{-9}$
ROV4 #3	17/11/07	8.648	0.951	$2.36503597 \cdot 10^{-9}$
ROV5 #1	18/11/07	8.905	0.935	$1.33067587 \cdot 10^{-9}$
ROV5 #2	18/11/07	8.697	0.951	$2.1126996 \cdot 10^{-9}$
ROV5 #3	18/11/07	8.802	0.951	$1.65896701 \cdot 10^{-9}$
ROV6 #1	23/11/07	9.353	0.942	$4.7088214 \cdot 10^{-10}$
ROV6 #2	23/11/07	9.113	0.945	$8.1597810 \cdot 10^{-10}$
ROV6 #3	23/11/07	9.134	0.948	$7.7457488 \cdot 10^{-10}$
ROV8 #1	25/11/07	9.354	0.834	$5.3037625 \cdot 10^{-10}$
ROV8 #2	25/11/07	9.400	0.849	$4.6915618 \cdot 10^{-10}$
ROV8 #3	25/11/07	9.347	0.858	$5.2417618 \cdot 10^{-10}$
ROV9 #1	27/11/07	8.478	0.915	$3.63407458 \cdot 10^{-9}$

Sample Name	Date	pH_{NBS}	$f_H(\mathbf{S}, \mathbf{T})$	$[\text{H}^+]_{SWS}$ in mol/l
ROV9 #2	27/11/07	8.481	0.919	$3.59605465 \cdot 10^{-9}$
ROV9 #3	27/11/07	8.530	0.912	$3.23718187 \cdot 10^{-9}$
ROV11 #1	30/11/07	8.536	0.935	$3.11223429 \cdot 10^{-9}$
ROV11 #2	30/11/07	8.275	0.938	$5.65763781 \cdot 10^{-9}$
ROV11 #3	30/11/07	8.530	0.942	$3.13265246 \cdot 10^{-9}$
ROV13 #1	03/12/07	8.680	0.838	$2.49352079 \cdot 10^{-9}$
ROV13 #2	03/12/07	8.760	0.857	$2.02798524 \cdot 10^{-9}$
ROV13 #3	03/12/07	8.088	0.856	$9.53405611 \cdot 10^{-9}$

B.3 Total alkalinity

Table B.3: Total alkalinity in $\mu\text{mol/l}$

Sample Name	Date	Total Alkalinity
ROV3 #1	14/11/07	5616.13
ROV3 #2	14/11/07	5671.62
ROV3 #3	14/11/07	5672.03
ROV4 #1	17/11/07	4802.84
ROV4 #2	17/11/07	4875.94
ROV4 #3	17/11/07	4825.49
ROV5 #1	18/11/07	4948.9
ROV5 #2	18/11/07	5105.02
ROV5 #3	18/11/07	5042.44
ROV6 #1	23/11/07	4746.13
ROV6 #2	23/11/07	4744.25
ROV6 #3	23/11/07	4709.42
ROV8 #1	25/11/07	2732.23
ROV8 #2	25/11/07	3068.32
ROV8 #3	25/11/07	3128.12
ROV9 #1	27/11/07	4484.54
ROV9 #2	27/11/07	4283.98
ROV9 #3	27/11/07	4383.5
ROV11 #1	30/11/07	4653.12

Sample Name	Date	Total Alkalinity
ROV11 #2	30/11/07	4659.36
ROV11 #3	30/11/07	4565.3
ROV13 #1	03/12/07	1987.98
ROV13 #2	03/12/07	2405.69
ROV13 #3	03/12/07	2350.35
Seawater sample	04/12/07	2218.39

Appendix C

Dissociation constants

Table C.1: pK_1 calculated at different salinities using the equations of different authors (see section 2.3.2)

Salinity	Hansson 1973	Mehrbach et al. 1973	Dickson and Millero 1987	Goyet et al. 1989	Roy et al. 1993	Mojica-Prieto and Millero 2002	Millero et al. 2006
10	6.2815	6.4185	6.2979	6.2623	6.2751	6.2999	6.2922
15	6.2416	6.3628	6.2534	6.2252	6.2369	6.2524	6.2456
20	6.2070	6.3186	6.2147	6.1928	6.2032	6.2118	6.2109
25	6.1776	6.2817	6.1818	6.1651	6.1737	6.1779	6.1829
30	6.1535	6.2501	6.1547	6.1422	6.1487	6.1509	6.1588
35	6.1346	6.2224	6.1334	6.1241	6.1279	6.1307	6.1371
40	6.1210	6.1979	6.1179	6.1107	6.1116	6.1174	6.1166

Salinity	Hansson 1973	Mehrbach et al. 1973	Dickson and Millero 1987	Goyet et al. 1989	Roy et al. 1993	Mojica-Prieto and Millero 2002	Millero et al. 2006
45	6.1126	6.1759	6.1082	6.1020	6.0995	6.1108	6.0968
50	6.1095	6.1561	6.1043	6.0981	6.0919	6.1111	6.0770
55	6.1116	6.1381	6.1062	6.0990	6.0885	6.1182	6.0569
60	6.1190	6.1217	6.1139	6.1046	6.0896	6.1321	6.0361
65	6.1316	6.1067	6.1274	6.1149	6.0949	6.1528	6.0144
70	6.1495	6.0929	6.1467	6.1300	6.1047	6.1804	5.9916
75	6.1726	6.0802	6.1718	6.1499	6.1187	6.2148	5.9675
80	6.2010	6.0685	6.2027	6.1745	6.1372	6.2559	5.9420
85	6.2346	6.0577	6.2394	6.2039	6.1599	6.3040	5.9150
90	6.2735	6.0478	6.2819	6.2380	6.1871	6.3588	5.8864
95	6.3176	6.0386	6.3302	6.2768	6.2185	6.4204	5.8561
100	6.3670	6.0301	6.3843	6.3204	6.2544	6.4889	5.8240

Table C.2: pK_2 calculated at different salinities using the equations of different authors (see section 2.3.2)

Salinity	Hansson 1973	Mehrbach et al. 1973	Dickson and Millero 1987	Goyet et al. 1989	Roy et al. 1993	Mojica-Prieto and Millero 2002	Millero et al. 2006
10	9.6978	10.3030	9.7484	9.7642	9.7307	9.8009	9.7515
15	9.6183	9.9793	9.6712	9.6757	9.6534	9.7051	9.6494
20	9.5454	9.7752	9.5998	9.5979	9.5823	9.6166	9.5775
25	9.4791	9.6364	9.5344	9.5309	9.5172	9.5355	9.5184

Salinity	Hansson 1973	Mehrbach et al. 1973	Dickson and Millero 1987	Goyet et al. 1989	Roy et al. 1993	Mojica-Prieto and Millero 2002	Millero et al. 2006
30	9.4194	9.5391	9.4748	9.4746	9.4583	9.4618	9.4629
35	9.3663	9.4704	9.4212	9.4290	9.4054	9.3954	9.4057
40	9.3198	9.4226	9.3734	9.3943	9.3587	9.3364	9.3434
45	9.2799	9.3908	9.3316	9.3702	9.3180	9.2848	9.2735
50	9.2466	9.3715	9.2956	9.3569	9.2835	9.2405	9.1942
55	9.2199	9.3625	9.2656	9.3544	9.2550	9.2036	9.1042
60	9.1998	9.3619	9.2414	9.3626	9.2327	9.1741	9.0025
65	9.1863	9.3683	9.2232	9.3816	9.2164	9.1519	8.8882
70	9.1794	9.3808	9.2108	9.4113	9.2063	9.1371	8.7607
75	9.1791	9.3984	9.2044	9.4517	9.2022	9.1296	8.6195
80	9.1854	9.4206	9.2038	9.5029	9.2043	9.1296	8.4640
85	9.1983	9.4468	9.2092	9.5649	9.2124	9.1369	8.2939
90	9.2178	9.4764	9.2204	9.6376	9.2267	9.1515	8.1089
95	9.2439	9.5092	9.2376	9.7211	9.2470	9.1735	7.9086
100	9.2766	9.5448	9.2606	9.8153	9.2735	9.2029	7.6928

Appendix D

Amount of the mineral ikaite in sea ice

Table D.1: Quantity of ikaite in sea ice in the Southern Ocean

Sample name	ikaite total in Sample	ikaite in mg/l melted ice
Iceberg core 101206 core section #2	0.28172724	0.12
iceberg core 101207, core section #1	0.15358148	0.07
Icecore 101207 iceberg core section #3	0.1745105	0.09
Prud' homme snow - 281107	0.12763714	0.13
ROV#6 CAC core can #5 20-30	0.10945075	0.18
ROV12 #25 20x20 Bio74 - 021207	0.09702853	0.18
ROV12 20x20 #1 135 - 021207	0.31179633	0.57
ROV12 20x20 #10 CAC9 - 021207	0.21967485	0.41
ROV12 20x20 #11 PR7 - 021207	0.03055119	0.05
ROV12 20x20 #12 DR5 - 021207	0.13428289	0.23
ROV12 20x20 #13 Bio34 - 021207	0.66072025	1.06
ROV12 20x20 #14 Prud1 - 021207	0.17191898	0.3
ROV12 20x20 #15 Pr6 - 021207	0.03488752	0.06
ROV12 20x20 #16 D15 - 021207	0.34061687	0.55
ROV12 20x20 #17 CAC1 021207	0.74505651	1.28
ROV12 20x20 #18 Bio29 - 021207	1.41470938	2.26
ROV12 20x20 #19 Bio62 - 021207	0.0960626	0.17
ROV12 20x20 #2 PR3 - 021207	0.20125996	0.33
ROV12 20x20 #20 PR4 - 021207	1.1494926	1.88
ROV12 20x20 #21 Bio69 - 021207	1.33463291	2.15
ROV12 20x20 #22 Bio80 - 021207	0.16345416	0.27

Sample name	ikaite total in Sample	ikaite in mg/l melted ice
ROV12 20x20 #23 Bio70 - 021207	0.8385324	1.4
ROV12 20x20 #24 PR8 - 021207	0.12647899	0.21
ROV12 20x20 #3 Bio37 - 021207	0.07345169	0.12
ROV12 20x20 #4 D12 - 021207	0.5825124	0.91
ROV12 20x20 #5 z - 021207	2.39459742	3.93
ROV12 20x20 #6 PR2 - 021207	0.07008656	0.11
ROV12 20x20 #7 Bio61	0.09154446	0.15
ROV12 20x20 #9 209 - 021207	0.32576286	0.56
ROV12 20x20 Bio91 #8 - 021207	0.27165232	0.46
ROV13 CAC Core CA6 #6 45-52 - 031207	2.32013359	3.54
ROV13 CAC core CAC #4 - 031207	0.01434085	0.03
ROV13 CAC core CAC3 - 031207	0.17995092	0.4
ROV13 CAC core CAC5 - 031207	0.80560806	3.66
ROV13 CAC2 - 031207	0.05155221	0.11
ROV15 2cm sect. 7 8-10cm - 051207	9.12635163	55.31
ROV15 ACA 2cm sect. 223 2-4cm - 051207	4.97915206	76.6
ROV15 CAC 2 cm sect. Bio12 4-6	8.5686141	73.87
ROV15 CAC 2 sect. 5-15 14-16	1.33390529	8.95
ROV15 CAC 2cm sect Bio32 6-8cm - 051207	11.9285453	125.56
ROV15 CAC 2cm sect. CAC8 10-12	0.87331761	4.41
ROV15 CAC 2cm sect. Sp7 12-14 - 051207	6.24470772	41.08
ROV15 CAC Bulk #1 - 051207	52.8920859	25.8
ROV15 Thin section 15-25 - 0-2 cm - 051207	6.37246242	104.47
ROV3 141107 #2 CAC	1.75045155	0.98
ROV3 141107 10-20 CAC Bio111	0.01984038	0.03
ROV3 141107 Bio56 CAC 40-50	0.03601437	0.06
ROV3 141107 CAC 20-30 Bio70	0.01357121	0.02
ROV3 30-40 Bio34 CAC 141107	0.01405106	0.02
ROV3 60-65 141107 CAC Bio23	0.02780401	0.08
ROV3 Bio69 50-60 141107	0.01882874	0.03
ROV3 CAC #1 141107	2.44778493	1.59
ROV3 CAC #3 141107	0.9231254	0.52
ROV3 CAC 0-20 209 141107	0.03825258	0.06

Sample name	ikaite total in Sample	ikaite in mg/l melted ice
ROV3 CAC 135 - 141107 snow/ice	0.30104579	1.2
ROV4 Bulk #1 171107	2.14875634	1.28
ROV4 CAC Bulk #2 171107	0.89986163	0.49
ROV4 CAC Bulk #3 171107	0.48457069	0.26
ROV4 CAC core # 7 - 171107	0.19139313	0.28
ROV4 CAC core #2 171107	0.14458717	0.25
ROV4 CAC core #3 - 171107	0.07284918	0.12
ROV4 CAC core #4 171107	0.0217203	0.04
ROV4 CAC core #5 171107	0.02230192	0.04
ROV4 CAC core #6 171107	0.04504007	0.07
ROV4 CAC core #8 171107	0.49734519	4.97
ROV4 Oberfläche 171107	25.5837878	93.03
ROV5 #1 CAC Bulk 181107	0.7868085	0.4
ROV5 #2(1) 191107 CAC Bulk	0.32062399	0.18
ROV5 181107 #3 CAC Bulk	0.15119816	0.08
ROV5 CaCO ₃ scratch 0.0025m ²	43.1964157	39.27
ROV6 3 40-50 CAC core 231107	0.05959638	0.1
ROV6 4 30-40 CAC core - 231107	0.00635018	0.01
ROV6 6-8cm surface D12 - 231107	0.34580967	2.47
ROV6 Bio23 2-4cm - 231107	8.54892668	85.49
ROV6 CAC Bulk #2 231107	5.00586754	1.22
ROV6 CAC Bulk #3 231107	5.90043399	1.46
ROV6 CAC Bulk1 - 231107	4.19498405	1.01
ROV6 CAC core #6 10-20 -231107	0.01546048	0.03
ROV6 CAC core #7 0-20 - 231107	0.99525846	3.11
ROV6 CAC core No. 2 50-60 - 231107	0.03065506	0.05
ROV6 surface 0-2 111 - 231107	1.43948006	22.15
ROV6 surface 135 4-6cm	0.1714411	1.22
ROV6 surface Bio74 8-10 - 231107	0.09386059	0.72
ROV7 135 10-12 Surface - 241107	0.02937237	0.21
ROV7 209 4-6 ice surface - 241107	0.21409176	3.76
ROV7 Bio23 12-14 surface ice 241107	0.14263445	1.06
ROV7 Bio66 20-30 CAC core - 241107	0.02354931	0.04

Sample name	ikaite total in Sample	ikaite in mg/l melted ice
ROV7 Bio69 8-10 surface ice	0.07375804	0.52
ROV7 Bio70 12-14cm snow/ice surface	0.2419277	1.79
ROV7 CAC core Bio 32 10-20 241107	0.13495409	0.23
ROV7 CAC core Bio113 30-40 - 241107	0.0208318	0.04
ROV7 CAC core Bio12 40-50	0.02394608	0.04
ROV7 CAC core Bio16 50-60 - 241107	0.05098578	0.09
ROV7 CAC core DMS-ED 0-10 241107	1.16289685	2.45
ROV7 CAC9 ice 0-2 cm surface 241107	11.3167967	103.82
ROV7 D12 14-16 surface snow - 241107	0.08850138	0.63
ROV7 D15 10-12 surface snow - 241107	0.07439681	0.53
ROV7 Ice surface CA1 6-8 - 241107	0.21094998	1.51
ROV7 surface 241107 Bio62 2-4cm snow	0.53265875	11.1
ROV7 Surface Bio34 8-10 - 241107	1.21633402	9.21
ROV7 surface Bio80 snow 4-6 - 241107	0.57789027	10.14
ROV7 Surface CAC8 241107 2-4 cm ice	0.81859022	5.76
ROV7 Surface No Bio74 snow 0-2cm 241107	0.67598797	16.09
ROV7 surface snow/ice 241107 Bio 111 6-6	2.55849986	38.77
ROV8 Sackhole #1 Bulk - 251107	3.02966404	1.59
ROV8 Sackhole Bulk #2 - 251107	1.83617266	1.01
ROV8 Sackhole Bulk #3 251107	3.77902716	2.15
ROV8 snow sample 251107	0.4809355	0.27
ROV9 CAC Bulk # 2 271107	1.17100109	0.71
ROV9 CAC Bulk #1 271107	1.19919897	0.67
ROV9 CAC Bulk #3 - 271107	0.35578221	0.2
ROV9 CAC core cac # 5 20-30 271107	0.12046014	0.21
ROV9 CAC core CAC #3 40-50 271107	0.05950809	0.1
ROV9 CAC core CAC #4 30-40 - 271107	0.01855872	0.03
ROV9 CAC core CAC #6 10-20 - 271107	0.15848423	0.26
ROV9 CAC core CAC#2 50-60 - 241107	0.02727413	0.05
ROV9 CAC core CAC#7 0-10 271107	1.75345279	5.01
ROV9 D15 Snow sample - 271107	1.83218576	4.95
ROV9 snow 40cm Bio 29 271107	0.01068644	0.02
SIPEX V1 2007/2008 A. Krell #1 221	0.10051816	0.16

Sample name	ikaite total in Sample	ikaite in mg/l melted ice
SIPEX V1 2007/2008 A. Krell #1 222	0.04553335	0.07
SIPEX V1 2007/2008 A. Krell #1 34	0.08008325	0.13
SIPEX V1 2007/2008 A. Krell #1 D14	0.12073526	0.22
SIPEX V1 2007/2008 A. Krell #10 109	0.02387699	0.04
SIPEX V1 2007/2008 A. Krell #10 116	0.02059701	0.03
SIPEX V1 2007/2008 A. Krell #10 201	0.05489664	0.1
SIPEX V1 2007/2008 A. Krell #10 224	0.30166909	0.55
SIPEX V1 2007/2008 A. Krell #10 D14	0.03076929	0.05
SIPEX V1 2007/2008 A. Krell #10 D16	0.05342693	0.09
SIPEX V1 2007/2008 A. Krell #11 1	0.02744052	0.05
SIPEX V1 2007/2008 A. Krell #11 33	0.03007865	0.05
SIPEX V1 2007/2008 A. Krell #11 34	0.03200004	0.05
SIPEX V1 2007/2008 A. Krell #11 D12	0.0198305	0.04
SIPEX V1 2007/2008 A. Krell #12 1	0.02981379	0.05
SIPEX V1 2007/2008 A. Krell #12 109	0.03721396	0.07
SIPEX V1 2007/2008 A. Krell #12 116	0.05466805	0.1
SIPEX V1 2007/2008 A. Krell #12 221	0.01803523	0.03
SIPEX V1 2007/2008 A. Krell #12 33	0.01595692	0.03
SIPEX V1 2007/2008 A. Krell #12 34	0.03253498	0.06
SIPEX V1 2007/2008 A. Krell #12 D14	0.04680567	0.08
SIPEX V1 2007/2008 A. Krell #12 D18	0.05879668	0.1
SIPEX V1 2007/2008 A. Krell #12 D3	0.03373983	0.06
SIPEX V1 2007/2008 A. Krell #13 118	0.03337631	0.06
SIPEX V1 2007/2008 A. Krell #13 135	0.03292963	0.06
SIPEX V1 2007/2008 A. Krell #13 222	0.10488048	0.17
SIPEX V1 2007/2008 A. Krell #13 224	0.03341781	0.06
SIPEX V1 2007/2008 A. Krell #13 D17	0.02389777	0.04
SIPEX V1 2007/2008 A. Krell #14 109	0.21464805	0.41
SIPEX V1 2007/2008 A. Krell #14 201	0.04619809	0.09
SIPEX V1 2007/2008 A. Krell #14 33	0.03021364	0.05
SIPEX V1 2007/2008 A. Krell #14 34	0.01314174	0.03
SIPEX V1 2007/2008 A. Krell #14 50	0.82575693	1.56
SIPEX V1 2007/2008 A. Krell #14 D14	0.03354244	0.06

Sample name	ikaite total in Sample	ikaite in mg/l melted ice
SIPEX V1 2007/2008 A. Krell #14 D14	0.01164198	0.02
SIPEX V1 2007/2008 A. Krell #2 1	0.13533333	0.28
SIPEX V1 2007/2008 A. Krell #2 33	0.05194173	0.09
SIPEX V1 2007/2008 A. Krell #2 D15	5.41124052	9.49
SIPEX V1 2007/2008 A. Krell #2 D3	0.06891287	0.11
SIPEX V1 2007/2008 A. Krell #3 109	0.17497249	0.3
SIPEX V1 2007/2008 A. Krell #3 15	1.30851518	2.08
SIPEX V1 2007/2008 A. Krell #3 27	0.09432297	0.14
SIPEX V1 2007/2008 A. Krell #4 1	0.02154061	0.04
SIPEX V1 2007/2008 A. Krell #4 109	0.06039612	0.11
SIPEX V1 2007/2008 A. Krell #4 15	0.08446631	0.15
SIPEX V1 2007/2008 A. Krell #4 224	0.06552171	0.12
SIPEX V1 2007/2008 A. Krell #4 27	0.06756789	0.12
SIPEX V1 2007/2008 A. Krell #4 33	0.12252179	0.22
SIPEX V1 2007/2008 A. Krell #5 116	2.43038959	4.08
SIPEX V1 2007/2008 A. Krell #5 135	0.56641372	1.05
SIPEX V1 2007/2008 A. Krell #5 43	0.17630675	0.31
SIPEX V1 2007/2008 A. Krell #5 C7	0.16406135	0.26
SIPEX V1 2007/2008 A. Krell #5 D12	0.41248962	0.76
SIPEX V1 2007/2008 A. Krell #5 D17	0.15229379	0.25
SIPEX V1 2007/2008 A. Krell #5 D18	0.0608946	0.11
SIPEX V1 2007/2008 A. Krell #6 1	0.02756515	0.05
SIPEX V1 2007/2008 A. Krell #6 135	0.01328713	0.02
SIPEX V1 2007/2008 A. Krell #6 15	0.15696773	0.26
SIPEX V1 2007/2008 A. Krell #6 224	0.10863018	0.18
SIPEX V1 2007/2008 A. Krell #6 27	0.05594049	0.09
SIPEX V1 2007/2008 A. Krell #6 33	0.0103141	0.02
SIPEX V1 2007/2008 A. Krell #6 43	0.33412611	0.59
SIPEX V1 2007/2008 A. Krell #6 D12	0.02439579	0.04
SIPEX V1 2007/2008 A. Krell #6 D17	0.50040907	0.84
SIPEX V1 2007/2008 A. Krell #7 221	0.05573794	0.11
SIPEX V1 2007/2008 A. Krell #7 222	0.04472332	0.08
SIPEX V1 2007/2008 A. Krell #7 34	0.10015474	0.17

Sample name	ikaite total in Sample	ikaite in mg/l melted ice
SIPEX V1 2007/2008 A. Krell #7 D16	0.01522626	0.03
SIPEX V1 2007/2008 A. Krell #7 D3	0.01938701	0.03
SIPEX V1 2007/2008 A. Krell #8 116	0.06784825	0.11
SIPEX V1 2007/2008 A. Krell #8 201	0.17410519	0.29
SIPEX V1 2007/2008 A. Krell #8 224	0.02344177	0.08
SIPEX V1 2007/2008 A. Krell #8 D14	0.05406564	0.09
SIPEX V1 2007/2008 A. Krell #9 135	0.05494857	0.1
SIPEX V1 2007/2008 A. Krell #9 221	0.44676424	0.79
SIPEX V1 2007/2008 A. Krell #9 222	0.02253563	0.04
SIPEX V1 2007/2008 A. Krell #9 34	0.0245895	0.04
SIPEX V1 2007/2008 A. Krell #9 43	0.02700434	0.05
SIPEX V1 2007/2008 A. Krell #9 D12	0.03860577	0.07
SIPEX V1 2007/2008 A. Krell #9 D17	0.02742495	0.05
SIPEX V1 2007/2008 A. Krell #9 D3	0.04075055	0.07

Appendix E

SIPEx data

Table E.1: SIPEx data

Station number	Date Labels	Time (UTC)	Latitude South	Longitude East	Depth from top	Bucket #	Vol. filtered in ml	Temp. in °C
#1	070911 Airtemp. -15.9 Total thickness: 51cm	04:00	64°13.773	127°57.132	0-11	34	630	-8.7
					11-21	221	620	-6.7
					21-31	222	608	-5.8
					31-41	D14	558	-4.1
#2	070912 Airtemp. -18.6 Total thickness: 98cm	06:00	64°29.42	128°03.29	41-51	224	520	-2.3
					0-10	D15	570	-9.6
					10-20	33	605	-7.6
					20-30	D3	610	-8.3

Station number	Date Labels	Time (UTC)	Latitude	Longitude South	Depth from top East	Bucket #	Vol. filtered ml	Temp. C°					
#6	070921 Airtemp. -11.7 Total thickness: 81cm		65°35.304	122°35.043	0-10	43	565	-9.1					
					10-20	D12	590	-8.6					
					20-30	D17	595	-7.4					
					30-40	15	600	-6.8					
					40-50	33	600	-5.3					
					50-60	27	600	-4.1					
					60-70	135	570	-3					
					70-81	1	610	-2					
#7	070922 Airtemp. -12.3 Total thickness: 53cm		65°33.492	121°31.640	0-10	34	595	-7.2					
					10-20	D16	570	-6.5					
					20-30	222	560	-5.3					
					30-40	D3	590	-3.9					
					40-50	221	520	-2.8					
					50-53	109	Chla						
					#8	070925 Airtemp. -7 Total thickness: 37cm		65°33.281	118°52.480	0-10	201	605	-4.9
										10-20	D14	605	-4.3
20-30	116	600	-3.5										
30-37	224	290	-2.4										

Station number	Date Labels	Time (UTC)	Latitude	Longitude South	Depth from top East	Bucket #	Vol. filtered ml	Temp. C°		
#9	070928 Airtemp: -11.1 Total thickness: 98		65°20.612	118°33.809	0-10	221	565	-4.9		
					10-20	222	530	-5.1		
					20-30	34	560	-4.6		
					30-40	135	545	-4.2		
					40-50	43	570	-3.3		
					50-60	D3	550	-3.1		
					60-70	D12	550	-2.6		
					70-80	D17	590	-2.1		
					80-90	D18		-2.1		
		90-98	1		-1.7					
#10	070930 Airtemp: -14.8 Total thickness: 133cm		64°56.549	119°07.976	0-10	224	545	-4		
					10-20	201	540	-5.8		
					20-30	D14	570	-6.4		
					30-40	D16	565	-6.5		
					40-50	116	590	-5.9		
					50-60	109	540	-5.6		
#11	071003 Airtemp:-7.3 Total thickness: 101cm		65°01.496	117°42.015	0-10	43	520	-6.8		
					10-20	222	560	-6.5		
					20-30	34	590	-6		

Station number	Date	Time (UTC)	Latitude	Longitude	Depth from top	Bucket #	Vol. filtered	Temp.
	Labels			South	East		ml	C°
					30-40	D12	560	-5.3
					40-50	33	550	-4.8
					50-60	1	585	-4.2
					60-70			-3.6
					70-80			-3.1
					80-90			-2.4
					90-101			-2
					snow	D3	560	
#12		071005			0-10	43	560	-6.5
					10-20	D12	550	-6.6
					20-30	34	540	-6.6
					30-40	D14	560	-6.4
					40-50	33	580	-6.1
					50-60	D3	575	-6.1
					60-70	221	540	-6
					70-80	D18	570	-5.7
					80-90	109	550	-5.1
					90-100	1	560	-5
					100-109	116	550	-4.7
					snow	201	305	

Airtemp: -6.9

Total thickness: 187cm

Station number	Date	Time (UTC)	Latitude	Longitude	Depth from top	Bucket #	Vol. filtered	Temp.
	Labels			South	East		ml	C°
#13	071006		64°44.436	116°49.274	0-10	27	565	-5.3
	Airtemp: -7.8				10-20	15	580	-4.8
	Total thickness: 78cm				20-30	135	530	-4.2
					30-40	224	590	-3.9
					40-50	D17	560	-3.4
					50-60	118	600	-2.9
					60-70	222	600	-2.4
				snow	D10	290		
#14	071007		64°18.483	116°49.594	0-10	50	530	-5.5
	Airtemp: -10.0				10-20	201	530	-4.6
	Total thickness: 64cm				20-30	D14	570	-3.7
					30-40	33	580	-3
					40-50	109	520	-2.6
					50-60	D12	545	-2.1
					snow	34	445	